REPORT NO.
UCB/EERC-83/09
JUNE 1983

EARTHQUAKE ENGINEERING RESEARCH CENTER

EFFECTS OF TRANSIENT FOUNDATION UPLIFT ON EARTHQUAKE RESPONSE OF STRUCTURES

by

CHIK-SING YIM
ANIL K. CHOPRA

A Report on Research Conducted Under
Grants PFR 79-08261 and CEE 81-05790
from the National Science Foundation

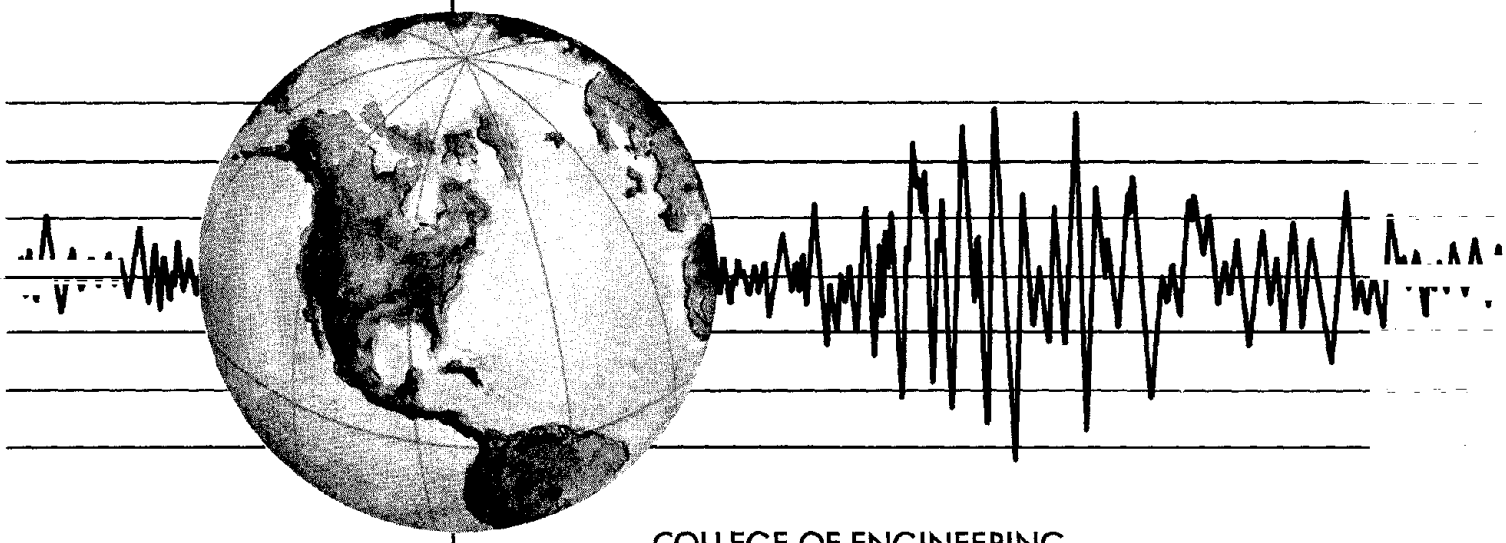

COLLEGE OF ENGINEERING

UNIVERSITY OF CALIFORNIA · Berkeley, California

For sale by the National Technical Information Service, U.S. Department of Commerce, Springfield, Virginia 22161.

See back of report for up to date listing of EERC reports.

DISCLAIMER

50272-101

REPORT DOCUMENTATION PAGE	1. REPORT NO. NSF/CEE-83014	2.	3. Recipient's Accession No. PB83 261396

4. Title and Subtitle
Effects of Transient Foundation Uplift on Earthquake Response of Structures

5. Report Date
June 1983

6.

7. Author(s)
Chik-Sing Yim and Anil K. Chopra

8. Performing Organization Rept. No.
UCB/EERC-83/09

9. Performing Organization Name and Address
Earthquake Engineering Research Center
University of California, Berkeley
47th Street & Hoffman Blvd.
Richmond, Calif. 94804

10. Project/Task/Work Unit No.

11. Contract(C) or Grant(G) No.
(C) PFR-79-08261
(G) CEE-81-05790

12. Sponsoring Organization Name and Address
National Science Foundation
1800 G. Street, N.W.
Washington, D.C. 20550

13. Type of Report & Period Covered

14.

15. Supplementary Notes

16. Abstract (Limit: 200 words)

The objective of this study is to develop a better understanding of the effects of transient foundation uplift on response of structures, so that the related reduction in earthquake forces can be considered in design of structures. The mathematical models chosen are simple, but incorporate the most important effects of soil flexibility and realistic mechanics of uplifting and impact. In its fixed base condition, the structure itself is idealized as a single-degree-of-freedom system attached to a flexibly supported rigid foundation mat. The flexibility and damping of the supporting soil are represented by two alternative idealizations: (1) two spring-damper elements, one at each edge of the foundation mat, or (2) Winkler foundation with spring-damper elements distributed over the entire width of the foundation mat.

Response spectra are presented, in which for each set of system parameters the maximum base shear is plotted against the natural vibration period of the corresponding rigidly-supported structure for two conditions of contact between the foundation mat and the supporting spring-damper elements: (a) bonded contact preventing uplift and (b) unbonded contact with uplift permitted.

Because foundation uplift is shown to reduce the structural deformations and forces, there is no need to prevent it but, on the contrary, it is desirable to permit it.

17. Document Analysis a. Descriptors

b. Identifiers/Open-Ended Terms

c. COSATI Field/Group

18. Availability Statement	19. Security Class (This Report)	21. No. of Pages
Release Unlimited		137
	20. Security Class (This Page)	22. Price

EFFECTS OF TRANSIENT FOUNDATION UPLIFT ON EARTHQUAKE RESPONSE OF STRUCTURES

by

Chik-Sing Yim

Anil K. Chopra

A Report on Research Conducted Under
Grants PFR 79-08261 and CEE 81-05790
from the National Science Foundation

Report No. UCB/EERC 83/09
Earthquake Engineering Research Center
University of California
Berkeley, California

June 1983

ABSTRACT

The earthquake induced lateral forces on a structure computed under the assumption that the foundation and soil remain in complete contact will often produce a base overturning moment that exceeds the available overturning resistance due to dead weight, thus implying that one edge of the foundation would uplift temporarily. Experiments on building frames with columns permitted to lift-off during vibration, conducted on the Berkeley shaking table, demonstrated that allowing column uplift under an extreme earthquake would enhance the chances of a structure surviving in a functional condition, with damage held to a minimum. Analytical studies have also indicated that uplifting tendency of the foundation may materially reduce the magnitude of the dynamic effects transmitted to the structure. The flexibility of supporting soil was ignored in these studies; it was not incorporated into the shaking table test either.

The objective of this study is to develop a better understanding of the effects of transient foundation uplift on response of structures, so that the related reduction in earthquake forces can be considered in design of structures. The mathematical models chosen are simple, but incorporate the most important effects of soil flexibility and realistic mechanics of uplifting and impact. In its fixed base condition, the structure itself is idealized as a single-degree-of-freedom system attached to a rigid foundation mat which is flexibly supported. The flexibility and damping of the supporting soil is represented by two alternative idealizations: (1) two spring-damper elements, one at each edge of the foundation mat, or (2) Winkler foundation with spring-damper elements distributed over the entire width of the foundation mat.

Analytical examination of the governing equations and system properties and the numerical results obtained in this study indicate that the earthquake response of uplifting structures is controlled by the following system parameters, listed in more or less descending order of importance:

- natural vibration frequency ω of the rigidly supported structure
- slenderness-ratio parameter α
- ratio γ of foundation mass to superstructure mass
- $\beta = \omega_v / \omega$ where ω_v is the vertical vibration frequency of the system with its foundation mat bonded to supporting elements
- damping ratio ξ of the rigidly supported structure
- damping ratio ξ_v in vertical vibration of the system with its foundation mat bonded to the supporting elements.

In order to study the effects of foundation-mat uplift on the maximum response of buildings, response spectra are presented. For each set of system parameters the maximum base shear is plotted against the natural vibration period of the corresponding rigidly-supported structure for two conditions of contact between the foundation mat and the supporting spring-damper elements: (a) bonded contact preventing uplift and (b) unbonded contact with uplift permitted. A study of these response spectra plots leads to the following conclusions:

1. The base shear developed in structures with relatively long vibration periods is below the static value at incipient uplift and the foundation mat does not uplift from its supporting elements.
2. For short period structures, the base shear exceeds the incipient-uplift value if foundation-mat uplift is prevented; for such structures, permitting uplift has the effect of reducing the base shear -- to values somewhat above the critical value.
3. Because the response of a structure with foundation mat permitted to uplift is controlled by the critical base shear, which is independent of the ground motion, the base shear is affected only slightly by earthquake intensity.

4. The foundation mat of a slender structure has a greater tendency to uplift resulting in greater reductions in base shear.

5. Because the critical base shear increases with mass ratio γ so does the maximum earthquake induced base shear.

6. The shape of the response spectrum is affected little by the frequency ratio β, but it does have the effect of shifting the response spectrum to the left with larger shift for smaller β, i.e. for the more flexible supporting elements.

Because foundation uplift is shown to reduce the structural deformations and forces, there is no need to prevent it but, on the contrary, it is desirable to permit it. The foundation, underlying soil and structural columns should be properly designed to accommodate the transient uplift and the effects of subsequent impact on contact.

ACKNOWLEDGEMENT

This research investigation was supported by the National Science Foundation under Grants PFR 79-08261 and CEE 81-05790. The authors are grateful for this support.

This report also constitutes Chik-Sing Yim's doctoral dissertation which has been submitted to the University of California, Berkeley. The dissertation committee consisted of Professors A. K. Chopra (Chairman), R. W. Clough and B. A. Bolt. Appreciation is expressed to Professors Clough and Bolt for reviewing the manuscript.

TABLE OF CONTENTS

1. INTRODUCTION

In dynamic analysis of response of buildings to earthquake ground motion it is usual to postulate that the free-field ground motion is directly transmitted to the base of the structure without any modification. Implicit in this approach are the assumptions that the soil underlying the structure is perfectly rigid and the structural foundation is firmly bonded to the soil. In reality soils are not infinitely stiff and the structural foundations are supported on the soil only through gravity forces.

During recent years considerable research has been devoted to removing the approximation implied by the first of these assumptions. By idealizing the underlying soil medium as a viscoelastic half space or as a system of finite elements, procedures have been developed to include the effects of soil-structure interaction arising from soil flexibility and inertia in the dynamic response of structures. These effects have been shown to be especially significant in the response of some types of structures, such as nuclear power plants and offshore structures. However much of the extensive work on soil-structure interaction was based on the second of the above mentioned assumptions, i.e. the foundation of the structure is firmly bonded to the soil.

Whether soil-structure interaction effects are considered or not, the earthquake induced lateral forces on a building, computed by dynamic analysis under the assumption that the foundation and soil are firmly bonded, will often produce a base overturning moment that exceeds the available overturning resistance due to gravity loads. The computed overload implies that a portion of the foundation mat or some of the individual column footings, as the case may be, would intermittently uplift for small time durations during an earthquake. Such uplift has been observed in several earthquakes. Several examples of towers and oil tanks uplifting from the underlying soil during Arvin Tehachapi (1952), Alaska (1964), and Imperial Valley (1979) earthquakes are cited in a recent work [1]. Uplift of multistory building foundations has rarely been observed because the uplift is expected to be small and the foundation-soil interface is often inaccessible for observation.

Until a few years ago the possibility of foundation uplift was not considered in the practical design of buildings because the design code forces were typically not large enough to initiate uplift. The situation changed after the San Fernando earthquake when the new hospital code required that hospitals in California be designed for much larger forces. In some cases the resulting base overturning moments exceeded the available overturning resistance due to gravity loads and to prevent uplift the designers anchored the foundation, a very expensive undertaking.

Housner was the first to recognize the correlation between foundation uplift and the good performance of seemingly unstable structures during earthquakes [2]. During the Chilean earthquakes of 1960, several golf-ball-on-a-tee type of elevated water tanks survived the ground shaking whereas much more stable appearing reinforced concrete elevated water tanks were severely damaged. Motivated by this anomalous behavior, Housner systematically investigated the dynamics of a rigid block rocking on a rigid horizontal base. He demonstrated that there is a scale effect which makes the larger of two geometrically similar blocks more stable than the smaller block. Moreover, the stability of a tall slender block subjected to earthquake motion is much greater than would be inferred from its stability against a static horizontal force. In order to take advantage of the beneficial effects of base uplift, it was proposed [3] to design the tall piers of a bridge to rock from side-to-side with vertical separation of parts of the pier from the supporting foundations. An earlier experimental study [4] suggested that tall structures allowed to rock on their foundations would be surprisingly stable during earthquakes.

Idealizing the structure as a one-degree-of-freedom oscillator, Meek was apparently the first to analytically investigate the effects of foundation uplift on the earthquake response of a flexible structure [5]. He concluded that foundation uplift leads to reduction in the structural deformation. Later he extended his study to multistory, braced-core buildings [6], and found that significant reduction in structural deformation can again be obtained by permitting uplift of the rigid base of the core. Experiments on steel building frames with columns permitted to lift-off during vibration, conducted on the Berkeley shaking table [7,8], demonstrated that

allowing column uplift under an extreme earthquake would enhance the chances of a structure surviving in a functional condition, with damage held to a minimum. In other words, it was demonstrated that the strength and ductility requirements for the frames can be reduced by permitting column uplift. The flexibility of the supporting soil was ignored in these analytical studies [5,6]; it was not incorporated in the shaking table tests either [7,8].

On the other hand, elaborate procedures have been developed to consider the effects of foundation uplift in the earthquake response of nuclear reactor structures. For example, the finite element method has been employed to model the nuclear reactor as well as the foundation in one study [9]. In another investigation, the nuclear reactor was idealized as a lumped mass system with many degrees-of-freedom and the foundation by equivalent translational and rotational stiffness and damping elements with their properties determined from elastic half space analyses [10]. These procedures, although suitable for analysis of particular structures, are not the most convenient to investigate, for a wide range of parameters, the effects of foundation uplift on structural response.

Recently, Psycharis [1] studied these effects using two simple models to represent foundation flexibility and energy dissipation: (a) two spring-damper elements symmetrically placed under the base of the structure, and (b) Winkler foundation with spring-damper elements distributed over the base of the structure. Considering the superstructure as a rigid block, he examined the undamped free vibration properties of the rigid block supported on the two foundation models for two situations: (a) small initial velocity not causing base uplift, and (b) large initial velocity resulting in motion dominated by base uplift most of the time. By matching the free vibration period and the displacement of the rigid block, excitation-dependent relations between the properties of the two foundation models were derived. In an effort to account for energy loss due to inelastic impact, radiation in the form of stress waves, and soil damping, three energy dissipating mechanisms were examined. It was concluded that the damping effects can be most efficiently represented by dashpots in parallel to the elastic springs. He also formulated the equations of motion for flexible structures supported on a foundation with two

spring-damper elements, and presented a procedure for analysis of structural response. Finally, he examined the effects of base uplift on the dynamic response of one example single-story structure and one mutistory superstructure. Based on theses results, he concluded that "for flexible superstructures, it seems that uplift always increases the angle of rotation of the foundation mat but the effects on the structural deflection and the resulting stresses are not clear. In general, it cannot be concluded whether uplift is beneficial to the structure or not, since this depends on the parameters of the system and the characteristics of the excitation."

The objective of this investigation is to develop a better understanding of the effects of transient foundation uplift on building response, considering a wide range of the important system parameters. For this purpose it is appropriate to choose structural idealizations that are relatively simple but realistic in the sense that they incorporate only the most important features of foundation uplift. In its fixed base condition, the structure is idealized as a single-degree-of-freedom (SDF) system attached to a rigid foundation mat which is flexibly supported. Two different models are employed to represent the flexibility and damping of the supporting soil: (a) two spring-damper (in parallel) elements, one at each edge of the foundation mat, and (b) Winkler foundation with spring-damper elements distributed over the entire width of the foundation mat.

In this investigation, the work of Psycharis is extended to include the following: The response of structures to horizontal ground excitations on the two foundation models are studied independently with equal emphasis; no equivalence relation between the two foundation models is assumed. Important system parameters are identified in nondimensional form. The effects of foundation uplift are studied by examining the time histories of free vibration responses and the response spectra of the structure-foundation systems, over a complete range of frequencies, to earthquake excitations for two conditions of contact between the foundation mat and the supporting spring-damper elements: (a) bonded contact preventing uplift, and (b) unbonded contact only through gravity with uplift permitted. A detailed parametric study on the sensitivity and the qualitative functional dependence of the dynamic response to each of the

important parameters is also conducted.

This report is organized in two major parts, chapters 2 and 3, corresponding to these two foundation models. At the expense of some duplication each chapter is developed to be self contained for easier reading. The conclusions of this work, presented for both foundation models, are summarized in chapter 4.

2. STRUCTURE ON TWO SPRING-DAMPER ELEMENT FOUNDATION

2.1 System Considered

It is desirable to begin with the simplest possible structural system, so for this purpose we consider the idealized representation of a one-story structure shown in Figure 2.1. It is a linear structure of mass m, lateral stiffness k and lateral damping c, which is supported through the foundation mat of mass m_0 resting on two spring-damper elements, one at each edge of the foundation mat, connected to the base which is assumed to be rigid. The column(s) is (are) assumed to be massless and axially inextensible, the foundation mat is idealized as a rigid rectangular plate of negligible thickness with uniformly distributed mass, and it is presumed that horizontal slippage between the mat and supporting elements is not possible. The mass and damping coefficients of the foundation model are assumed constant, independent of displacement amplitude or excitation frequency. Thus the frequency dependence of these coefficients, as for a viscoelastic half space [11], is not recognized; nor is the strain dependence of these coefficients for soils [12] considered in this study.

Prior to the dynamic excitation, the foundation mat rests on the spring-damper elements only through gravity and is not bonded to these supporting elements. Thus a supporting element can provide an upward reaction force to the foundation mat but not a downward pull. During vibration of the system this upward reaction force will vary with time. At any instant of time the total reaction force -- which for a supporting element consisting of a spring and damper in parallel is the sum of the elastic and damping forces -- reaches zero, one edge of foundation mat is in the condition of incipient uplift from the supporting element.

In particular, if the damper is absent, the relation between the reaction force and displacement of an edge i (left or right) of the foundation mat is shown in Figure 2.2a. The upward reaction force is related linearly to the downward displacement of the foundation mat through the spring stiffness k_f, but no reaction force is developed if the displacement is upward; the displacements are measured from the unstressed position of the springs. If the foundation mat were bonded to the supporting elements the force-displacement relation will be linear, as shown

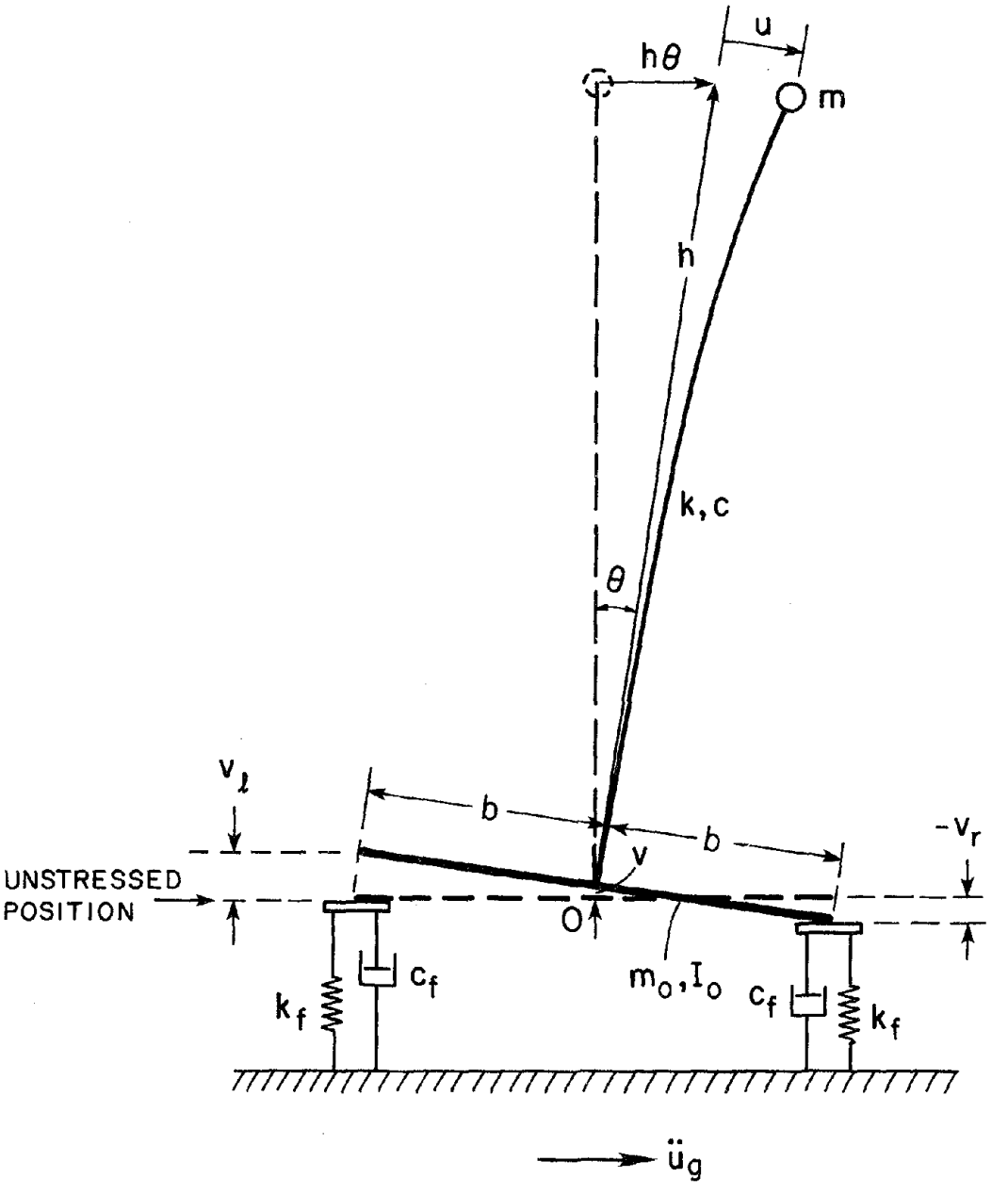

FIGURE 2.1 Flexible structure on two spring-damper element foundation.

in Figure 2.2a, valid for downward as well as upward displacements.

Consider the foundation mat and its supporting elements without the superstructure with a static force p acting in the downward direction at its center of gravity (c.g). The relation between the static moment M applied at the c.g and the resulting foundation-mat rotation θ, limited to angles much smaller than the slenderness ratio b/h, is shown in Figure 2.2b for unbonded as well as bonded conditions. If the mat is not bonded to the supporting elements the $M-\theta$ relation is linear until the foundation mat uplifts from one of the supporting elements; thereafter no additional moment can be developed. Uplift occurs when the rotation reaches $\theta_c = p/2k_f b$ with the corresponding moment $M_c = pb$. The downward force is $p = (m + m_o)g$, the combined weight of the superstructure and foundation mat, prior to any dynamic excitation, but would vary with time during vibration.

Next consider the entire structural system with a gradually increasing force f_s applied in the lateral direction. If the foundation mat is bonded to the supporting elements, which along with the structure have linear properties, the lateral force can increase beyond limit if the overturning effects of gravity forces are neglected. However, if the mat is not bonded to the supporting elements, one edge of the foundation mat is at incipient uplift when the lateral force reaches $f_{sc} = (m + m_o)gb/h$. Thus the maximum base shear that can be developed under the action of static forces is

$$V_c = (m + m_o)\, g \frac{b}{h} \tag{2.1a}$$

The structural deformation associated with this base shear is

$$u_c = \frac{(m + m_o)\, g}{k} \frac{b}{h} \tag{2.1b}$$

and at incipient uplift, the foundation-mat rotation

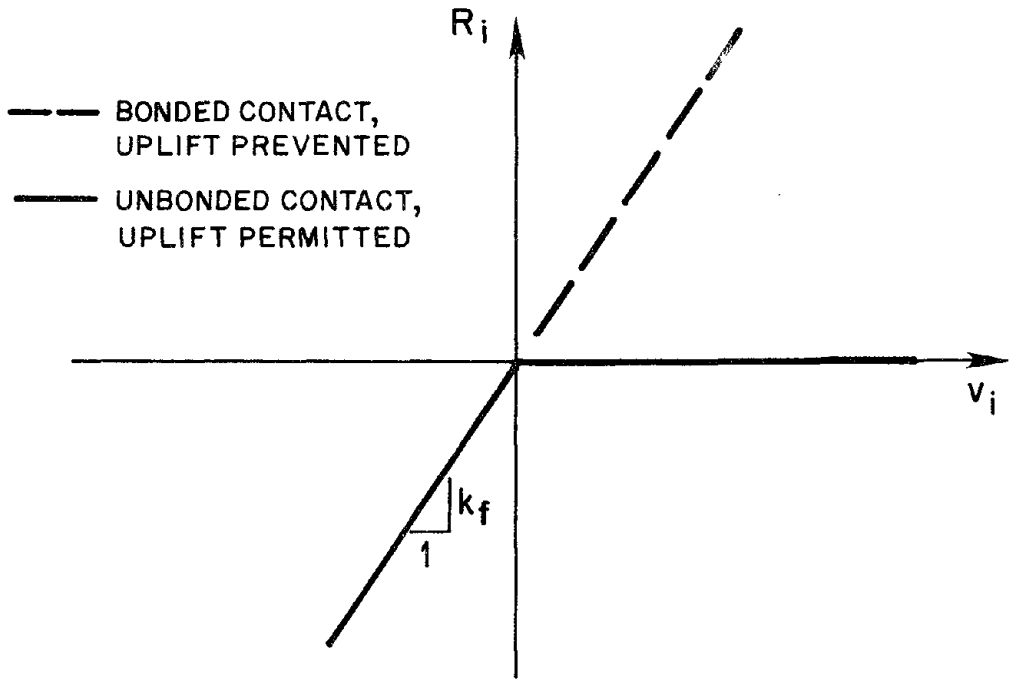

(a) Reaction force-displacement relation for supporting element

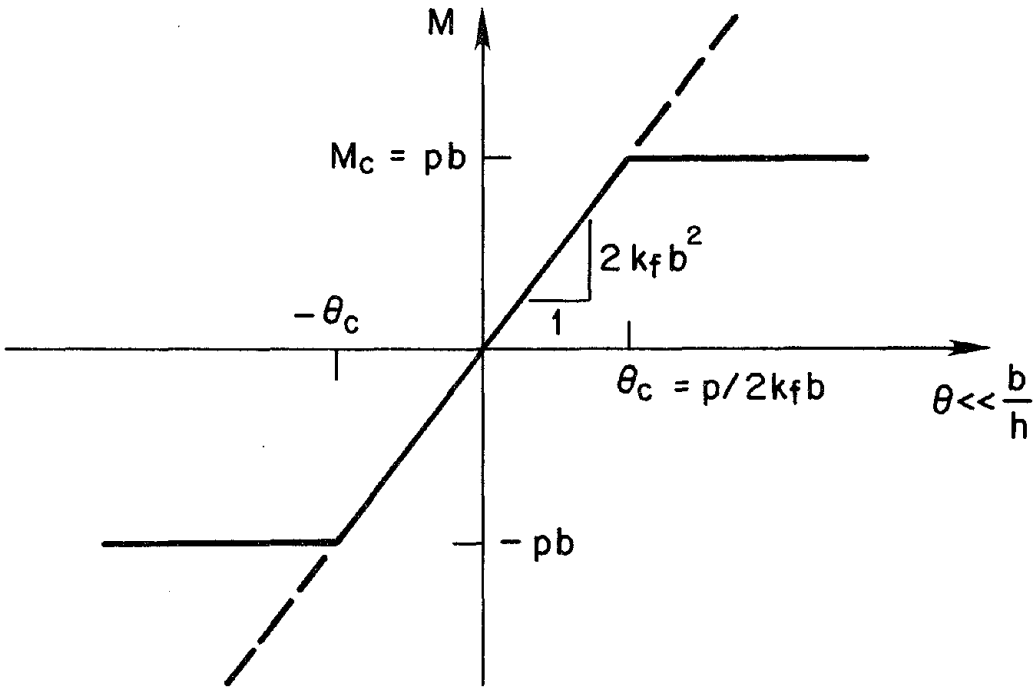

(b) Moment-rotation relation for foundation mat

FIGURE 2.2 Properties of two spring-damper element foundation.

$$\theta_c = \frac{(m + m_o)\, g}{2k_f\, b} \tag{2.1c}$$

which is consistent with the preceding paragraph and Figure 2.2b.

The base excitation is specified by the horizontal ground motion with displacement $u_g(t)$ and acceleration $\ddot{u}_g(t)$. The vertical component of ground motion is not considered in this study.

Under the influence of this excitation the foundation mat would rotate through an angle $\theta(t)$ and undergo a vertical displacement $v(t)$, defined at its c.g relative to the unstressed position. Prior to dynamic excitation, the vertical displacement is $v_s = (m + m_o)\, g / 2k_f$, the static displacement due to the total weight of the superstructure and foundation mat. During the dynamic excitation, the vertical displacement v will remain constant at the initial static value if the foundation mat is bonded to the supporting elements, but it will vary with time in the unbonded case.

The displaced configuration of the structure at any instant of time can be defined by the deformation $u(t)$, foundation-mat rotation $\theta(t)$, and vertical displacement $v(t)$ at the center of gravity of the foundation mat.

2.2 Equations of Motion

The differential equations governing the small-amplitude motion of the system of Figure 2.1 can be derived by considering the lateral equilibrium of forces acting on the structural mass m, and moment and vertical equilibrium of forces acting on the entire system (Appendix B). Assuming that the structural-foundation system and excitation are such that the amplitudes of the resulting displacement and rotation responses are small so that $\sin\theta$ and $\cos\theta$ may be approximated by θ and 1, respectively, these equations may be expressed as

$$m\ddot{u} + m\,(h\ddot{\theta}) + c\dot{u} + ku = -m\ddot{u}_g(t) \tag{2.2a}$$

$$\frac{m_o b^2}{3h^2}(h\ddot{\theta}) - c\dot{u} + \epsilon_1 c_f \frac{b^2}{h^2}(h\dot{\theta}) + \epsilon_2 c_f \frac{b}{h}\dot{v}$$

$$- ku + \epsilon_1 k_f \frac{b^2}{h^2}(h\theta) + \epsilon_2 k_f \frac{b}{h} v = 0 \tag{2.2b}$$

$$(m + m_o)\ddot{v} + \epsilon_1 c_f \dot{v} + \epsilon_2 c_f \frac{b}{h}(h\dot{\theta}) + \epsilon_1 k_f v + \epsilon_2 k_f \frac{b}{h}(h\theta) = -(m + m_o) g \tag{2.2c}$$

where ϵ_1 and ϵ_2 depend on whether one or both edges of the foundation mat are in contact with the supporting elements:

$$\epsilon_1 = \begin{cases} 2 & \textit{contact at both edges} \\ 1 & \textit{left or right edge uplifted} \end{cases}$$

$$\epsilon_2 = \begin{cases} -1 & \textit{left edge uplifted} \\ 0 & \textit{contact at both edges} \\ 1 & \textit{right edge uplifted} \end{cases}$$

A supporting spring-damper element provides an upward reaction force to the foundation mat

$$R_i(t) = -k_f v_i(t) - c_f \dot{v}_i(t), \qquad i = l,r \tag{2.3a}$$

where

$$v_i(t) = v(t) \pm b\theta(t), \qquad i = l,r \tag{2.3b}$$

As mentioned earlier, a downward reaction force cannot be developed because the foundation mat is not bonded to the supporting elements, i.e. $R_i(t) \geq 0$, $i = l,r$. If, at some instant of time, this condition is not satisfied at the left or right edge of the foundation mat, i.e.

$$R_i(t) < 0 \qquad i = l \text{ or } r \tag{2.4a}$$

that particular edge uplifts from the supporting element which no longer provides any reaction to the foundation mat. Because the spring-damper element cannot extend above its initial unstressed position, i.e. $v_i(t) \leqslant 0$, $i = l,r$, an edge of the foundation mat would uplift at the instant of time this condition is not satisfied, i.e.

$$v_i(t) > 0 \qquad i = l \text{ or } r \tag{2.4b}$$

The two uplift criteria, equations 2.4a and 2.4b, are equivalent if each supporting element included only a spring.

The earthquake response of the system depends on the following dimensionless parameters:

$\omega = \sqrt{k/m}$, the natural frequency of the rigidly supported structure

$\xi = c/2m\omega$, the damping ratio of the rigidly supported structure

$\beta = \omega_v/\omega$, where $\omega_v = \sqrt{2k_f/(m+m_o)}$ is the vertical vibration frequency of the system of Figure 2.1 with its foundation mat bonded to the supporting elements

$\xi_f = 2c_f/2(m+m_o)\omega_v$, the damping ratio in vertical vibration of the system of Figure 2.1 with its foundation mat bonded to the supporting elements

$\alpha = h/b$, a slenderness-ratio parameter

$\gamma = m_o/m$, the ratio of foundation mass to superstructure mass

When the equations of motion and uplift criterion are expressed in terms of these dimensionless parameters, for a given excitation, it is observed that, under the small-amplitude assumption, the foundation-mat rotation response θ depends on the width of the foundation mat; however, u, the structural deformation, θb, the product of the foundation-mat rotation and half base width, and v, the vertical displacement, do not depend on the size of the structure. If we were to consider the large-amplitude motion of the structure including the possibility of its overturning, the size parameter h would play an important role, just as in the dynamics of rigid blocks [2]. However, the foundations of most buildings are expected to undergo only small

rotations and uplift displacements. At these small-amplitude motions the deformation response of the system depends on the h / b ratio but not separately on h.

The equations of motion for the system of Figure 2.1 are nonlinear as indicated by the dependence of the coefficients ϵ_1 and ϵ_2 (equation 2.2) on whether one or both edges of the foundation mat are in contact with the supporting elements, the left edge is uplifted, or the right edge is uplifted. However, for each of the three contact conditions the governing equations are linear, but they depend on the contact condition. Thus, during the time duration that one particular contact condition is valid, the system behaves as a linear system, but the vibration properties of the linear system are different for the three contact conditions. Thus the dynamic response of the nonlinear system of Figure 2.1 can be viewed as the sequential response of three linear systems.

The equations of motion can be specialized for the undamped system with massless foundation mat by substituting $m_o = 0$, and $c = c_f = 0$. In particular, the inertia and damping terms in equation 2.2b are zero and, following the usual approach to static condensation, θ can be expressed in terms of u and v from

$$- ku + \epsilon_1 k_f \frac{b^2}{h^2} (h\theta) + \epsilon_2 k_f \frac{b}{h} v = 0 \tag{2.5}$$

and substituted into equations 2.2a and 2.2c. The reduced system consists of the resulting two differential equations in the two unknown dynamic degrees-of-freedom. As discussed later, this reduced system of equations provides a basis for approximate analysis of the systems with damping and foundation-mat mass, i.e. $c \neq 0$, $c_f \neq 0$, and $m_o \neq 0$.

2.3 Natural Vibration Frequencies and Modes

It is useful to study the vibration properties of the three linear systems. These vibration properties will be examined in detail for the special case of massless foundation mat, i.e., $\gamma = 0$; the effect of foundation-mat mass will be examined subsequently. For the special case

of $\gamma = 0$, the natural frequencies and mode shapes of the system of Figure 2.1 can be determined by solving the eigenvalue problems associated with the reduced version of equation 2.2. The resulting 2-DOF eigenvalue problem is solved for the three linear systems corresponding to the three sets of values for ϵ_1 and ϵ_2 .

The natural frequencies of the linear system with both edges of the foundation mat in contact with the supporting elements are

$$\omega_1 = \omega\bar{\omega}_1 \tag{2.6a}$$

$$\omega_2 = \omega_v = \omega\beta \tag{2.6b}$$

where

$$\bar{\omega}_1 = \sqrt{\frac{\beta^2}{\alpha^2 + \beta^2}} \tag{2.6c}$$

and the corresponding mode shapes are

$$\boldsymbol{\phi}_1{}^T = < \ \bar{\omega}_1{}^2 \quad (1-\bar{\omega}_1{}^2) \quad 0 \ > \tag{2.7a}$$

$$\boldsymbol{\phi}_2{}^T = < \ 0 \quad 0 \quad 1 \ > \tag{2.7b}$$

where the three terms in each mode shape are ordered to correspond to

$$\mathbf{r}^T = < \ u \quad h\theta \quad v \ >$$

As shown in Figure 2.3a, the system vibrating in the second mode undergoes uncoupled vertical motion, without lateral deformation of the structure or rotation of the foundation mat, at the natural frequency ω_v defined earlier. The motion of the system vibrating in the first mode consists of lateral deformation of the structure and rotation of the foundation mat without any vertical displacement of its c.g (relative to its static equilibrium position).

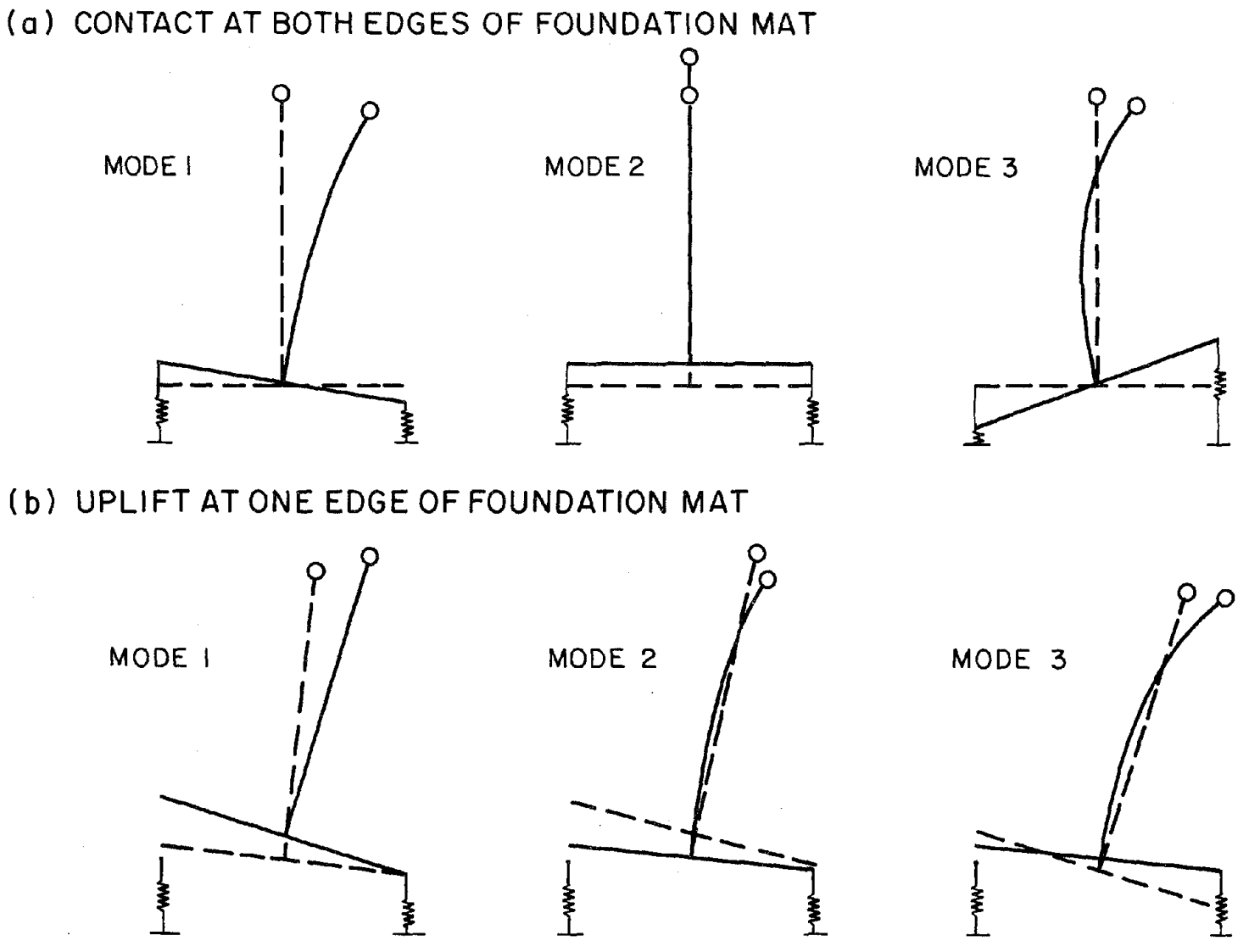

FIGURE 2.3 Free vibration mode shapes for two cases: (a) Foundation mat in contact with supporting elements at both edges, and (b) One edge of the foundation mat uplifted.

The natural frequencies of the linear system with uplift at one edge (left or right edge) of the foundation mat are

$$\lambda_1 = 0 \tag{2.8a}$$

$$\lambda_2 = \omega\bar{\lambda}_2 \tag{2.8b}$$

where

$$\bar{\lambda}_2 = \sqrt{\frac{(1+\alpha^2)\beta^2}{2\alpha^2+\beta^2}} \tag{2.8c}$$

and the corresponding mode shapes are

$$\psi_1{}^T = < \ 0 \quad 1 \quad \pm 1/\alpha \ > \tag{2.9a}$$

$$\psi_2{}^T = < \ \bar{\lambda}_2{}^2 \quad (1-\bar{\lambda}_2{}^2) \quad \mp\alpha \ > \tag{2.9b}$$

Equations 2.8 and 2.9 are applicable to the system with uplift at left or right edge of the foundation mat. Wherever both algebraic signs appear simultaneously the upper sign applies to uplift at the left edge and the lower sign to uplift at the right edge. The mode shapes described by equation 2.9 are plotted in Figure 2.3b relative to an initial reference position (shown in dashed lines) which is somewhat arbitrary. The system vibrating in the first mode undergoes rigid body rotation about one edge of the foundation mat, whereas in the second mode motion occurs in all three degrees of freedom: lateral deformation of the structure, vertical displacement and rotation of the foundation mat. If the frequency ratio β exceeds the slenderness-ratio parameter α, which in turn is much larger than unity, it can be shown that $\bar{\lambda}_2$ is close to α, the value determined directly for the structure of Figure 2.1 but supported directly on the rigid base without the spring-damper elements [5].

For the general case with some foundation-mat mass ($\gamma \neq 0$), the natural frequencies and mode shapes can be determined by solving the eigenvalue problem associated with equation

2.2. The 3-DOF eigenvalue problem is solved for the three linear systems corresponding to the three sets of values for ϵ_1 and ϵ_2 . The resulting analytical expressions are available (Section C.1.1, Appendix C) and will not be repeated here. For the present purpose it suffices to numerically study the dependence of frequencies and mode shapes on the mass ratio γ.

For the linear system with both edges of the foundation-mat in contact with the supporting elements, the first two natural frequencies and modes are described by equations 2.6a and 2.6b and Figure 2.3 even when the foundation mat has some mass. However, now $\bar{\omega}_1$ depends also on γ and is no longer described by equation 2.6c. Because the natural frequency and the shape of the first mode involves $\bar{\omega}_1$ (equations 2.6a and 2.7a), they also depend on γ. The numerical results presented in Figure 2.4 display the influence of γ on $\bar{\omega}_1$ which decreases monotonically as γ becomes smaller. For a fixed value of the frequency ratio β, the natural frequency and shape of the second mode is independent of the mass ratio γ. A third vibration mode appears (Figure 2.3a) when the foundation mat has some mass. Just like the first mode, the third mode includes lateral deformation of the structure and rotation of the foundation mat without any vertical displacement of its c.g (relative to its static equilibrium position). It can be shown through numerical results and a mathematical limiting process that the natural frequency of the third mode is at least an order of magnitude higher than the other two frequencies, and it tends to infinity as the mass of the foundation mat approaches zero.

For the linear system with uplift at one edge of the foundation mat, the first two natural frequencies and modes are described by equations 2.8 and 2.9 and Figure 2.3b, even when the foundation mat has some mass. However, $\bar{\lambda}_2$ is no longer described by equation 2.8c and depends on γ, as indicated by the numerical results presented in Figure 2.4. The effect of mass ratio γ on the natural frequency and shape of the second mode decreases monotonically with γ. The natural frequency and shape of the first mode, which is a rigid body mode, is independent of the mass ratio γ. The third vibration mode, which appears when the foundation has some mass, includes displacements in all the three degrees of freedom just as in the second mode. Just as in the earlier case, the natural frequency of the third mode is at least an order of

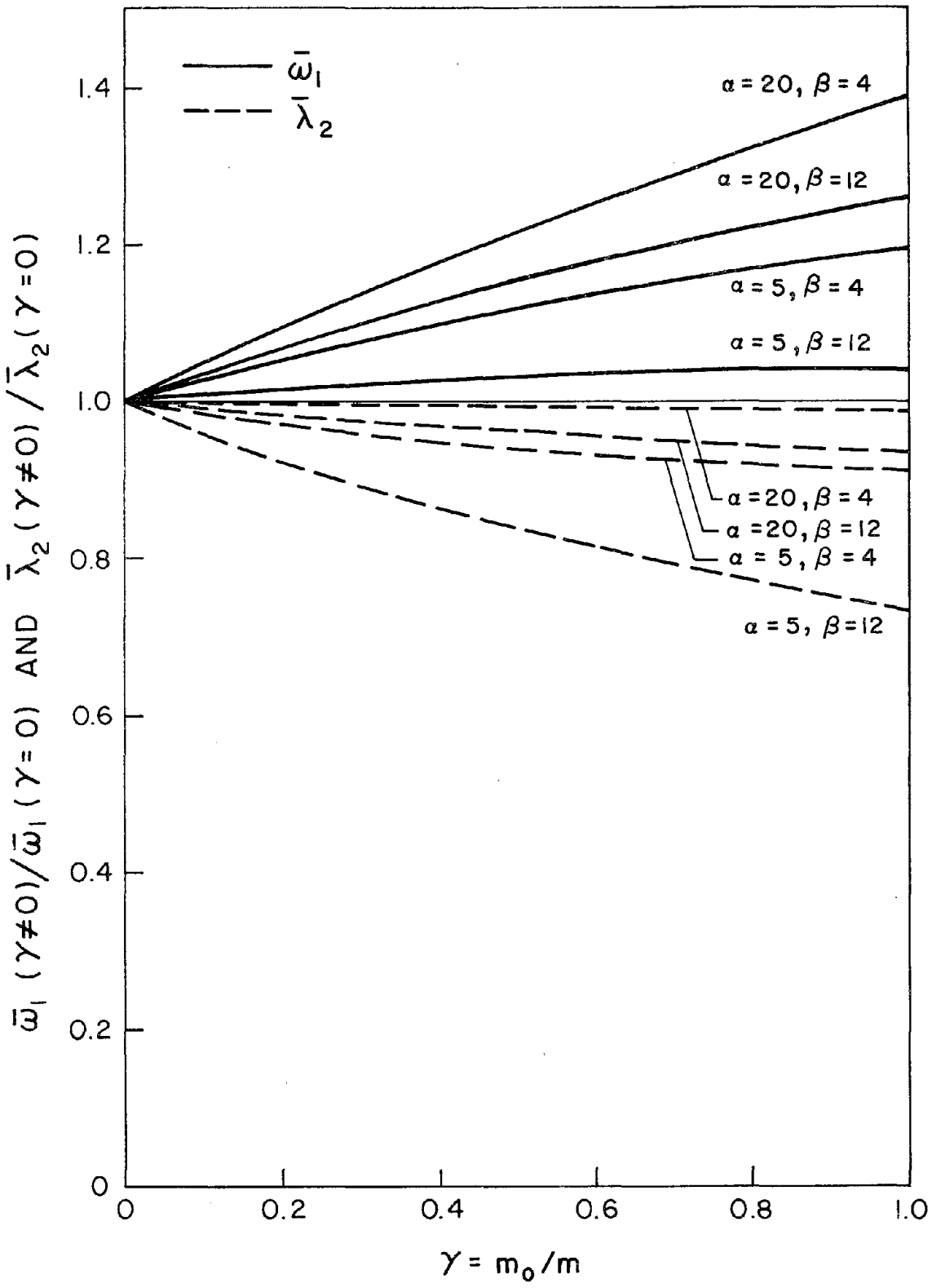

FIGURE 2.4 Variation of vibration frequency and mode shape parameters $\bar{\omega}_1$ and $\bar{\lambda}_2$ with mass ratio γ for various values of system parameters α and β.

magnitude higher than the second mode frequency and it tends to infinity as the foundation-mat mass approaches zero.

2.4 Free Vibration Response

Before studying the response of the system of Figure 2.1 to earthquake excitations, wherein we will have to depend entirely on numerical computations, it is useful to analytically examine some features of the system in free vibration. Restricting this section to massless foundation mats, the response of undamped systems is studied first, followed by the effects of damping.

2.4.1 Undamped System

Starting with the initial state of the structural system of Figure 2.1, wherein both edges of the foundation mat are in contact with the supporting elements, the response of the system to any initial displacements and velocities can be determined as the superposition of the free vibration responses in the two modes of vibrations $\boldsymbol{\phi}_1$, and $\boldsymbol{\phi}_2$. In particular, if an initial velocity $\dot{x}(0)$ is imparted in the lateral direction to the mass m of the superstructure, the second vibration mode will not be excited and the response will be entirely due to the first mode. The structural displacement vector $\mathbf{r}^T = < \; u \qquad h\theta \qquad v \; >$ is then described by

$$\mathbf{r}(t) = \frac{\dot{x}(0)}{\omega_1}\boldsymbol{\phi}_1 \sin \omega_1 t - v_s \boldsymbol{\phi}_2 \tag{2.10}$$

provided the motion is small enough that both edges of the foundation mat remain in contact with the supporting elements. From equation 2.10, the structural displacements at the point of incipient uplift of one edge of the foundation mat are

$$u_c = \frac{g}{\alpha\omega^2} \tag{2.11a}$$

$$h\theta_c = \frac{\alpha g}{\beta^2\omega^2} \tag{2.11b}$$

These displacements are same as those presented in equation 2.1, specialized for massless foundation mat, which were obtained from static considerations.

The critical velocity $\dot{x}(0)_c$ is defined as the initial velocity that results in the maximum displacements $\mathbf{r}(t)$, from equation 2.10, equal to the displacements given by equation 2.11. It can be shown that

$$\dot{x}(0)_c = \frac{\sqrt{\alpha^2+\beta^2}}{\alpha\beta}\frac{g}{\omega} \tag{2.12}$$

and it depends on the slenderness-ratio parameter α and frequency ratio β. For purposes of the subsequent discussion it is useful to introduce the normalized initial velocity

$$\bar{\dot{x}}(0) = \dot{x}(0)/\dot{x}(0)_c \tag{2.13}$$

If the initial velocity is less than the critical velocity, i.e., $\bar{\dot{x}}(0) < 1$, both edges of the foundation mat will remain in contact with the supporting elements and no uplift will occur; the free vibration response will be described by equation 2.10.

If the initial velocity exceeds the critical velocity, i.e., $\bar{\dot{x}}(0) > 1$, equation 2.10 will be valid only until the first uplift occurs. One edge of the foundation mat will uplift at the time instant $u(t)$ given by equation 2.10 reaches the u_c value of equation 2.11a. During the time duration that uplift of this edge continues, the displacement response can be expressed as

$$\mathbf{r}(\bar{t}) = \left[\mp\frac{1}{2}\frac{\alpha}{1+\alpha^2}g\bar{t}^2 + C_1\bar{t} + C_3\right]\boldsymbol{\psi}_1 + \left[C_2\sin(\lambda_2\bar{t}+\delta) + \frac{1}{\lambda_2^2}\left(\frac{\alpha}{1+\alpha^2}\right)g\right]\boldsymbol{\psi}_2 \tag{2.14}$$

wherein $\bar{t}$ is the time measured from the onset of uplift and, where two algebraic signs appear, the upper sign is to be used if the left edge of the foundation mat uplifts and the lower sign applies to uplift of the right edge. The four constants C_1, C_2, C_3 and δ can be determined from the displacements and velocities of the system at the onset of uplift, by transforming them to modal coordinates.

After vibration of the structure for some time with one edge of the foundation mat uplifted, as described by equation 2.14, the foundation mat will re-establish contact with supporting elements at both its edges. Measuring time t' from this instant, the response of the structure during the time span it continues to vibrate without uplift is given by

$$\mathbf{r}(t) = D_1\boldsymbol{\phi}_1 \sin(\omega_1 t' + \delta_1) + D_2\boldsymbol{\phi}_2 \sin(\omega_2 t' + \delta_2) - v_s\boldsymbol{\phi}_2 \tag{2.15}$$

Both vibration modes may now contribute to the response, in contrast to equation 2.10 wherein the second vibration mode did not appear. The four constants D_1, D_2, δ_1 and δ_2 can be determined by standard procedures from the displacements and velocities of the structure at the time contact at both edges of the foundation mat is re-established.

Numerical results for the response of a structure to normalized initial velocity $\bar{\dot{x}}(0) = 2$ are presented in Figure 2.5 for two conditions of contact between the foundation mat and the supporting spring-damper elements: (a) bonded contact preventing uplift and (b) unbonded contact only through gravity with uplift permitted. The response quantities presented as a function of time are deformation u, foundation-mat rotation θ, total lateral displacement $x = u+h\theta$, vertical displacements v_l and v_r of the left and right edges of the foundation mat, and uplift index which is zero if there is no uplift, +1 if the left edge uplifts and -1 if the right edge uplifts.

If the foundation mat is bonded to the supporting elements, the structural response is described by equation 2.10 for all time. The frequency of this simple harmonic motion is ω_1, defined in equation 2.6a, and the amplitudes of the response quantities are given by the critical

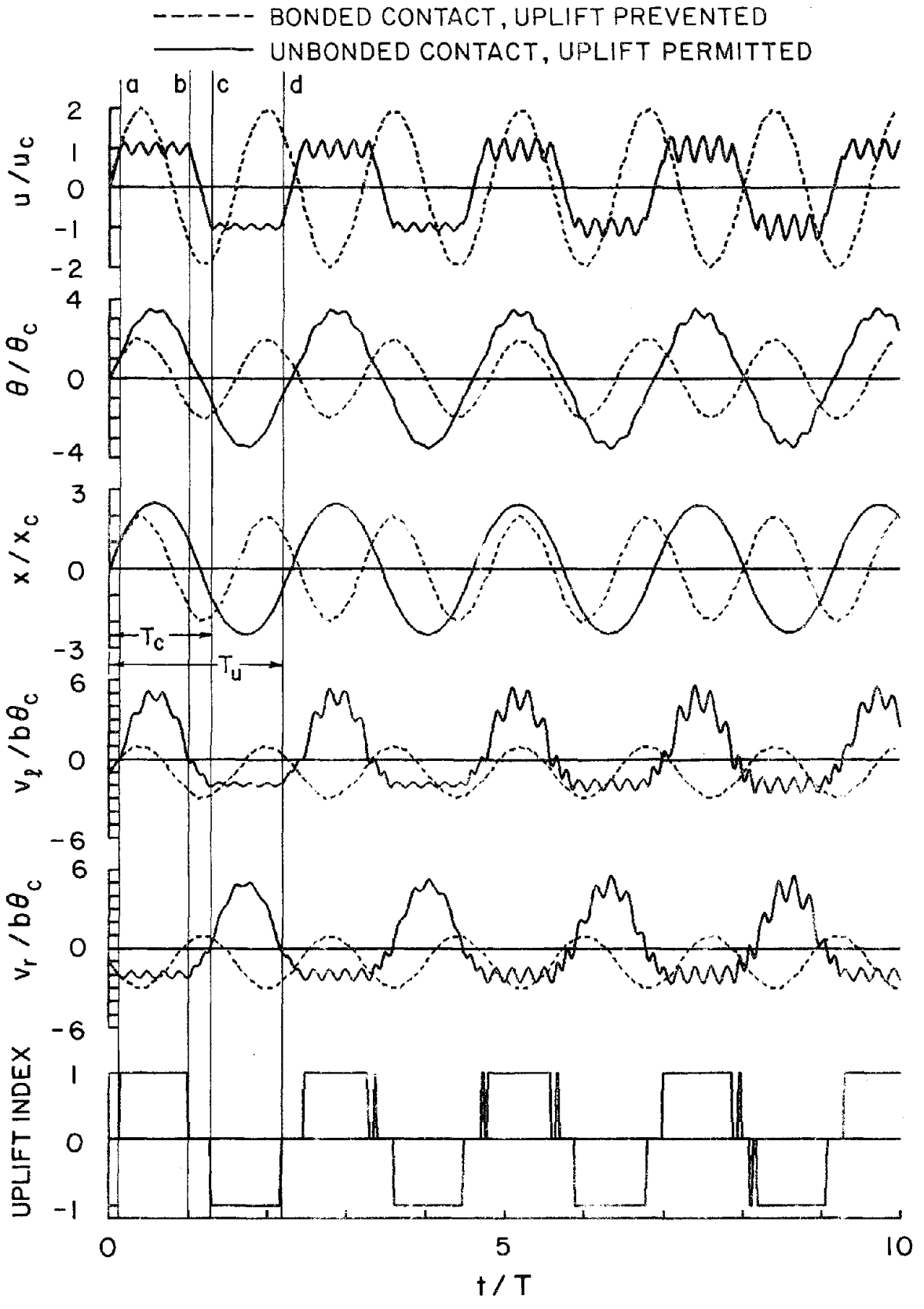

FIGURE 2.5 Response of an undamped structure ($\alpha = 10$, $\beta = 8$, $\gamma = 0$) to initial velocity $\dot{\bar{x}}(0) = 2$ for two conditions of contact between the foundation mat and the supporting elements: (a) Bonded contact preventing uplift, and (b) Unbonded contact only through gravity with uplift permitted.

value of equation 2.11 multiplied by the normalized initial velocity, which is 2 in this case.

The structural response is initially described by equation 2.10 even when uplift is permitted, resulting in response identical to the bonded case. When the deformation u and foundation-mat rotation θ reach their critical values (equation 2.11), the left edge of the mat uplifts at time a (Figure 2.5) and the subsequent response is described by equation 2.14. The deformation u oscillates with frequency λ_2 about a value $= (\alpha/1+\alpha^2)(g/\omega^2)$ which for a wide range of α is close to u_c (equation 2.11a). This higher frequency response appears also in $v_l(t)$ and $v_r(t)$ and slightly in $\theta(t)$, but the total lateral displacement $x(t)$ varies smoothly with time without any noticeable contribution of the higher frequency mode. Contact at both edges of the foundation mat is re-established at time b and the response is described by equation 2.15 until the right edge uplifts at time c; at which time equation 2.14 takes over again until contact at both edges is re-established at time d and equation 2.15 is back in the picture. This response behavior is repeated during every cycle of free vibration as seen in Figure 2.5. However, the response is almost, but not precisely, periodic because the initial conditions are not exactly repeated at the beginning of each vibration cycle. Whereas no vertical velocity is imparted to the structural mass when free vibration is initiated at $t = 0$, a small vertical velocity may be present at the beginning of subsequent cycles of free vibration. In addition to the slight differences in the response details from one cycle to the next, this perturbation can produce additional very short duration uplift episodes, as seen in the lowest portion of Figure 2.5.

Because of uplift of the foundation mat, the maximum structural deformation u is reduced but the maximum values of all the other response quantities -- θ, x, v_l and v_r -- are increased.

Noting that the time scale in Figure 2.5 is normalized with respect to the natural vibration period T of the rigidly supported structure, it is apparent that the flexibility of the supporting elements has the effect of lengthening the vibration period to T_c, and uplift of the foundation mat results in even a longer period T_u. From equation 2.6a the period ratio

$$\frac{T}{T_c} = \bar{\omega}_1 \tag{2.16}$$

wherein, for a fixed mass ratio γ, $\bar{\omega}_1$ depends only on α and β and not on $\bar{\dot{x}}(0)$ or T; in particular it is given by equation 2.6c if $\gamma = 0$. An analytical expression for the period ratio T_u/T does not appear to be derivable because the system is nonlinear when uplift of the foundation mat is permitted. However, based on numerical results it can be shown that, for a fixed value of γ, T_u/T depends on α, β and $\bar{\dot{x}}(0)$ but, over a useful range of parameters, it does not depend on T. Because as discussed earlier the mass ratio γ has little effect on the vibration properties of the three linear systems (Figure 2.4), its influence on these period ratios is also small.

Presented in Figure 2.6 are the ratios T_c/T and T_u/T as a function of the frequency ratio β for three values of the slenderness ratio parameter α. Whereas the ratio T_c/T is independent of $\bar{\dot{x}}(0)$, because the system is linear if uplift of the foundation mat is not permitted, T_u/T does depend on this parameter and the results of Figure 2.6 are for $\bar{\dot{x}}(0) = 4$. For a fixed α, the period ratios decrease as the frequency ratio β increases, approaching their asymptotic values as β increases. The asymptotic value for $T_c/T = 1$ because T_c approaches T as the support system becomes stiffer. Beyond a certain value of β, which depends on α, the period ratios are affected little by further increase in β. The lengthening of vibration period due to support flexibility and foundation-mat uplift is greater for the larger value of α, i.e., for the more slender buildings.

As mentioned earlier, T_c/T depends on α and β but not on $\bar{\dot{x}}(0)$, T , or γ; and T_u/T depends on α, β and $\bar{\dot{x}}(0)$ but not on T or γ. Numerical results have demonstrated that the ratio T_u/T_c depends on the normalized initial velocity $\bar{\dot{x}}(0)$ as shown in Figure 2.7, essentially independent of all other parameters. For a known T and given system properties α and β, the periods T_c and T_u can be estimated from equation 2.16, wherein $\bar{\omega}_1$ can be computed from equation 2.6c, and Figure 2.7.

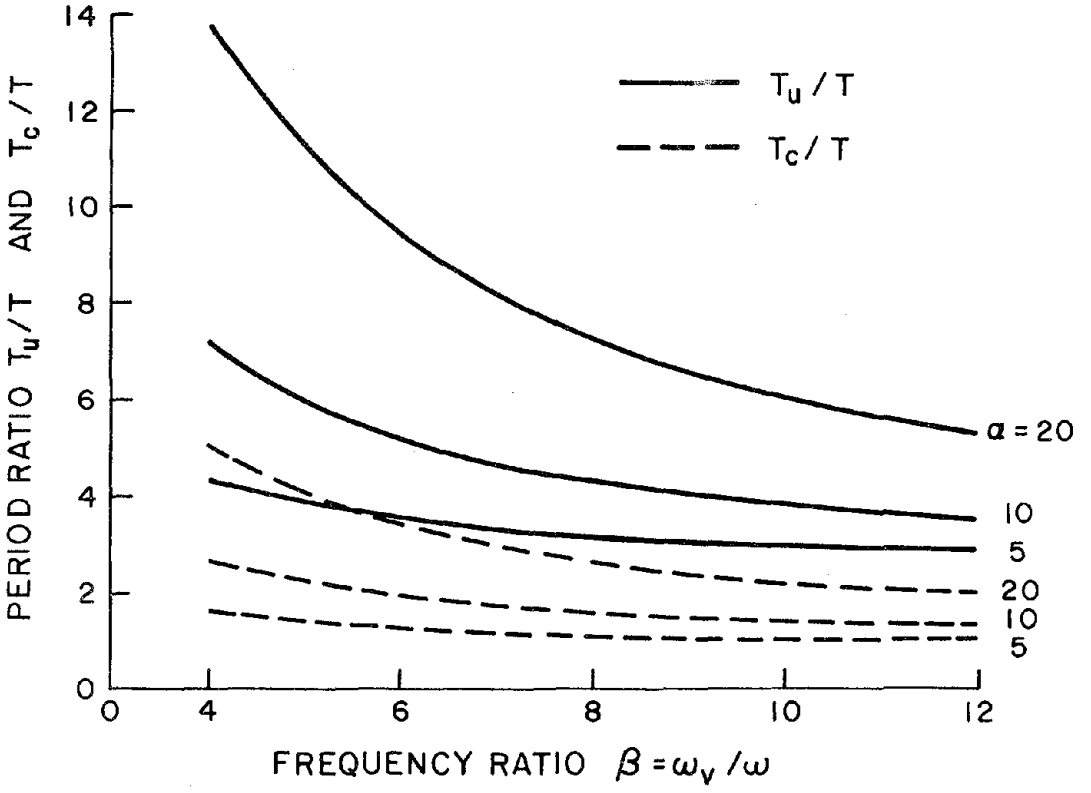

FIGURE 2.6 Variation of period ratio with β and α. Results for T_c/T are independent of $\bar{x}(0)$, but T_u/T values correspond to $\bar{x}(0) = 4$.

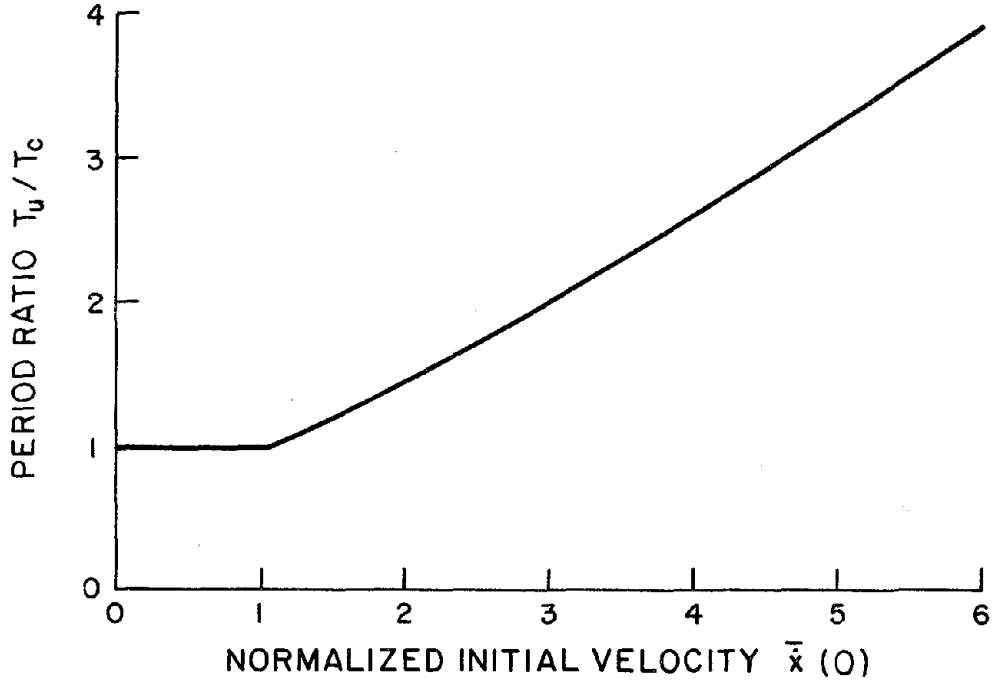

FIGURE 2.7 Variation of period ratio T_u/T_c with normalized initial velocity $\bar{x}(0)$.

2.4.2 Effects of Damping

Expressed as a combination of modal contributions, the response of the undamped system to an initial velocity was given by equation 2.10 during the time that both edges of the foundation mat remain in contact with the supporting elements, by equation 2.14 during the time one edge is uplifted, and by equation 2.15 after contact has been re-established at both edges. When damping in the structure and the supporting elements is included, the responses of a system with massless foundation mat will be described by equations 2.10, 2.14, and 2.15 with appropriated modifications to account for modal damping. In equations 2.10 and 2.15, these include exponential decay terms $e^{-\xi_n \omega_n t}$ and $e^{-\xi_n \omega_n t'}$, respectively; and substitution of the damped frequency ω'_n instead of ω_n in the harmonic terms, where $\omega'_n = \omega_n \sqrt{1 - \xi_n^2}$ and the modal damping ratios are

$$\xi_1 = \frac{\beta^3}{(\alpha^2 + \beta^2)^{3/2}} \left(\xi + \frac{\alpha^2}{\beta^3} \xi_v \right) \tag{2.17a}$$

$$\xi_2 = \xi_v \tag{2.17b}$$

In equation 2.14 only the harmonic term is modified to include the exponential decay term $e^{-\zeta_2 \lambda_2 \bar{t}}$ and the damped frequency λ'_2 is substituted instead of the undamped frequency λ_2, where $\lambda'_2 = \lambda_2 \sqrt{1 - \zeta_2^2}$ and the damping ratio

$$\zeta_2 = \frac{\beta^3 (1 + \alpha^2)^{1/2}}{(2\alpha^2 + \beta^2)^{3/2}} \left(\xi + \frac{2\alpha^2}{\beta^3} \xi_v \right) \tag{2.18}$$

Consider first the case of the structure with both edges of the foundation mat in contact with the supporting elements. The damping ratio for the second vibration mode -- which involves uncoupled vertical motion without lateral deformation or base rotation -- is simply ξ_v, the damping ratio of the structure in vertical vibration (equation 2.17b). In the first mode which includes lateral deformation of the structure coupled with rotation of the foundation mat about its c.g, the damping ratio is a linear combination of ξ_v and ξ, where the latter is the

damping ratio of the rigidly supported structure in lateral vibration.

For the linear system with uplift at one edge, the first vibration mode is a rigid-body mode without any damping. The damping ratio for the second vibration mode, which includes lateral structural deformation coupled with foundation-mat rotation, is a linear combination of ξ_v and ξ.

The response of the structure considered earlier, but now including damping in the structure as well as supporting elements, to normalized initial velocity $\bar{\dot{x}}(0) = 2$ is presented in Figure 2.8. From the selected values $\xi = 0.05$, and $\xi_v = 0.4$, equations 2.17 and 2.18 lead to $\xi_1 = 0.03$, $\xi_2 = 0.4$ and $\zeta_2 = 0.25$. If the foundation mat is bonded to the supporting elements and its uplift is thus prevented, the deformation u and base rotation θ decay exponentially at a rate defined only by the first mode damping ratio ξ_1, because the second mode does not contribute to these response quantities.

Several observations regarding the effects of damping can be made by comparing the responses of the structure, with uplift of the foundation mat permitted, in Figures 2.5 and 2.8 : The tendency of the foundation mat to uplift, is reduced, resulting in the uplift duration decreasing with each vibration cycle; after a few cycles the foundation mat remains in a continuous contact with the supporting elements and the responses u, θ and x decay exponentially at a rate controlled by ξ_1. The vibratory term in the response during the time one edge is uplifted (equation 2.14) decays exponentially at a rate defined by ζ_2, which in this case is large and results in a quick decay of the high-frequency oscillations in u about the u_c value, and the maximum deformation is essentially equal to u_c. The corresponding high-frequency effects in the other responses also disappear.

Based on the above discussion and numerical results of Figure 2.8, we can examine the dependence of damping effects on the normalized initial velocity $\bar{\dot{x}}(0)$. If $\bar{\dot{x}}(0)$ exceeds 1 only slightly, the foundation mat will uplift from its supporting elements only for relatively short durations of time; for most of the time, neither edge of the foundation mat will uplift. The

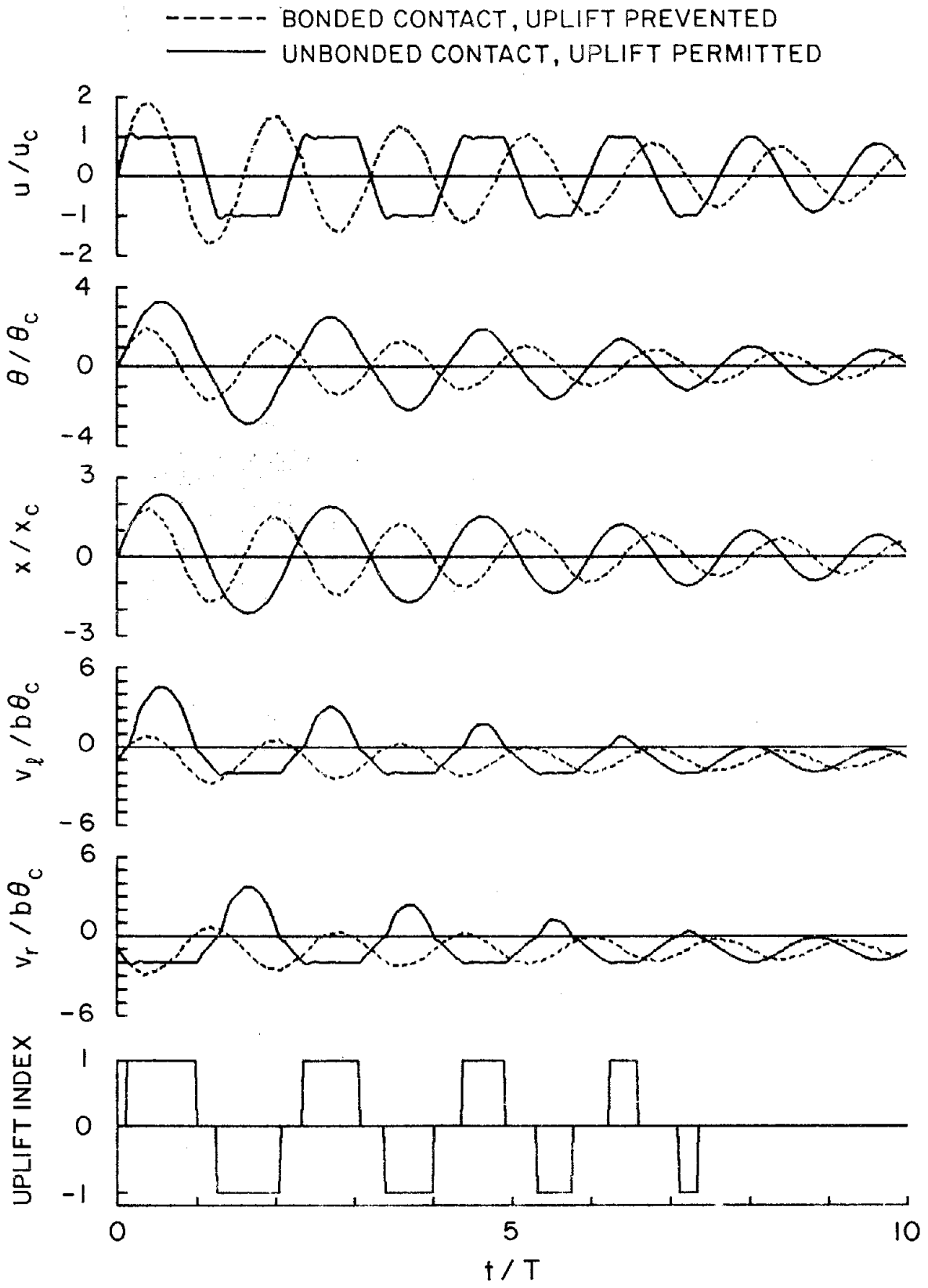

FIGURE 2.8 Response of a damped structure ($\xi = 0.05$, $\xi_v = 0.4$, $\alpha = 10$, $\beta = 8$, $\gamma = 0$) to initial velocity $\bar{x}(0) = 2$, for two conditions of contact between the foundation mat and the supporting elements: (a) Bonded contact preventing uplift, and (b) Unbonded contact only through gravity with uplift permitted.

response of the structure will therefore be dominated by equation 2.15. The second mode does not contribute to the structural deformation, which will therefore decay exponentially at a rate controlled by the damping ratio ξ_1 for the first mode. As discussed earlier, this damping ratio is a linear combination of ξ and ξ_v.

If the normalized initial velocity $\bar{\dot{x}}(0)$ is much larger than 1, the foundation mat will remain in contact with its supporting elements only for a small fraction of a vibration cycle, too short to cause any significant decay of response. The left or right edge of the foundation mat will be uplifted during a major part of a vibration cycle. In this condition, the rotation and vertical displacement of the foundation mat are primarily due to the undamped rigid-body mode. The high-frequency ($= \lambda_2$) contributions to the structural deformation and vertical displacements at the edges of the foundation mat (Figure 2.5) essentially disappear due to damping (Figure 2.8), because they are due to the second mode (equation 2.14) which has a modal damping ζ_2. For typical parameter values, λ_2 is several times higher than the overall frequency, thus several vibration cycles of the second mode occur during each uplift phase (Figure 2.5). The number of cycles is sufficient to essentially eliminate this high frequency response for a wide range of values of damping and other structural parameters. Considering that the rigid body mode is undamped and the high frequency response is eliminated by damping, the structural deformation response is insensitive to the damping values ξ and ξ_v if $\bar{\dot{x}}(0)$ is significantly larger than 1. This conclusion is supported by numerical results not presented here.

2.5 Analysis Procedure

The response of the system of Figure 2.1 to specified ground motion can be analyzed by numerical solution of the equations of motion (equation 2.2). These equations are nonlinear as indicated by the dependence of the coefficients ϵ_1 and ϵ_2 on whether one or both edges of the foundation mat are in contact with the supporting elements. For each of the three contact conditions -- contact at both edges, left edge uplifted, and right edge uplifted -- the governing equations are linear, but they depend on the contact condition. Thus, during the time duration

that one particular contact condition is valid, the system behaves as a linear system, but vibration properties of the linear system are different for the three contact conditions. Thus, at any time, the numerical analysis of response over the next time-increment consists of two steps: (1) determining the contact condition valid for that time increment, and (2) solution of the equations of motion with the corresponding values for ϵ_1 and ϵ_2.

As mentioned earlier, for each contact condition the linear system has three degrees-of-freedom and the natural frequency of the third mode is at least an order of magnitude higher than the second mode frequency, and it tends to infinity as the mass of the foundation-mat approaches zero (Section C.2, Appendix C). Because the time-increment employed in numerical analysis of response is controlled by the vibration frequency of the highest mode, very short time increments must be used to accurately represent the contributions of the third mode. Because its frequency is at least an order of magnitude higher than that of the second mode, the time-increment would be so short to be almost impractical. Fortunately, the contribution of the third mode to the response of each of the three linear systems (corresponding to the three contact conditions) is negligible (Section C.3, Appendix C). By eliminating the effects of this high frequency mode in the numerical analysis, the time increment will be controlled by the natural frequencies of the first two vibration modes.

The obvious procedure to eliminate the high frequency effects is to express the structural displacements as a linear combination of the first two vibration modes of the system for the appropriate contact condition. However, this approach has the disadvantage that the choice of the time-varying modal coordinates depends on the contact condition. The more convenient approach is to transform the equations of motion to a set of displacements that can be used for all contact conditions. To this end the rotation θ is expressed in terms of u and v from equation 2.5:

$$h\theta = \frac{1}{\epsilon_1}\left[\frac{k}{k_f}\left(\frac{h}{b}\right)^2 u - \epsilon_2\left(\frac{h}{b}\right)v\right] \tag{2.19}$$

The displacement vector can therefore be expressed as

$$\begin{Bmatrix} u \\ h\theta \\ v \end{Bmatrix} = \begin{bmatrix} 1 & 0 \\ \frac{1}{\epsilon_1}\frac{k}{k_f}\left(\frac{h}{b}\right)^2 & -\frac{\epsilon_2}{\epsilon_1}\left(\frac{h}{b}\right) \\ 0 & 1 \end{bmatrix} \begin{Bmatrix} u \\ v \end{Bmatrix} \tag{2.20a}$$

or,

$$\mathbf{r} = \mathbf{T}\,\bar{\mathbf{r}} \tag{2.20b}$$

Substituting the transformation of equation 2.20 into equation 2.2 and premultiplying both sides by the transpose of the transformation matrix T leads to a reduced system of two differential equations in the two unknown u and v.

The eigenvalue problem associated with the reduced system of two differential equations was solved. The resulting natural frequencies and shapes of the two vibration modes were compared with the 'exact' values for the lower two modes, obtained from analysis of the original 3-DOF eigenvalue problem. The agreement was found to be excellent over a wide range of the system parameters γ, α and β (Section C.3, Appendix C). Thus the reduced system of equations accurately retains the vibration properties of the lower two vibration modes, while eliminating the high-frequency third mode.

The reduced system of equations is integrated numerically using an implicit method with linear variation of acceleration in each time-step. Appropriate governing equations are used, consistent with the contact condition at the beginning of the time-step. Appropriate modifications are incorporated if the contact condition changes during a time-step (Appendix D). By eliminating the high-frequency, third vibration mode it was possible to employ a much larger integration time-step than would otherwise be practical. The integration time-step

$\Delta t = 0.01$ sec. used in this investigation is ten times longer than that necessary to accurately solve the original equations of motion [1], resulting in considerable saving in computational effort.

The procedure described above to eliminate the contributions of the high-frequency, third vibration mode may be viewed as an application of the classical Rayleigh-Ritz method, wherein the two Ritz vectors are described by the columns of the transformation matrix T. If the foundation mat is massless, this procedure is equivalent to the static condensation approach outlined in Section 2.2.

2.6 Earthquake Responses

The response of a structural system to the north-south component of the El Centro, 1940, ground motion computed by the numerical procedures described in Section 2.5 is presented in Figure 2.9. Responses are shown for two conditions of contact between the foundation mat and the supporting spring-damper elements: (a) bonded contact preventing uplift and (b) unbonded contact only through gravity with uplift permitted. In the first case, the structural response is entirely due to the first natural vibration mode of the system with both edges of the foundation mat in contact with the supporting elements (see Section 2.3). Thus the response behavior is similar to a SDOF system. When uplift of the foundation mat is permitted, the response behavior is much more complicated. During the initial phase of the ground shaking, both edges of the foundation mat remain in contact with the supporting elements. As the ground motion intensity builds up, the two edges of the foundation mat alternately uplift in a vibration cycle. In this example uplift occurs every vibration cycle during the strong phase of ground shaking, with the duration of uplift depending on the amplitudes of foundation mat rotation. As the intensity of ground motion decays toward the later phase of the earthquake, the foundation mat no longer uplifts, and both edges remain in contact with the supporting elements.

The effects of foundation-mat uplift on the maximum response of the structure due to

earthquake ground motion are similar to those observed in Section 2.4 during free vibration. The maximum deformation of the structure is very close to u_c (equation 2.11a) when foundation-mat uplift is permitted, which is a significant reduction compared to the response when foundation-mat uplift is prevented. Because of damping, the small-amplitude oscillations at the frequency λ_2 (Figure 2.5) damp out and are not present in the earthquake response results of Figure 2.9. The rotation of the foundation mat and vertical displacements of the two edges of the foundation mat are significantly increased due to the rigid body rocking mode of the system, permitted by uplift. This mode provides the dominant contribution to these responses during uplift but does not affect the structural deformation.

In order to study the effects of foundation-mat uplift on the maximum response of structures, response spectra are presented. The base shear coefficient

$$V_{\max} = \frac{\mathbf{V}_{\max}}{w} = \frac{ku_{\max}}{mg} = \left(\frac{2\pi}{T}\right)^2 \frac{u_{\max}}{g} \tag{2.21}$$

where $\mathbf{V}_{\max}$ is the maximum base shear and w is the weight of the superstructure, is plotted as a function of the natural vibration period of the corresponding rigidly supported structure. For each set of system parameters α, β, γ, ξ and ξ_y, such a response spectrum plot is presented for two conditions of contact between the foundation mat and the supporting spring-damper elements: (a) bonded contact preventing uplift, and (b) unbonded contact only through gravity with uplift permitted. Also presented are the results for the corresponding rigidly supported structure, which is simply the standard pseudo-acceleration response spectrum, normalized with respect to gravitational acceleration. Included in the response spectra plots is V_c, the critical base shear coefficient associated with the maximum value of base shear, $\mathbf{V}_c$, obtained from static considerations (equation 2.1a):

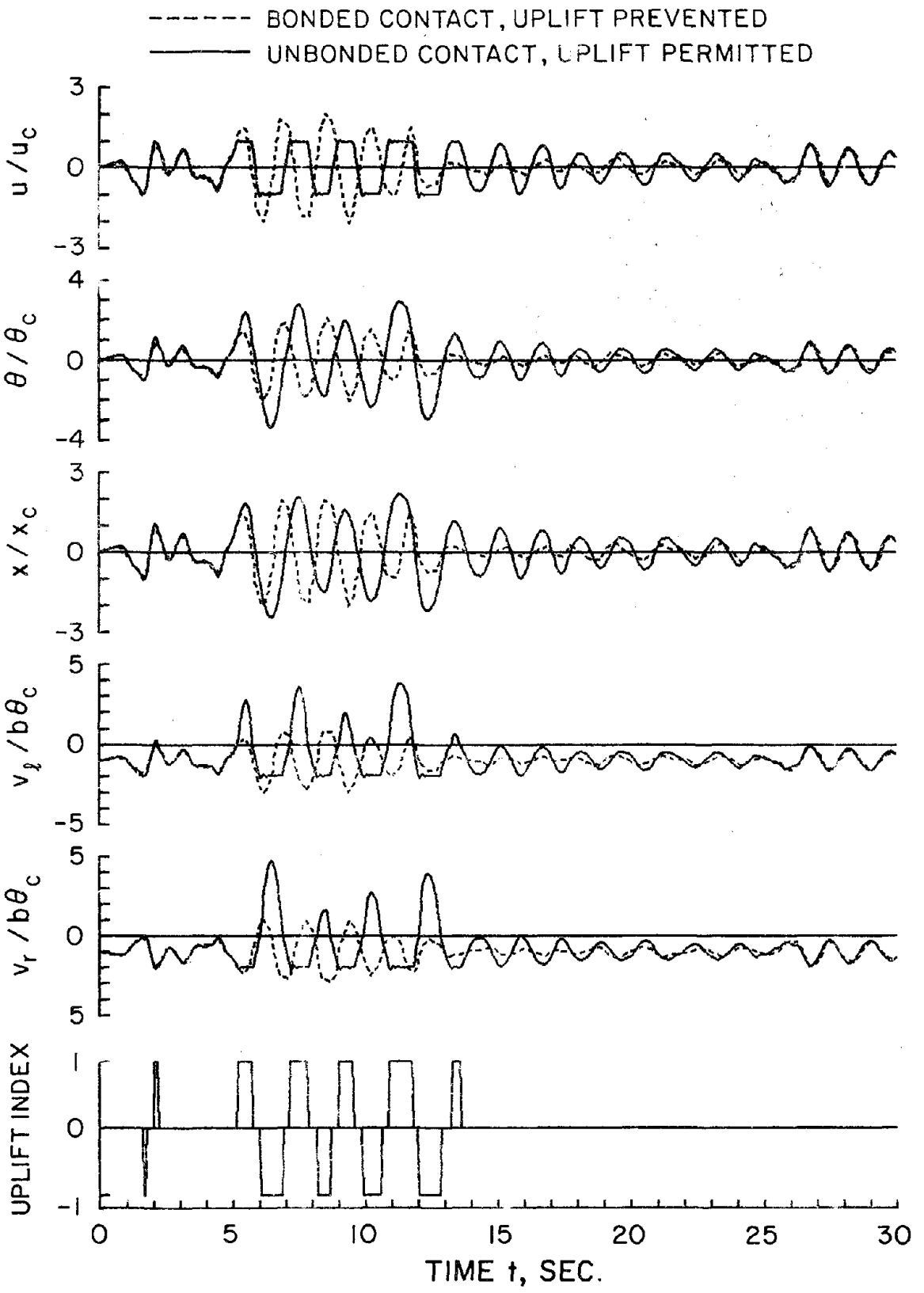

FIGURE 2.9 Response of a structure ($\alpha = 10$, $\beta = 8$, $\gamma = 0$, $T = 1$ sec., $\xi = 0.05$, $\xi_v = 0.4$) to El Centro ground motion for two conditions of contact between the foundation mat and the supporting elements: (a) Bonded contact preventing uplift, and (b) Unbonded contact only through gravity with uplift permitted.

$$V_c = \frac{\mathbf{V}_c}{w} = \frac{1+\gamma}{\alpha} \tag{2.22}$$

This critical base shear coefficient depends on the mass ratio γ and slenderness-ratio parameter α, but is independent of the vibration period T.

The response spectra presented in Figure 2.10 are for systems with massless foundations ($\gamma = 0$) and a fixed set of system parameters α, β, ξ, and ξ_v subjected to the El Centro ground motion. The differences between the response spectra for the two linear systems, the structure with foundation mat bonded to the supporting elements and the corresponding rigidly supported structure, are due to the change in period and damping resulting from support flexibility (equations 2.6 and 2.17). The base shear developed in structures with relatively long vibration periods is below the critical value and the foundation mat does not uplift from its supporting elements. If foundation mat uplift is prevented, the maximum base shear at some vibration periods may exceed the critical values; for the selected system parameters and ground motion Figure 2.10 indicates that the critical value is exceeded for all vibration periods shorter than the period where the linear spectrum first attains the critical value. If the foundation mat of such a structure rests on the spring-damper elements only through gravity and is not bonded to these elements, uplift occurs and this has the effect of reducing the base shear. However, the base shear is not reduced to as low as the critical value based on static considerations (equation 2.1a). Although foundation-mat uplift is initiated at the time instant the base shear in a vibrating structure reaches the instantaneous dynamic critical value, depending on the state -- displacement, velocity and acceleration -- of the system the deformation and base shear may continue to exceed the critical values. Furthermore the dynamic, critical base shear may exceed the static critical value because the time-dependent vertical force p may exceed the gravity loads, see section 2.1. Because the base shear developed in linear structures (foundation-mat uplift prevented) tends to exceed the critical value by increasing margins as the vibration period decreases, the foundation mat of a shorter-period structure has a greater

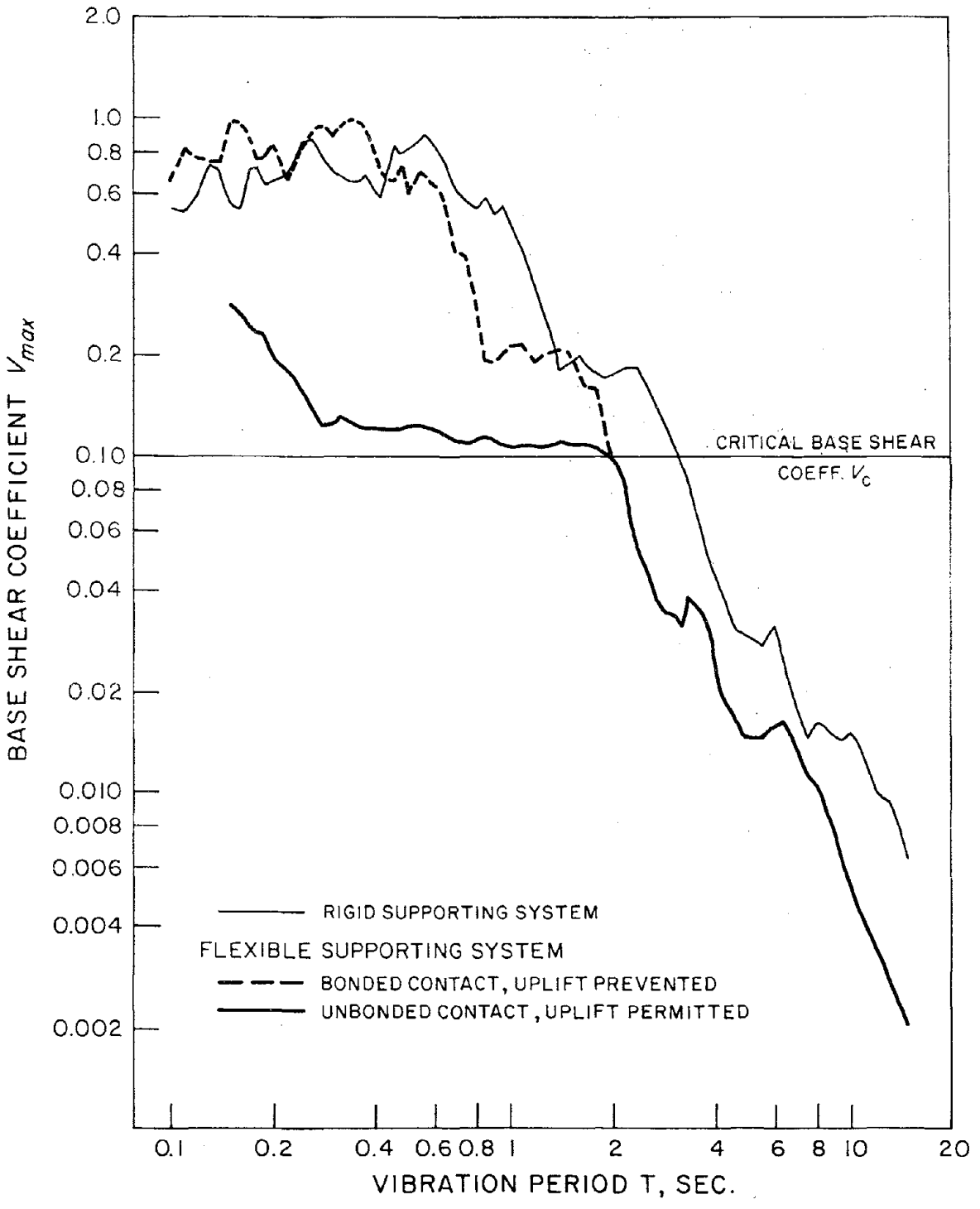

FIGURE 2.10 Response spectra for structures ($\alpha = 10$, $\beta = 8$, $\gamma = 0$, $\xi = 0.05$, $\xi_v = 0.4$) subjected to El Centro ground motion for three support conditions.

tendency to uplift, which in turn causes the critical base shear to be exceeded by a greater margin, although it remains well below the linear response.

The effects of ground motion intensity on the dynamic response of structures is displayed in Figure 2.11, wherein the response spectra for El Centro ground motion amplified by a factor of 2 are compared with the corresponding plots for the unscaled ground motion. If the foundation mat is bonded to the supporting elements and it can not uplift, the structural system is linear and the response spectrum is amplified by the same factor of 2. However, the response of a structure with foundation mat permitted to uplift is controlled by the critical base shear coefficient V_c which is a property of the system, independent of the ground motion intensity. Thus, the base shear is increased only slightly although the earthquake intensity is doubled. Because the base shear attains its critical value at a slightly longer period when earthquake intensity is increased, uplift of the foundation mat is initiated at a slightly longer period.

The response spectra presented in Figure 2.12 are for two values of the frequency ratio β with all other system parameters kept constant. As mentioned earlier, the differences in the response spectra for the two linear systems, the structure with foundation mat bonded to the supporting elements and the corresponding rigidly supported structure, are due to the change in period and damping resulting from support flexibility (equations 2.6 and 2.17). The period change appears as a shift in the response spectrum to the left, with larger shift for smaller values of β, i.e. for the more flexible supporting elements. The nonlinear response spectrum for the structure with foundation mat permitted to uplift shifts similarly to the left, with uplift initiated at longer periods as β increases. But for the period shift, the shape of the linear as well as nonlinear response are affected little by the frequency ratio β.

As presented in equation 2.22, the critical base shear coefficient is inversely proportional to the slenderness-ratio parameter α. This would suggest that maximum base shear will be smaller for relatively slender structures, which is confirmed by response spectra presented in Figure 2.13. The foundation mat of a slender structure has a greater tendency to uplift

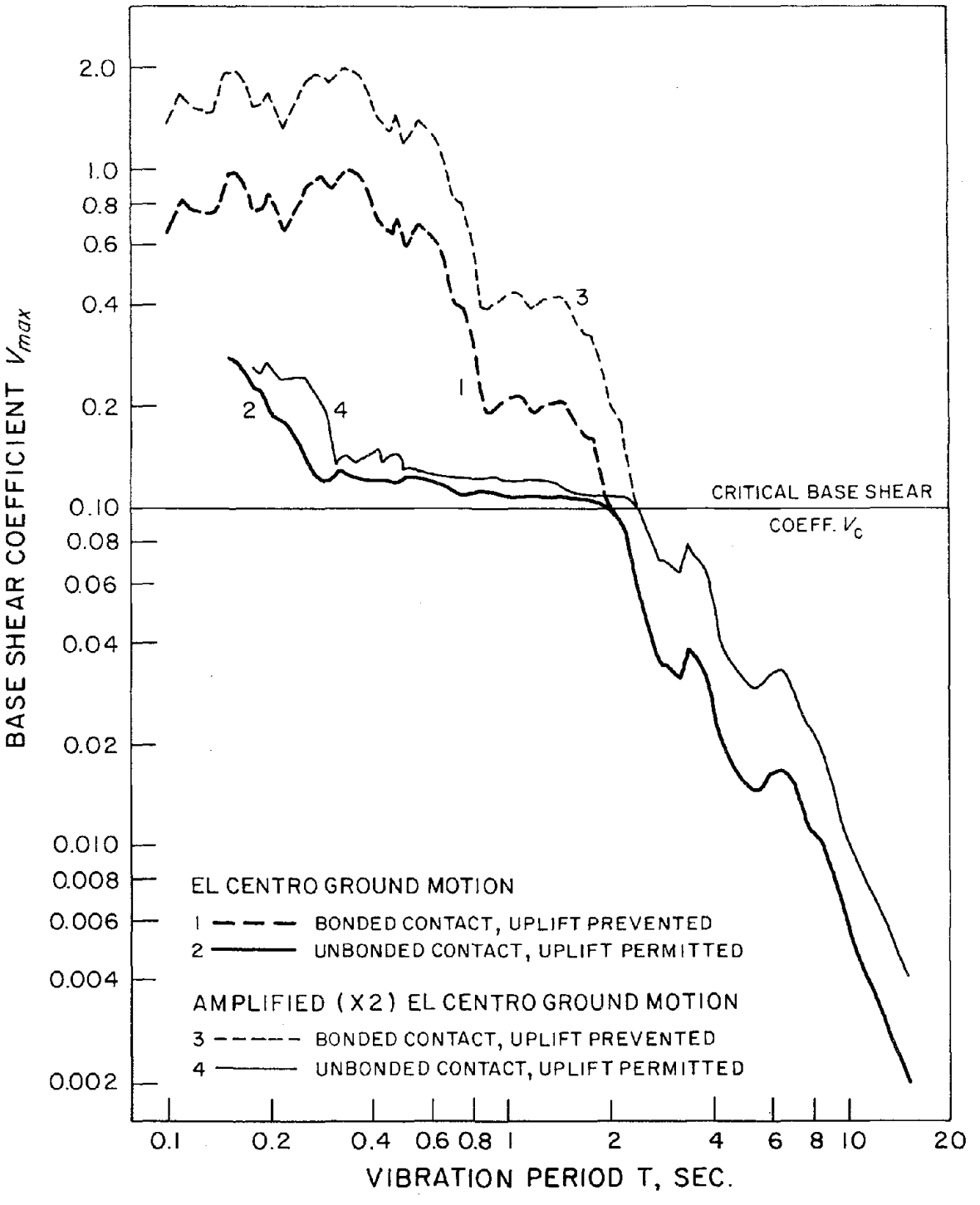

FIGURE 2.11 Effects of ground motion intensity on response spectra for structures ($\alpha = 10$, $\beta = 8$, $\xi = 0.05$, $\xi_v = 0.4$).

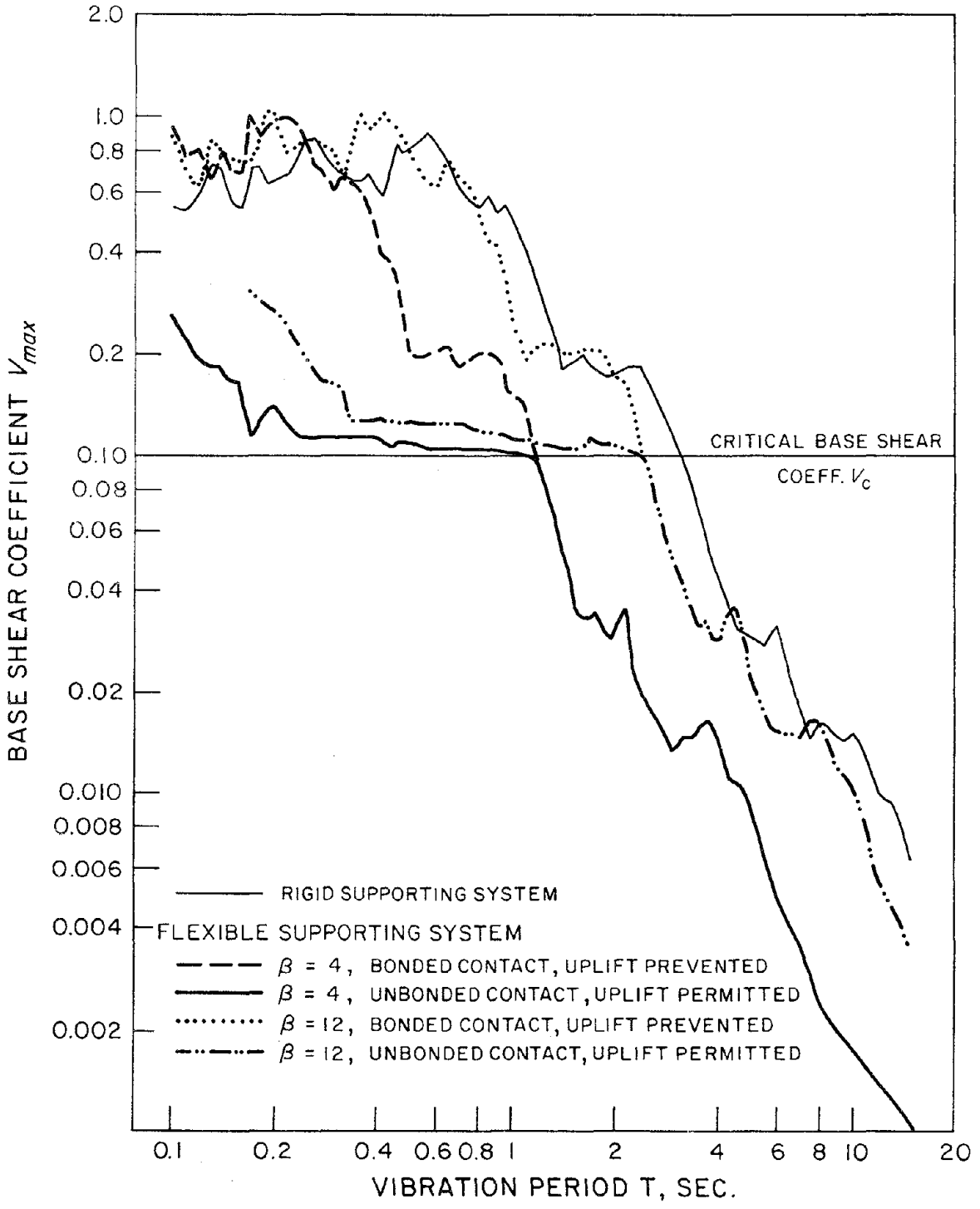

FIGURE 2.12 Response spectra for structures ($\alpha = 10$, $\gamma = 0$, $\xi = 0.05$, $\xi_v = 0.4$) subjected to El Centro ground motion for two values of frequency ratio $\beta = 4$ and 12.

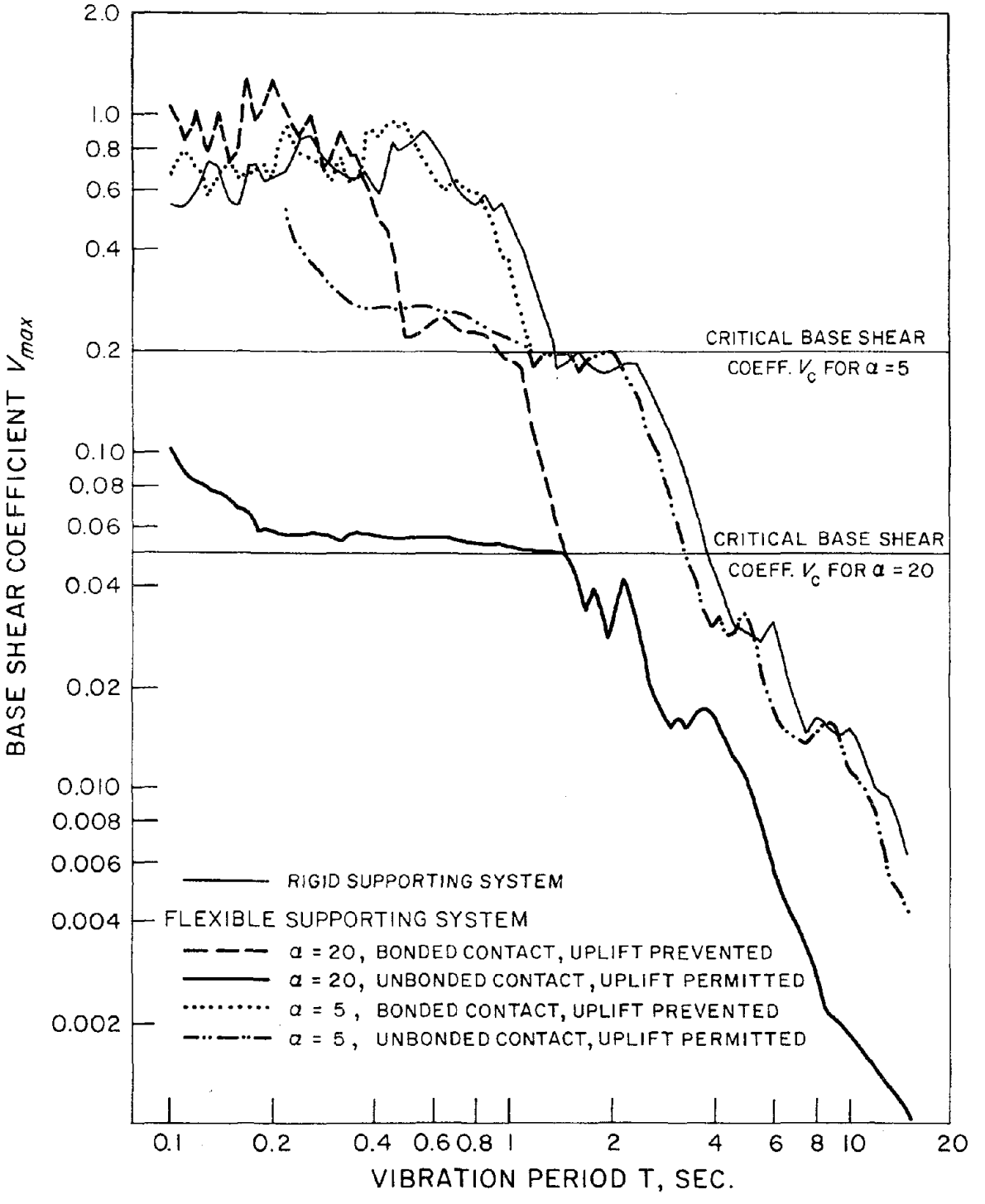

FIGURE 2.13 Response spectra for structures ($\beta = 8$, $\gamma = 0$, $\xi = 0.05$, $\xi_v = 0.4$) subjected to El Centro ground motion for two values of slenderness ratio parameter $\alpha = 5$ and 20.

resulting in greater reductions in the base shear. Uplift of the foundation mat occurs at all vibration periods shorter than the period where the linear response spectrum attains the critical value. This period depends on the slenderness ratio α in a complicated manner, because the critical base shear coefficient as well as the period shift of the linear response spectrum (relative to the standard pseudo-acceleration spectrum) both depend on α. For relatively slender structures the critical base shear coefficient is smaller (equation 2.22), but the period shift is larger (equation 2.6).

The critical base shear coefficient increases with mass ratio γ as indicated by equation 2.22; for systems with massless foundation mat ($\gamma = 0$) this coefficient is $1/\alpha$ and it increases to $2/\alpha$ for systems with equal foundation-mat and structural masses ($\gamma = 1$). The response spectra for these two mass ratios are presented in Figure 2.14 which indicate that the effects of foundation-mat mass are to reduce the short period range over which the foundation mat uplifts; to approximately double the maximum base shear over this period range; and to introduce a period shift in the linear response spectrum, with little influence on the shape of the spectrum.

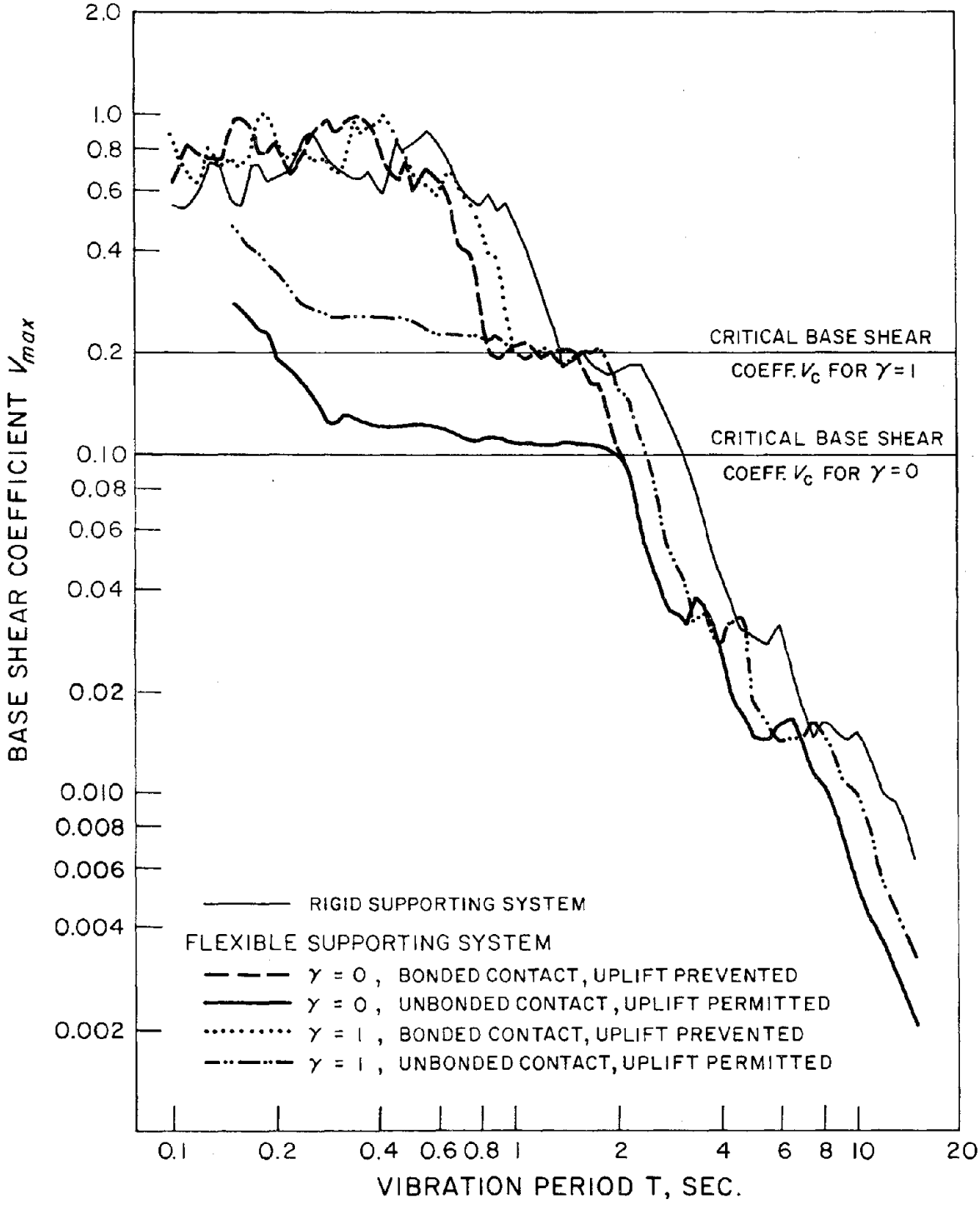

FIGURE 2.14 Response spectra for structures ($\alpha = 10$, $\beta = 8$, $\xi = 0.05$, $\xi_\nu = 0.4$) subjected to El Centro ground motion for two values of mass ratio $\gamma = 0$ and 1.

3. STRUCTURE ON WINKLER FOUNDATION

3.1 System Considered

The effects of transient foundation uplift on the dynamics of the simplest possible structural system were studied in Chapter 2 wherein the foundation mat was supported on two spring-damper elements, one at each edge. In order to make the supporting system more representative of actual conditions, the two spring-damper elements are replaced by a continuous series of elements resulting in the well known Winkler foundation.

The resulting system shown in Figure 3.1 consists of a linear structure of mass m , lateral stiffness k and lateral damping c, which is supported through the foundation mat of mass m_o resting on a Winkler foundation, with spring-damper elements distributed over the entire width of the foundation mat, connected to the base which is assumed to be rigid. The column(s) is (are) assumed to be massless and axially inextensible, the foundation mat is idealized as a rigid rectangular plate of negligible thickness with uniformly distributed mass, and it is presumed that horizontal slippage between the mat and supporting elements is not possible. The mass and damping coefficient of the foundation model are assumed constant, independent of displacement amplitude or excitation frequency. Thus the frequency dependence of these coefficients, as for a viscoelastic half space [11], is not recognized; nor is the strain dependence of these coefficients for soils [12] considered in this study.

Prior to the dynamic excitation, the foundation mat rests on the Winkler spring-damper elements only through gravity and is not bonded to these supporting elements. Thus the supporting elements can provide an upward force to the foundation mat but not a downward pull. During vibration of the system this upward resultant reaction force will vary with time. At any instant of time when one edge of the foundation mat reaches the natural unstressed level of the spring elements, that edge is in the condition of incipient uplift from the supporting elements. As the upward displacement of that edge continues, an increasing portion of the foundation mat uplifts from the supporting elements.

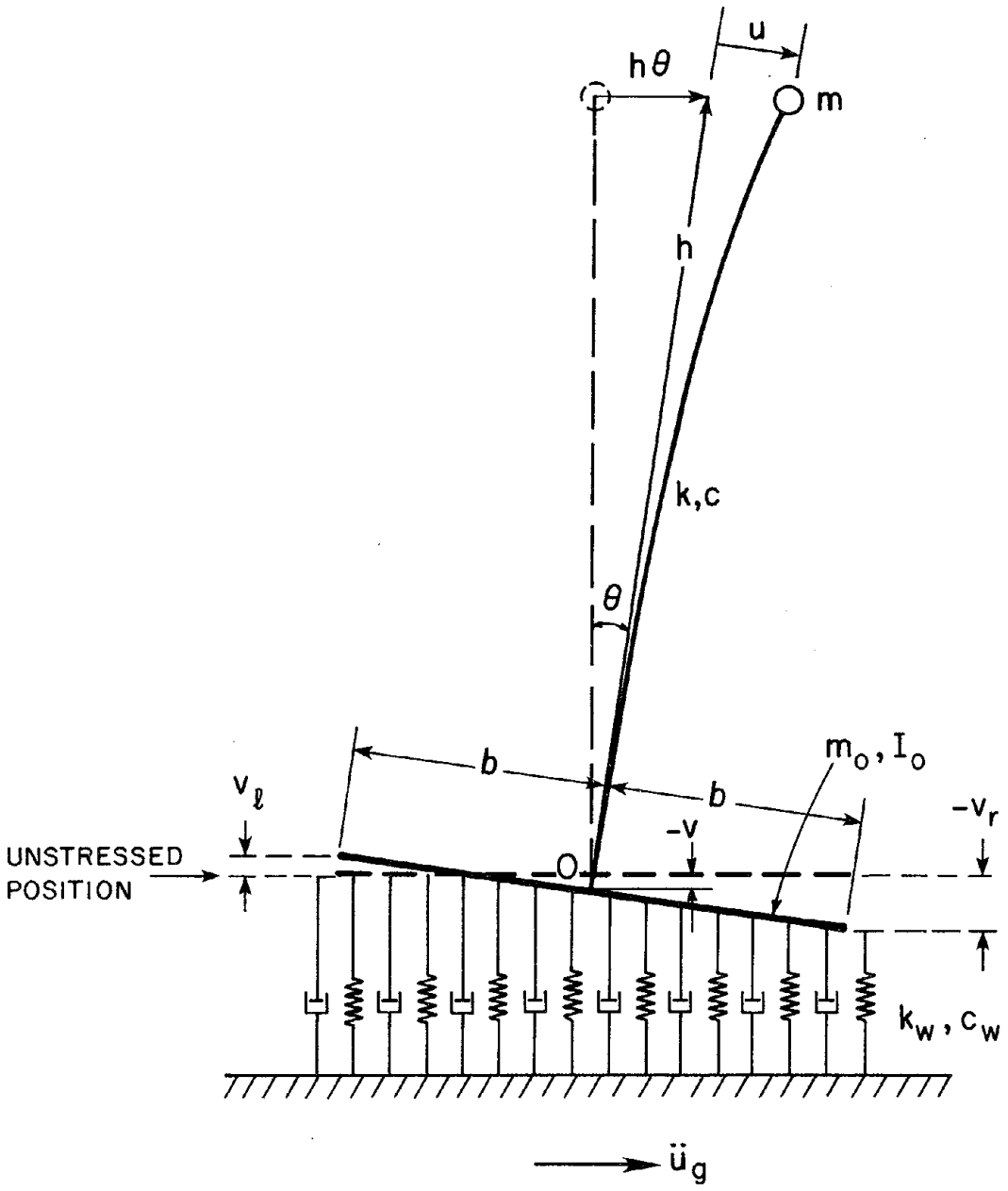

FIGURE 3.1 Flexible structure on Winkler foundation.

In particular, if the dampers are absent, the relation between the displacement and reaction force per unit width of the foundation mat is shown in Figure 3.2a. The upward reaction force is related linearly to the downward displacement through k_w, the spring stiffness per unit width, but no reaction force is developed if the displacement is upward; the displacements are measured from the unstressed position of the springs. If the foundation mat were bonded to the supporting elements the force-displacement relation will be linear, as shown in Figure 3.2a, valid for downward as well as upward displacements.

Consider the foundation mat and its supporting elements without the superstructure with a static force p acting in the downward direction at its center of gravity (c.g). The relation between the static moment M applied at the c.g and the resulting foundation-mat rotation θ, limited to angles much smaller than the slenderness ratio b/h, is shown in Figure 3.2b for unbonded as well as bonded conditions. If the mat is not bonded to the supporting elements the $M-\theta$ relation is linear, implying constant rotational stiffness, until one edge of the foundation mat uplifts from the supporting elements; thereafter the rotational stiffness decreases monotonically with increasing θ, which implies an expanding foundation-mat width over which uplift occurs. Uplift is initiated when the rotation reaches $\theta_u = p/2k_w b^2$ with the corresponding moment $M_u = pb/3$. The $M-\theta$ curve asymptotically approaches the critical moment, $M_c = pb$, corresponding to uplift of the entire foundation mat from the supporting elements except for one edge. The downward force is $p = (m + m_o)g$, the combined weight of the superstructure and foundation mat, prior to any dynamic excitation, but would vary with time during vibration.

Next consider the entire structural system with a gradually increasing force f_s applied in the lateral direction. If the foundation mat is bonded to the supporting elements, which along with the structure have linear properties, the lateral force can increase without limit if the overturning effects of gravity forces are neglected. However, if the mat is not bonded to the supporting elements, one edge of the foundation mat is at incipient uplift when the lateral force reaches $f_{su} = (m + m_o)g\frac{b}{3h}$. Thus the corresponding base shear at incipient uplift under

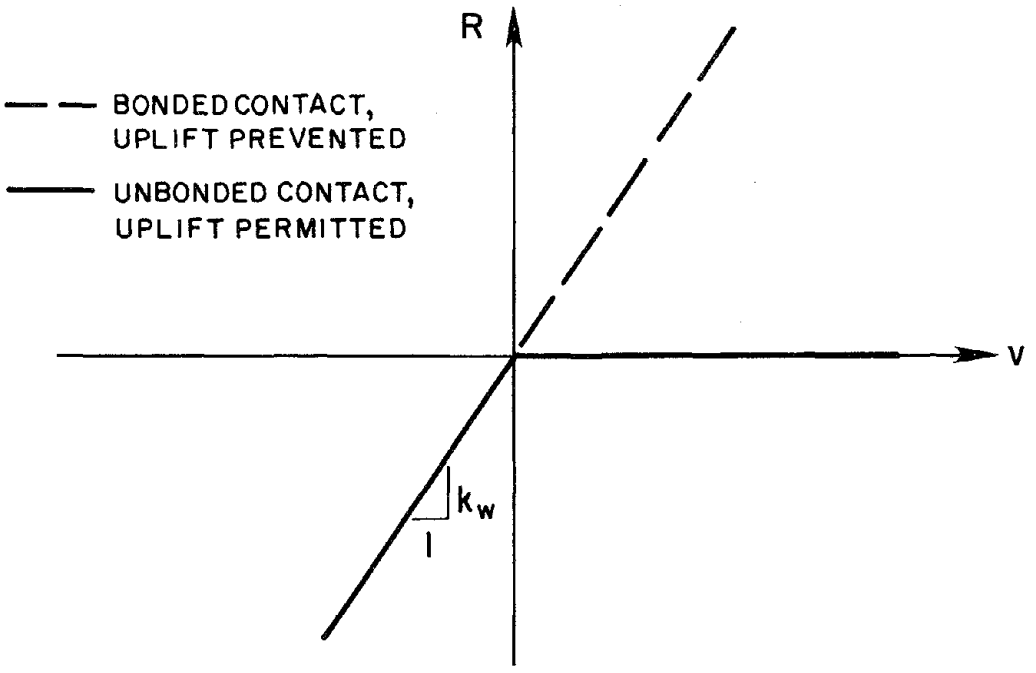

(a) Reaction force-displacement relation for unit width of the supporting elements

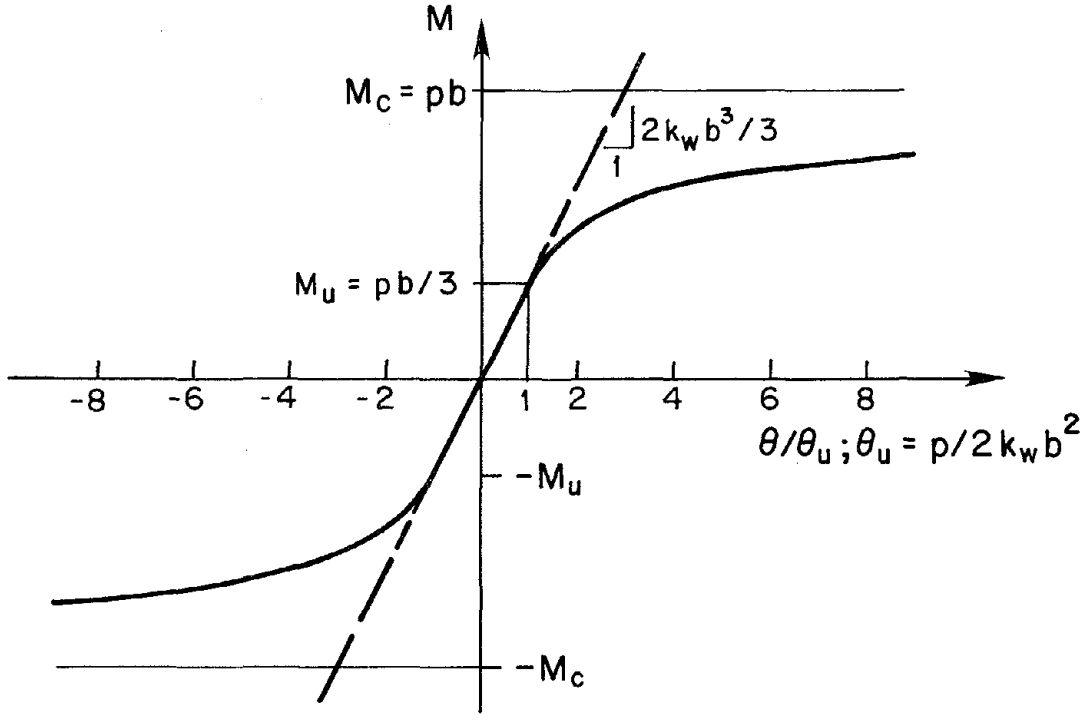

(b) Moment-rotation relation for foundation mat

FIGURE 3.2 Properties of Winkler foundation.

the action of static force is

$$\mathbf{V_u} = (m + m_o)\, g\, \frac{b}{3h} \tag{3.1a}$$

The structural deformation associated with this base shear is

$$u_u = \frac{(m + m_o)\, g}{k}\, \frac{b}{3h} \tag{3.1b}$$

and the corresponding foundation-mat rotation

$$\theta_u = \frac{(m + m_o)\, g}{2k_w b^2} \tag{3.1c}$$

which is consistent with the preceding paragraph and Figure 3.2b.

As the lateral force continues to increase beyond f_{su}, the lateral force corresponding to incipient uplift, the foundation mat separates over increasing width from its supporting elements. Finally when the lateral force reaches $f_{sc} = (m + m_o)\, g\, \frac{b}{h}$ the separation extends to the entire width and the contact is reduced to one edge. Thus the maximum base shear that can be developed under the action of static forces is

$$\mathbf{V_c} = (m + m_o)\, g\, \frac{b}{h} \tag{3.1d}$$

The structural deformation due to this base shear is

$$u_c = \frac{(m + m_o)\, g}{k}\, \frac{b}{h} \tag{3.1e}$$

The base excitation is specified by the horizontal ground motion with displacement $u_g(t)$ and acceleration $\ddot{u}_g(t)$. The vertical component of ground motion is not considered in this study.

Under the influence of this excitation the foundation mat would rotate through an angle $\theta(t)$ and undergo a vertical displacement $v(t)$, defined at its c.g relative to the unstressed position. Prior to the dynamic excitation, the vertical displacement is $v_s = (m + m_o)\, g / 2k_w b$, the static displacement due to the total weight of the superstructure and foundation mat. During the dynamic excitation, the vertical displacement v will remain constant at the initial static value if the foundation mat is bonded to the supporting elements, but it will vary with time in the unbonded case.

The displaced configuration of the structure at any instant of time can be defined by the deformation $u(t)$, foundation-mat rotation $\theta(t)$, and vertical displacement $v(t)$ at the center of gravity of the foundation mat.

3.2 Equations of Motion

The differential equations governing the small-amplitude motion of the system of Figure 3.1 can be derived by considering the lateral equilibrium of forces acting on the structural mass m, and moment and vertical equilibrium of forces acting on the entire system (Appendix B). Assuming that the structural-foundation system and the excitation are such that the amplitudes of the resulting displacement and rotation responses are small so that $\sin\theta$ and $\cos\theta$ can be approximated by θ and 1, respectively, these equations may be expressed as

$$m\ddot{u} + m(h\ddot{\theta}) + c\dot{u} + ku = -m\ddot{u}_g(t) + \frac{m(u + h\theta)}{h}(\ddot{v} + g) \tag{3.2a}$$

$$\frac{m_o b^2}{3h^2}(h\ddot{\theta}) - c\dot{u} + (1 + \epsilon_1^3)\, c_w \frac{b^3}{3h^2}(h\theta) + (1 - \epsilon_1^2)\, \epsilon_2 c_w \frac{b^2}{2h}\dot{v}$$

$$- ku + (1 + \epsilon_1^3)\, k_w \frac{b^3}{3h^2}(h\theta) + (1 - \epsilon_1^2)\, \epsilon_2 k_w \frac{b^2}{2h} v = 0 \tag{3.2b}$$

$$(m + m_o)\,\ddot{v} + (1 + \epsilon_1)\,c_w b\dot{v} + (1 - \epsilon_1^2)\,\epsilon_2 c_w \frac{b^2}{2h}\,(h\dot{\theta})$$

$$+ (1 + \epsilon_1)\,k_w bv + (1 - \epsilon_1^2)\,\epsilon_2 k_w \frac{b^2}{2h}\,(h\theta) = -(m + m_o)\,g \qquad (3.2c)$$

where contact coefficient ϵ_1 is equal to unity during full contact but depends continuously on foundation-mat rotation θ and vertical displacement v during partial uplift as follows:

$$\epsilon_1 = \begin{cases} 1 & \textit{contact at both edges} \\ \epsilon_2 v / b\theta & \textit{left or right edge uplifted} \end{cases} \qquad (3.3a)$$

and contact coefficient ϵ_2 depends on whether one or both edges of the foundation mat are in contact with the supporting elements:

$$\epsilon_2 = \begin{cases} -1 & \textit{left edge uplifted} \\ 0 & \textit{contact at both edges} \\ 1 & \textit{right edge uplifted} \end{cases} \qquad (3.3b)$$

The vertical displacements at the edges of the foundation mat, measured from the initial unstressed position, are

$$v_i = v \pm b\theta(t) \qquad i = l,r \qquad (3.4a)$$

Because the Winkler foundation cannot extend above its initial unstressed position an edge of the foundation mat would uplift at the time instant when

$$v_i(t) > 0 \qquad i = l,r \qquad (3.4b)$$

The foundations of most buildings are expected to undergo only small rotations and uplift displacements, so that complete separation of the foundation mat from its supporting elements is unrealistic, i.e. the vertical displacement $v_i(t)$ will be always less than zero at one of the edges of the foundation mat.

The earthquake response of the system depends on the following dimensionless parameters:

$\omega = \sqrt{k/m}$, the natural frequency of the rigidly supported structure

$\xi = c/2m\omega$, the damping ratio of the rigidly supported structure

$\beta = \omega_v/\omega$, where $\omega_v = \sqrt{2k_w b/(m + m_o)}$ is the vertical vibration frequency of the system of Figure 3.1 with its foundation mat bonded to the supporting elements

$\xi_v = 2c_w b/2(m + m_o)\omega_v$, the damping ratio in vertical vibration of the system of Figure 3.1 with its foundation mat bonded to the supporting elements

$\alpha = h/b$, a slenderness-ratio parameter

$\gamma = m_o/m$, the ratio of foundation mass to superstructure mass

The foundations of most buildings are expected to undergo only small rotations and uplift displacements, far short of overturning. At these small amplitude motions, and if $p-\delta$ effects represented by the second term in the right side of equation 3.2a are neglected, for a given excitation, the deformation response of the system depends on the slenderness parameter but not separately on the size. This can be shown by expressing the equations of motion and uplift criterion in terms of the above mentioned dimensionless parameters; the deformation response is seen to depend on h/b ratio but not separately on h. If we were to consider the large-amplitude motion of the structure including the possibility of its overturning, the size parameter h would play an important role. Similarly the size parameter would influence the small-amplitude response if $p-\delta$ effects are considered, but, as will be seen later, these effects appear to be insignificant for most buildings.

The equations of motion for the system of Figure 3.1 are nonlinear as indicated by the dependence of the coefficients ϵ_1 and ϵ_2 (equation 3.3) on whether the foundation mat is in full or partial contact with the supporting system; and on the degree of uplift.

The equations of motion can be specialized for the undamped system with massless foundation mat by substituting $m_o = 0$, and $c = c_f = 0$. In particular, the inertia and damping terms in equation 3.2b are zero and, following the usual approach to static condensation, θ can be expressed in terms of u and v from

$$-ku + (1 + \epsilon_1^3)\, k_w \frac{b^3}{3h^2}(h\theta) + (1 - \epsilon_1^2)\, \epsilon_2 \frac{b^2}{2h} v = 0 \tag{3.5}$$

and substituted into equations 3.2a and 3.2c. The reduced system consists of the resulting two differential equations in the two unknown dynamic degrees-of-freedom. As discussed later, this reduced system of equations provides a basis for approximate analysis of systems with damping and foundation-mat mass, i.e. $c \neq 0$, $c_f \neq 0$, and $m_o \neq 0$.

3.3 Equivalent Two-Element Foundation System

The equations of motion for the idealized one-story structure supported through a foundation mat resting on a Winkler foundation were presented in Section 3.2 and those for a two-element foundation in Section 2.2. If the foundation mat is bonded to the supporting elements the equations of motion for the structure supported on Winkler foundation are identical to those for the same structure on a two-element foundation with the following properties: $k_f = bk_w$, $c_f = bc_w$ and half base-width $= b/\sqrt{3}$. This two-element foundation is exactly equivalent to the Winkler foundation if uplift is not permitted.

Consider the foundation mat and its supporting elements without the superstructure with a static force p acting in the downward direction at the center of gravity (c.g). If the mat is not bonded to the supporting elements, the relation between the static moment M applied at the c.g and the resulting foundation-mat rotation is shown in Figure 3.3 for the two systems. The $M-\theta$ relation is linear with the same rotational stiffness for the two systems until θ reaches $\theta_u = p/2k_w b^2$ when one edge of the foundation mat on Winkler foundation is at incipient uplift. For larger rotation angles the $M-\theta$ relation for the two systems are different. The

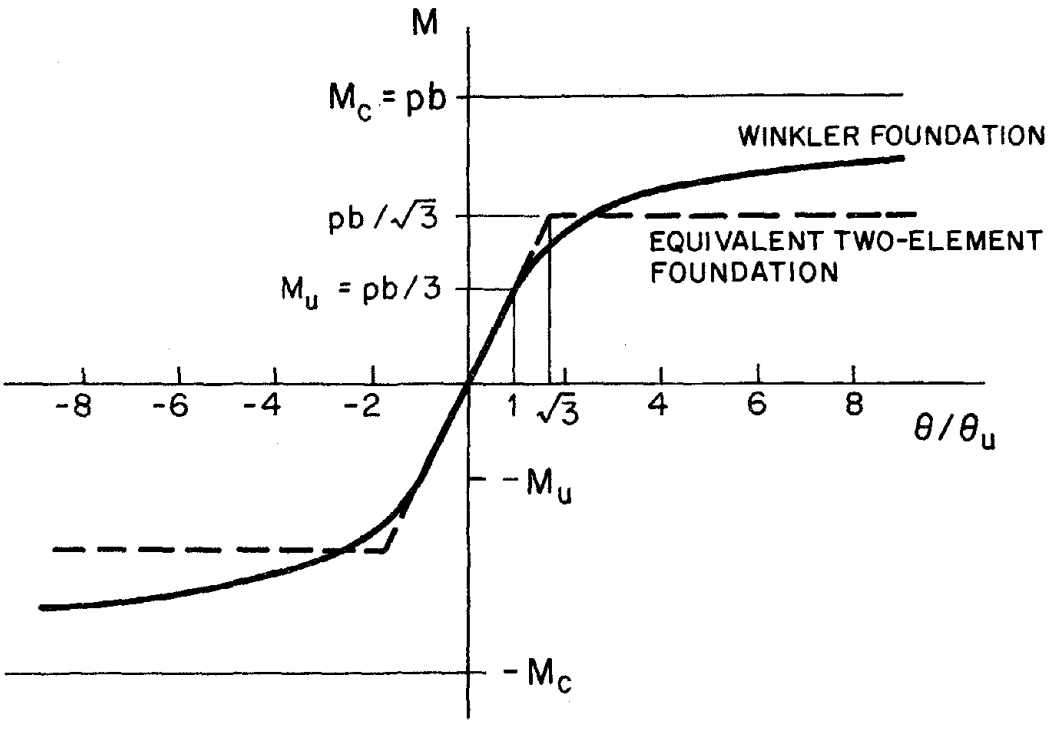

FIGURE 3.3 Moment-rotation relations for foundation mat on Winkler foundation and on equivalent two-element foundation.

constant rotational stiffness implied by the linear $M-\theta$ relation continues to apply for the equivalent two-element supporting system until θ reaches $\theta_u\sqrt{3}$ when one edge of the foundation mat uplifts from one of the supporting elements; thereafter no additional moment can be developed. On the other hand the $M-\theta$ relation for the Winkler supporting system is nonlinear for $\theta > \theta_u$ with the rotational stiffness decreasing monotonically with increasing θ. The $M-\theta$ curve asymptotically approaches the critical moment $M_c = pb$. Whereas the equivalent two-element supporting system is an exact representation of the Winkler foundation system for rotation angles $\theta < \theta_u$, it is at best an approximation if the ground motion is intense enough to cause significant uplift. Figure 3.3 suggests that the approximation is likely to deteriorate for the larger angles.

The parameters of a two-element foundation system, which is equivalent to the Winkler system after uplift, can also be determined. Because the width of the foundation mat in contact with Winkler foundation varies with time, the parameters of such an equivalent two-element system will be time-dependent. Constant parameter values were obtained by using the temporal average of the contact width during free vibration of the structure [1].

Thus, it is possible to establish relations between the parameters of the two-element and Winkler models so that the two models are equivalent for the two cases of full contact and uplift. However, if the structure vibrates in both states for significant portions of the response, neither of these parameter sets is expected to provide a good agreement between the responses of the two models. The two parameter sets have been combined to obtain general expressions valid for both regimes of response [1]. These expressions are based on free vibration response of the undamped structure and are not directly extendable to a damped structure subjected to arbitrary earthquake excitation. Consequently these general expressions for parameters of the equivalent two-element system are not utilized in this investigation. Instead the parameters defined earlier for the case of foundation mat bonded to the supporting elements are used.

3.4 Analysis Procedure

The response of the system of Figure 3.1 to specified ground motion can be analyzed by numerical solution of the equations of motion (equation 3.2). The equations are nonlinear as indicated by the dependence of the stiffness and damping coefficients on whether the foundation mat is in full contact with the supporting elements or it has partially uplifted; in the latter case, the coefficients depend continuously on ϵ_1 which is a measure of the contact width (equation 3.3). However, a linear system corresponding to any instantaneous contact condition of the foundation mat can be defined. This linear system has three degrees-of-freedom and the natural frequency of the third mode is at least an order of magnitude higher than the second mode frequency and it tends to infinity as the foundation-mat mass approaches zero. Because the contribution of the third mode to the instantaneous response of this linear system is negligible, it can be eliminated with the advantage that the integration time-step would not be controlled by the very short vibration period of the third mode.

The obvious procedure to eliminate the high frequency effects is to express the structural displacements as a linear combination of the first two vibration modes of the system for the instantaneous contact condition:

$$\begin{Bmatrix} u \\ h\theta \\ v \end{Bmatrix} = \begin{bmatrix} \psi_{11} & \psi_{12} \\ \psi_{21} & \psi_{22} \\ \psi_{31} & \psi_{32} \end{bmatrix} \begin{Bmatrix} Z_1 \\ Z_2 \end{Bmatrix} \tag{3.7a}$$

or

$$\mathbf{r} = \mathbf{\Psi Z} \tag{3.7b}$$

where the eigenvectors $\boldsymbol{\psi}_1$ and $\boldsymbol{\psi}_2$ depend continuously on the contact coefficient ϵ_1. Substituting this transformation into equation 3.2 and premultiplying both sides by the transpose of the transformation matrix $\mathbf{\Psi}$ leads to a reduced system of differential equations in the generalized coordinates Z_1 and Z_2. The stiffness and damping coefficients in the reduced equation system

are also continuous functions of the contact coefficient ϵ_1.

The reduced system of equations is integrated numerically using an implicit method with linear variation of acceleration in each time-step with dynamic equilibrium satisfied by iteration at the end of the time-step (Appendix D). Even though the high-frequency, third vibration mode was eliminated, the time-step used has to be short enough to ensure convergence within a few iteration cycles. The integration time-step used is $\Delta t = 0.001$ sec., ten times shorter than that employed for the system with two-element foundation.

3.5 Free Vibration Response

Before studying the response of the system of Figure 3.1 to complex ground motion such as earthquake excitation, it is useful to examine some features of the system in free vibration. Restricting this section to massless foundation mats, the response of undamped systems is studied first, followed by the effects of damping.

3.5.1 Undamped System

Starting with the initial state of the structural system of Figure 3.1 wherein the entire width of the foundation mat is in contact with the supporting elements, the response of the system to any initial displacements and velocities can be determined as the superposition of the free vibration responses in the two modes of vibration $\boldsymbol{\phi}_1$ and $\boldsymbol{\phi}_2$, which are similar to those described in equation 2.7 (Section C.1.2, Appendix C). The system vibrating in the second mode undergoes uncoupled vertical motion, without lateral deformation of the structure or rotation of the foundation mat. The motion of the system vibrating in the first mode consists of lateral deformation of the structure and rotation of the foundation mat without any vertical displacement at its c.g. In particular, if an initial velocity $\dot{x}(0)$ is imparted in the lateral direction to the mass m of the superstructure, the second vibration mode will not be excited and the response will be entirely due to the first mode. The structural displacement vector

$\mathbf{r}^T = < u \quad h\theta \quad v >$ is then described by

$$\mathbf{r}(t) = \frac{\dot{x}(0)}{\omega_1} \boldsymbol{\phi}_1 \sin \omega_1 t - v_s \boldsymbol{\phi}_2 \tag{3.8}$$

where

$$\omega_1 = \omega \bar{\omega}_1 \tag{3.9a}$$

$$\bar{\omega}_1 = \sqrt{\frac{\beta^2}{3\alpha^2 + \beta^2}} \tag{3.9b}$$

$$\boldsymbol{\phi}_1 = < \bar{\omega}_1 \quad (1 - \bar{\omega}_1^2) \quad 0 > \tag{3.9c}$$

and

$$\boldsymbol{\phi}_2 = < 0 \quad 0 \quad 1 > \tag{3.9d}$$

provided the motion is small enough that, over its entire width, the foundation mat remains in contact with the supporting elements. Equation 3.8 is of the same form as equation 2.10 which describes the initial free vibration motion of the two-element system. The structural displacements in the first mode at the point of incipient uplift of one edge of the foundation mat for the Winkler foundation are

$$u_u = \frac{g}{3\alpha\omega^2} \tag{3.10a}$$

and

$$h\theta_u = \frac{\alpha g}{\beta^2 \omega^2} \tag{3.10b}$$

These displacements are same as those presented in equations 3.1b and 3.1c specialized for massless foundation mat, which were obtained from static considerations.

The initial velocity $\dot{x}(0)_u$ that results in the maximum displacement $\mathbf{r}(t)$, from equation 3.8, equal to the displacements given by equation 3.10 is given by

$$\dot{x}(0)_u = \frac{\sqrt{3\alpha^2+\beta^2}}{3\alpha\beta}\frac{g}{\omega} \tag{3.11}$$

and it depends on the slenderness-ratio parameter α and frequency ratio β. For purposes of the subsequent discussion it is useful to introduce the normalized initial velocity

$$\bar{\dot{x}}(0) = \dot{x}(0)/\dot{x}(0)_u \tag{3.12}$$

If the initial velocity is less than $\dot{x}(0)_u$, i.e. $\bar{\dot{x}}(0) < 1$, both edges of the foundation mat will remain in contact with the supporting elements and no uplift will occur; the free vibration response will be described by equation 3.8.

If the initial velocity exceeds $\dot{x}(0)_u$, i.e., $\bar{\dot{x}}(0) > 1$, equation 3.8 will be valid only until the first uplift occurs. One edge of the foundation mat will begin to uplift from its supporting elements at the time instant $u(t)$ given by equation 3.8 reaches the incipient-uplift value of equation 3.10a. Uplift of the foundation mat from the supporting elements will gradually continue to extend over increasing width with the maximum uplifted width depending on the magnitude of the normalized initial velocity $\bar{\dot{x}}(0)$; then followed by a gradual decrease in the uplifted width until full contact is re-established. During the time duration that this edge remains uplifted, unlike the two-element system where motion is governed by a linear differential equation with solution consisting of constant and harmonic vibration parts (equation 2.14), the displacement response is nonlinear and no analytical expression for the solution is possible and we must resort to numerical computations. Measuring time t' from the instant when full base contact is re-established, the response of the structure during the time span it continues to vibrate without uplift is given by

$$\mathbf{r}(t) = D_1\boldsymbol{\phi}_1 \sin(\omega_1 t' + \delta_1) + D_2\boldsymbol{\phi}_2 \sin(\omega_2 t' + \delta_2) - v_s\boldsymbol{\phi}_2 \tag{3.13}$$

where

$$\omega_2 = \omega_v = \omega\beta \tag{3.14}$$

Both vibration modes may now contribute to the response, in contrast to equation 3.8 wherein the vertical vibration mode did not appear. The four constants D_1, D_2, δ_1, and δ_2 can be determined by standard procedures from the displacements and velocities of the structure at the time contact at both edges of the foundation mat is re-established. Equation 3.13 is also of the same form as equation 2.15 which describes the subsequent motion of the two-element system during full contact.

Numerical results for the response of a structure to normalized initial velocity $\bar{\dot{x}}(0) = 4$ obtained by the procedures described in Section 3.4 are presented in Figure 3.4 for two conditions of contact between the foundation mat and the supporting spring-damper elements: (a) bonded contact preventing uplift and (b) unbonded contact only through gravity with uplift permitted. The response quantities presented as a function of time are deformation u, foundation-mat rotation θ, total lateral displacement $x = u + h\theta$, vertical displacements v_l and v_r of the left and right edges of the foundation mat, and uplift index which is the ratio of foundation-mat width separated from the Winkler foundation to the full mat-width; the uplift index is positive for uplift of the left edge and negative for uplift of right edge.

If the foundation mat is bonded to the supporting elements, the structural response is described by equation 3.8 for all time. The frequency of this simple harmonic motion is ω_1, defined in equation 3.9, and the amplitudes of the response quantities are given by the values at incipient uplift (equation 3.10) multiplied by the normalized initial velocity, which is 4 in this case.

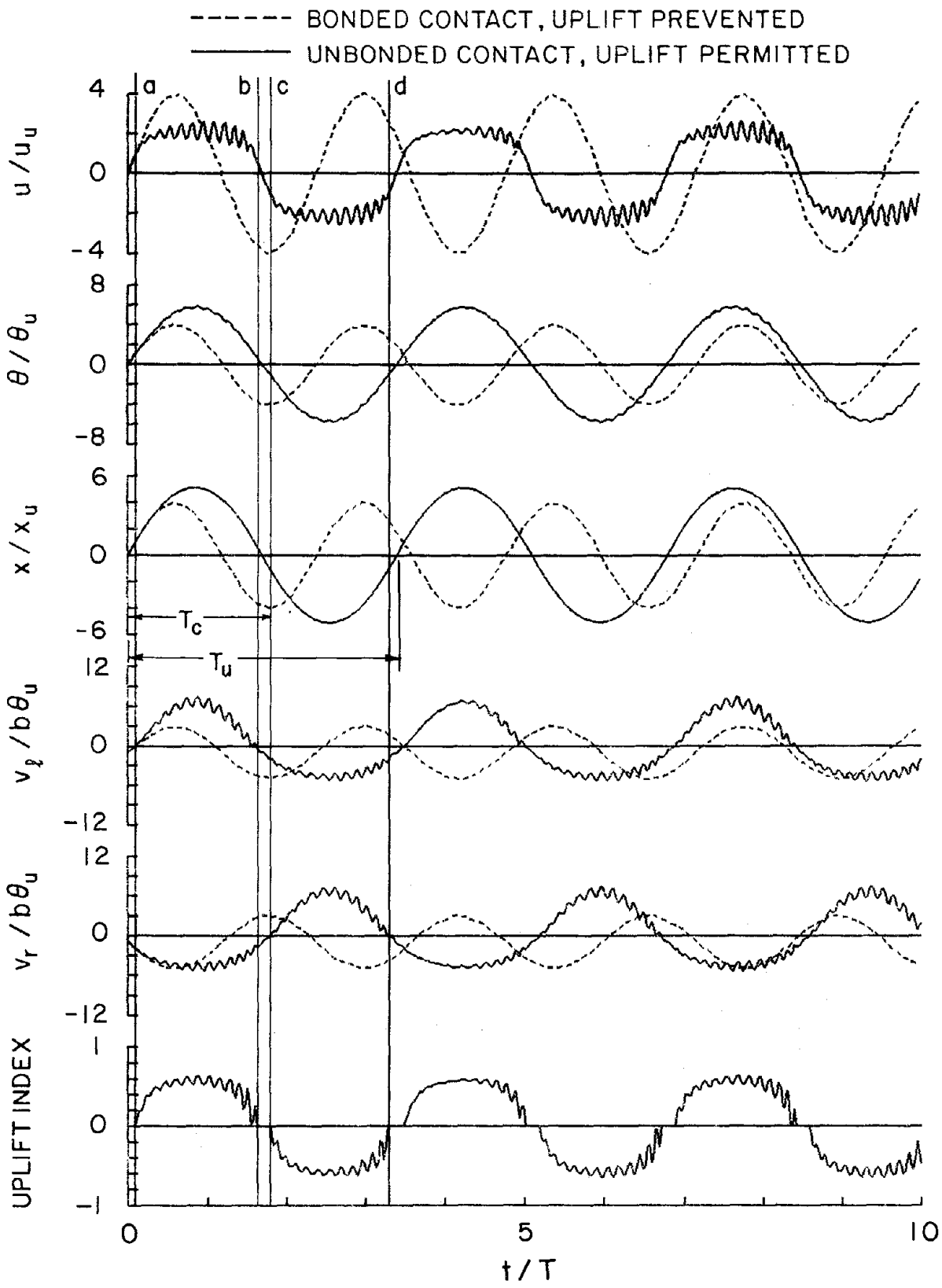

FIGURE 3.4 Response of an undamped structure ($\alpha = 10$, $\beta = 8$, $\gamma = 0$) to initial velocity $\dot{\bar{x}}(0) = 4$, for two conditions of contact between the foundation mat and the supporting elements: (a) Bonded contact preventing uplift, and (b) Unbonded contact only through gravity with uplift permitted.

The structural response is initially described by equation 3.8 even when uplift is permitted, resulting in response identical to the bonded case (Figure 3.4). When the deformation u and foundation-mat rotation θ reach their incipient-uplift values (equation 3.10), the left edge of the mat begins to separate from the supporting elements at time a (Figure 3.4) and the subsequent response is nonlinear. The deformation u oscillates at a much higher frequency, analogous to the frequency λ_2 in the two-element case, except that this frequency in the Winkler foundation case is amplitude-dependent. In this particular example, this is about 8 times the fixed base frequency, which is equal to the frequency of the vertical vibration mode during full contact, thus demonstrating the contribution of the second mode even under nonlinear vibration. This higher frequency response appears also in $v_l(t)$ and $v_r(t)$ and slightly in $\theta(t)$, but the total lateral displacement $x(t)$ varies smoothly with time without any noticeable contribution of the higher frequency motion. Full contact of the foundation mat is re-established at time b and the response is described by equation 3.13 until the right edge begins to separate from the supporting elements at time c; at which time the response motion is again nonlinear until full contact of the foundation mat is re-established at time d and equation 3.13 is back in the picture. This response behavior is repeated during every cycle of free vibration as seen in Figure 3.4. However, the response is not precisely periodic although it appears to be nearly so because the initial conditions are not exactly repeated at the beginning of each vibration cycle. Whereas no vertical velocity is imparted to the structural mass when free vibration is initiated at $t = 0$, a small vertical velocity may be present at the beginning of subsequent cycles of free vibration. The uplift index shows that during a half-cycle of partial separation of the foundation mat from its supporting elements, the separated width of the foundation mat remains essentially constant, at about 60 percent in this case, with small fluctuations occurring at a high frequency as in deformation response $u(t)$.

Because of uplift of the foundation mat, the maximum structural deformation u for this system is reduced but the maximum values of all the other response quantities -- θ, x, v_l and v_r -- are increased.

Noting that the time scale in Figure 3.4 is normalized with respect to the natural vibration period T of the rigidly supported structure, it is apparent that the flexibility of the supporting elements has the effect of lengthening the vibration period to T_c, and uplift of the foundation mat results in even a longer period T_u. From equation 3.9a the period ratio

$$\frac{T}{T_c} = \bar{\omega}_1 \tag{3.15}$$

wherein for a fixed mass ratio γ , $\bar{\omega}_1$ depends only on α and β and not on $\bar{x}(0)$ or T; in particular it is given by equation 3.9b if $\gamma = 0$. An analytical expression for the period ratio T_u / T does not appear to be derivable because the system is nonlinear when uplift if the foundation mat is permitted. However, based on numerical results it can be shown that, for a fixed value of γ, T_u / T depends on α, β and $\bar{x}(0)$ but over a useful range of parameters, it does not depend on T. Like the two-element system, the mass ratio γ has little effect on the vibration properties thus its influence on these period ratios is expected to be small. Numerical results for free vibration response of several systems with parameters α and β varied over a wide range support this claim.

In order to examine whether the free vibration response behavior observed above is typical, results are also presented for another system. Compared to the one considered earlier, the slenderness ratio parameter α for this system is smaller and frequency ratio β is higher. Numerical results for the response of a structure to normalized initial velocity $\dot{x}(0) = 4$ are presented in Figure 3.5. Comparing it with Figure 3.4 indicates that the high-frequency response component is now much more pronounced, to the extent that foundation mat uplift does not necessarily reduce the maximum structural deformation u. The behavior of a squatty structure (smaller α) with a rather stiff supporting system (higher β) is dominated by the rapid fluctuations in the portion of the foundation mat over which uplift occurs.

The response of the system considered in Figure 3.4 is recomputed including the second term on the right side of equation 3.2a associated with $p-\delta$ effects and the results are presented

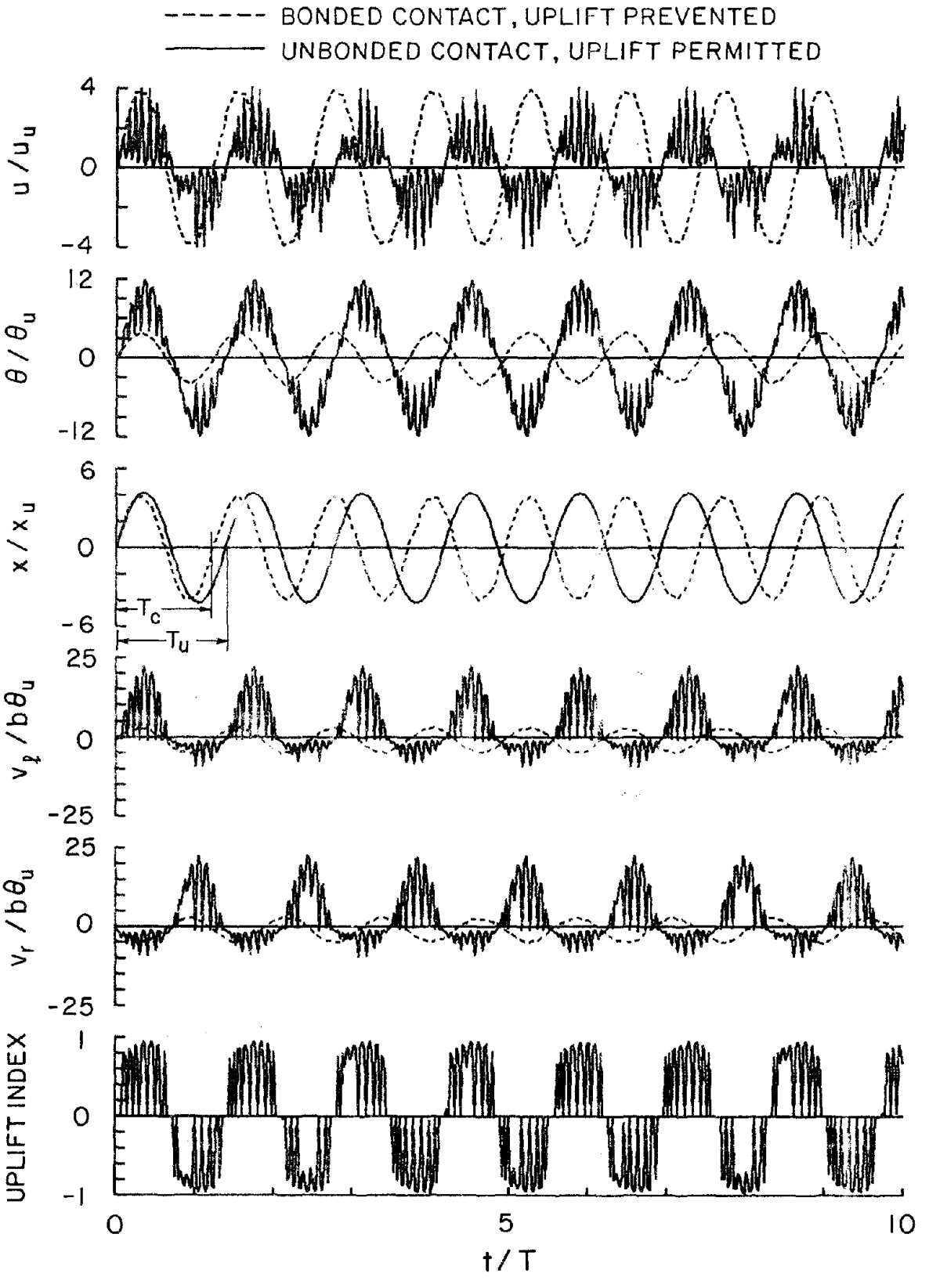

FIGURE 3.5 Response of an undamped structure ($\alpha = 5$, $\beta = 12$, $\gamma = 0$) to initial velocity $\dot{x}(0) = 4$, for two conditions of contact between the foundation mat and the supporting elements: (a) Bonded contact preventing uplift, and (b) Unbonded contact only through gravity with uplift permitted.

in Figure 3.6. Comparison of Figure 3.4 and 3.6 indicates that $p-\delta$ effects have little influence on the response of the structure under either contact condition. The response is essentially unaffected by $p-\delta$ effects if the foundation mat is bonded to the supporting elements. If the foundation mat is permitted to uplift, the total displacement x increases only slightly, by about 8 percent, with a similar lengthening of the vibration period T_u, whereas the maximum deformation is essentially unaffected.

3.5.2 Effect of Damping

The response of the undamped system to an initial velocity was given by equation 3.8 during the time the foundation mat remains fully in contact with the supporting elements. Because the system is nonlinear with properties depending on the width of the uplifted portion of the foundation mat, analytical expression for free vibration response during uplift are not derivable. After full contact has been re-established the response is described by equation 3.13. When damping in the structure and the continuous supporting elements is included, the responses of a system with massless foundation mat during initial and subsequent full contact will be described by equations 3.8 and 3.13 with appropriate modification to include exponential terms $e^{-\xi_n \omega_n t}$ and $e^{-\xi_n \omega_n t'}$, respectively; and substitution of the damped frequency ω'_n instead of ω_n in the harmonic terms, where $\omega'_n = \omega_n \sqrt{1-\xi_n^2}$ and the modal damping ratios are

$$\xi_1 = \frac{\beta^3}{(3\alpha^2+\beta^2)^{3/2}} \left(\xi + \frac{3\alpha^2}{\beta^3}\xi_v\right) \tag{3.16a}$$

$$\xi_2 = \xi_v \tag{3.16b}$$

Like the two-element system, the damping ratio for the second vibration mode -- which involves uncoupled vertical motion without lateral deformation or base rotation -- is simply ξ_v, the damping ratio of the structure in vertical vibration (equation 3.16b). In the first mode which includes lateral deformation of the structure coupled with rotation of the foundation mat

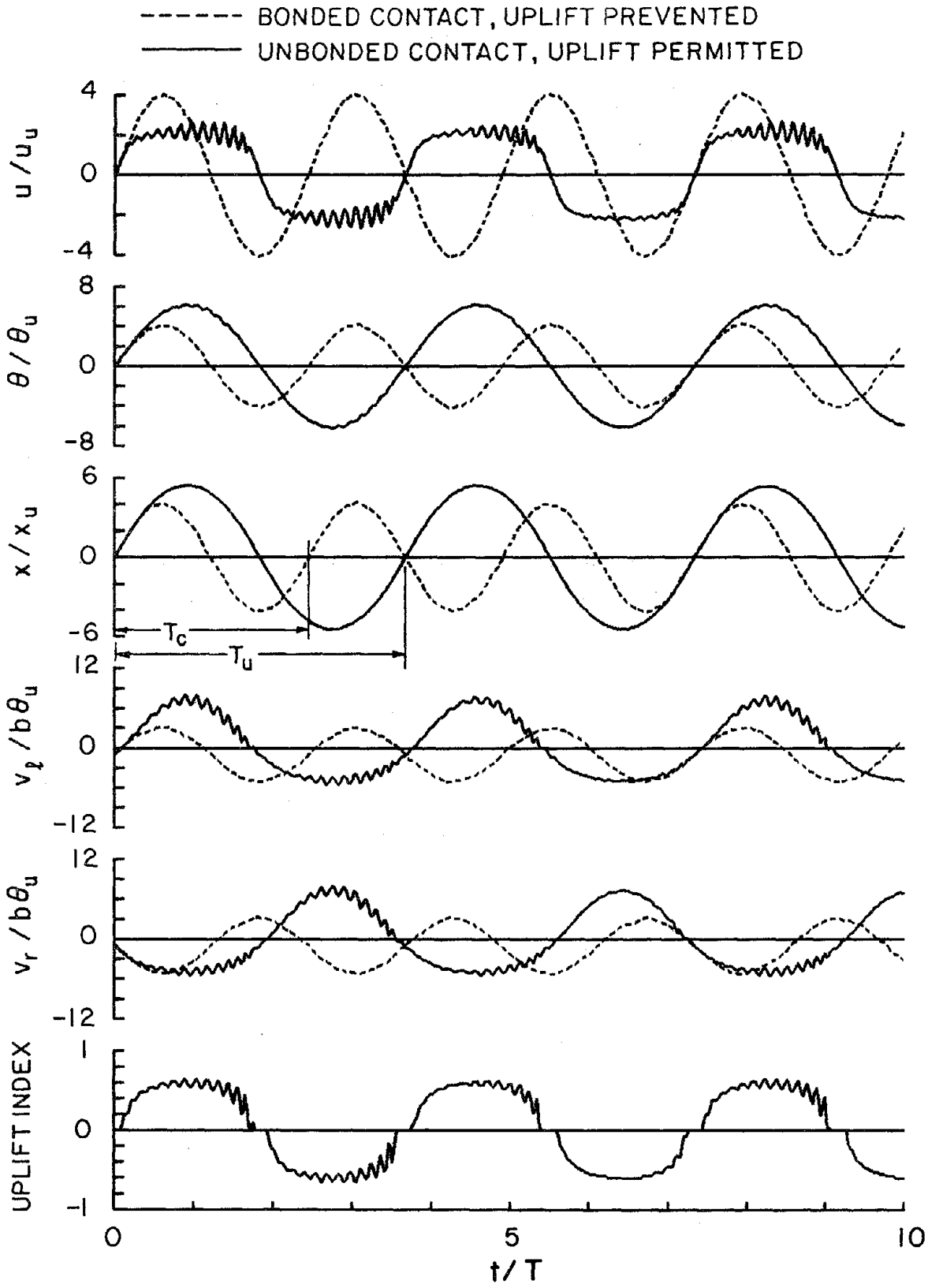

FIGURE 3.6 Response of an undamped structure ($\alpha = 10$, $\beta = 8$, $\gamma = 0$) including $p-\delta$ effects, to initial velocity $\bar{x} = 4$, for two conditions of contact between the foundation mat and the supporting elements: (a) Bonded contact preventing uplift, and (b) Unbonded contact only through gravity with uplift permitted.

about its c.g, the damping ratio is a linear combination of ξ_v and ξ, where the latter is the damping ratio of the rigidly supported structure in lateral motion. Based on the notion of equivalent base width introduced in Section 3.3, it can be readily seen that equation 3.16a can be reduced to equation 2.17a.

Although there is no analytical expression available for free vibration during uplift of the system with Winkler foundation, the damping properties of the system during large base uplift are expected to resemble qualitatively those of a system with two-element foundation with similar system parameters. Specifically, the rocking vibration mode is expected to be nearly undamped during large uplift, while the damping ratio for the high frequency mode will be similar in magnitude to the second mode damping ratio of the two-element system standing on one edge (equation 2.18). This damping ratio is

$$\zeta_2 = \frac{\beta^3 (1+\alpha^2)^{1/2}}{(2\alpha^2+\beta^2)^{3/2}} \left(\xi + \frac{2\alpha^2}{\beta^3}\xi_v\right) \tag{3.16c}$$

where ξ_v may be taken equal to the vertical mode damping ratio for the Winkler system. For a fixed pair of damping ratios ξ and ξ_v, ζ_2 decreases with decreasing slenderness ratio parameter α and increasing frequency ratio β. The over all damping effect on the high frequency vibration mode of the structure with Winkler foundation is thus a function of the vertical damping ratio during full contact ξ_v, and the estimated damping ratio during large uplift ζ_2.

The response of the first structure considered earlier, with $\alpha = 10$ and $\beta = 8$, but now including damping in the structure as well as supporting elements, to normalized initial velocity $\bar{\dot{x}}(0) = 4$ is presented in Figure 3.7. From the selected values $\xi = 0.05$ and $\xi_v = 0.4$, and equations 3.16a, 3.16b and 3.16c, $\xi_1 = 0.006$ and $\xi_2 = 0.4$ and damping ratio for the high frequency mode is of the order of magnitude $\zeta_2 = 0.25$ during large uplift. If the foundation mat is bonded to the supporting elements and its uplift is thus prevented, the deformation u and base rotation θ decay exponentially at a rate defined only by the first mode damping ratio ξ_1, because the second mode does not contribute to these response quantities.

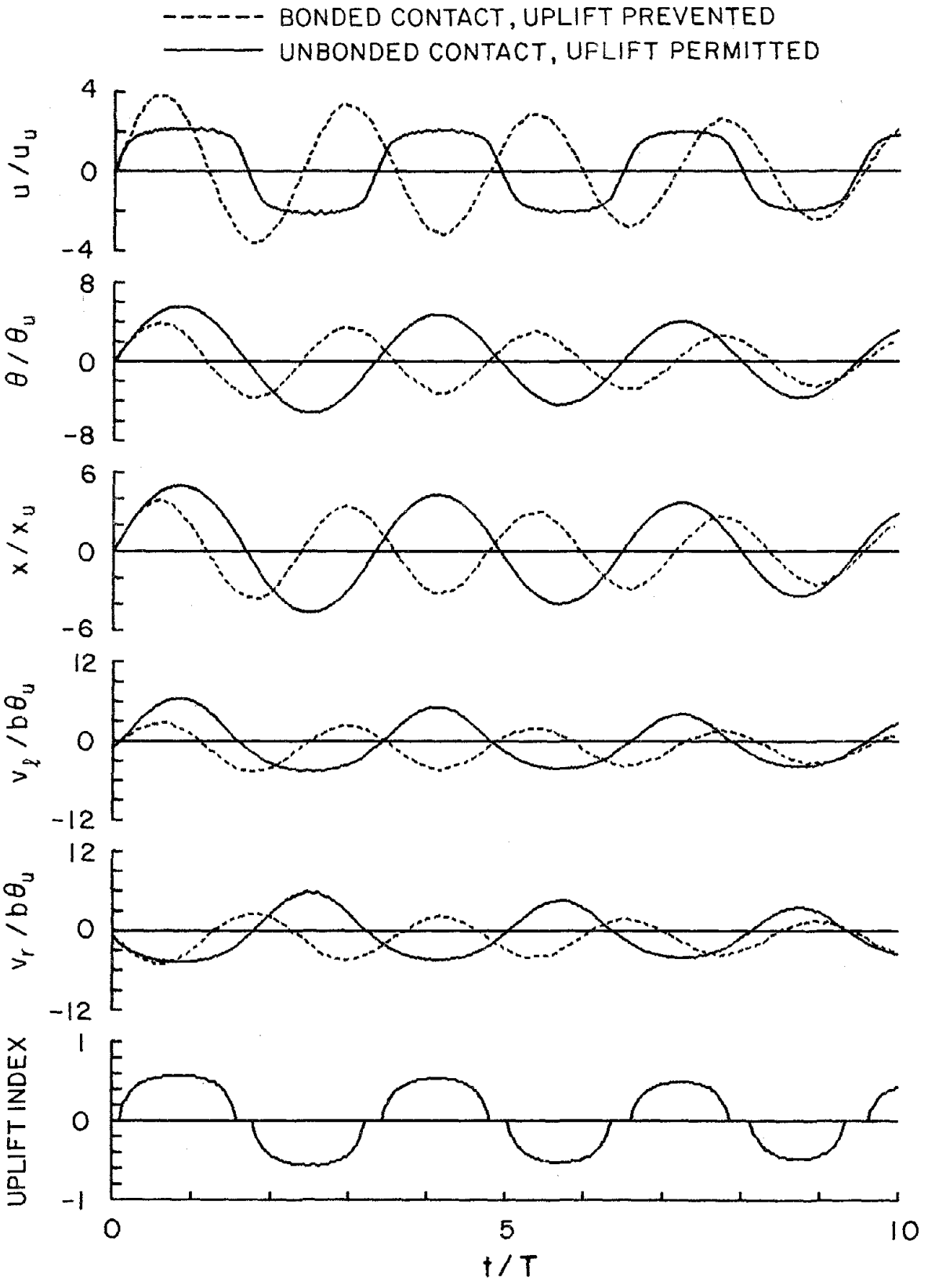

FIGURE 3.7 Response of a damped structure ($\xi = 0.05$, $\xi_y = 0.4$, $\alpha = 10$, $\beta = 8$, $\gamma = 0$) to initial velocity $\bar{\dot{x}} = 4$, for two conditions of contact between the foundation mat and the supporting elements: (a) Bonded contact preventing uplift, and (b) Unbonded contact only through gravity with uplift permitted.

Several observations regarding the effects of damping can be made by comparing the responses of the structure, with uplift of the foundation mat permitted, in Figures 3.4 and 3.7: The tendency of the foundation mat to uplift, is reduced, resulting in the uplift duration decreasing slowly with each vibration cycle. Just as in the two-element system the higher frequency oscillations are heavily damped and decay rapidly at a rate closely related to the second mode damping ratio ξ_2 during full contact and to the damping ratio ζ_2 for high frequency mode during large uplift. Although uplift of the foundation mat increases the maximum downward edge displacement in the undamped case, the effect of damping in the second mode during full contact, and the high frequency mode during uplift, which are excited when uplift is permitted, is so strong that downward edge displacement is actually slightly reduced by permitting uplift.

The response of the second structure considered earlier with $\alpha = 5$ and $\beta = 12$, but now including damping is presented in Figure 3.8. From the selected values $\xi = 0.05$ and $\xi_v = 0.4$, and equations 3.16a, 3.16b and 3.16c, $\xi_1 = 0.036$ and $\xi_2 = 0.4$ and the high frequency mode damping ratio $\zeta_2 = 0.05$ which is much smaller compared to the system with $\alpha = 10$ and $\beta = 8$ due to reduction in α and increase in β as discussed earlier. For bonded foundation support, the deformation u and base rotation θ decay exponentially at a rate defined by ξ_1 like the response of the first structure.

However, when uplift is allowed, the damped responses differ significantly from those of the first structure. While the uplift duration decreases with each cycle, the contribution of the high frequency component to deformation u, base rotation θ, edge displacements v_l and v_r, and uplift index remain dominant in the first few cycles despite of having a greater linear first mode damping ratio than the first structure. The maximum uplift index remains almost at a constant high level (approximately 95%) for each half cycle of the first six and a half cycles, and then drops off to a very low level (approximately 20%) and becomes negligible after another cycle. As discussed above neglecting the fluctuations, the structure can be viewed as if it is standing on two stiff spring elements and the motion resembles that of a structure rocking on a two-element foundation. Fluctuations in the uplift width are caused by the significantly smaller

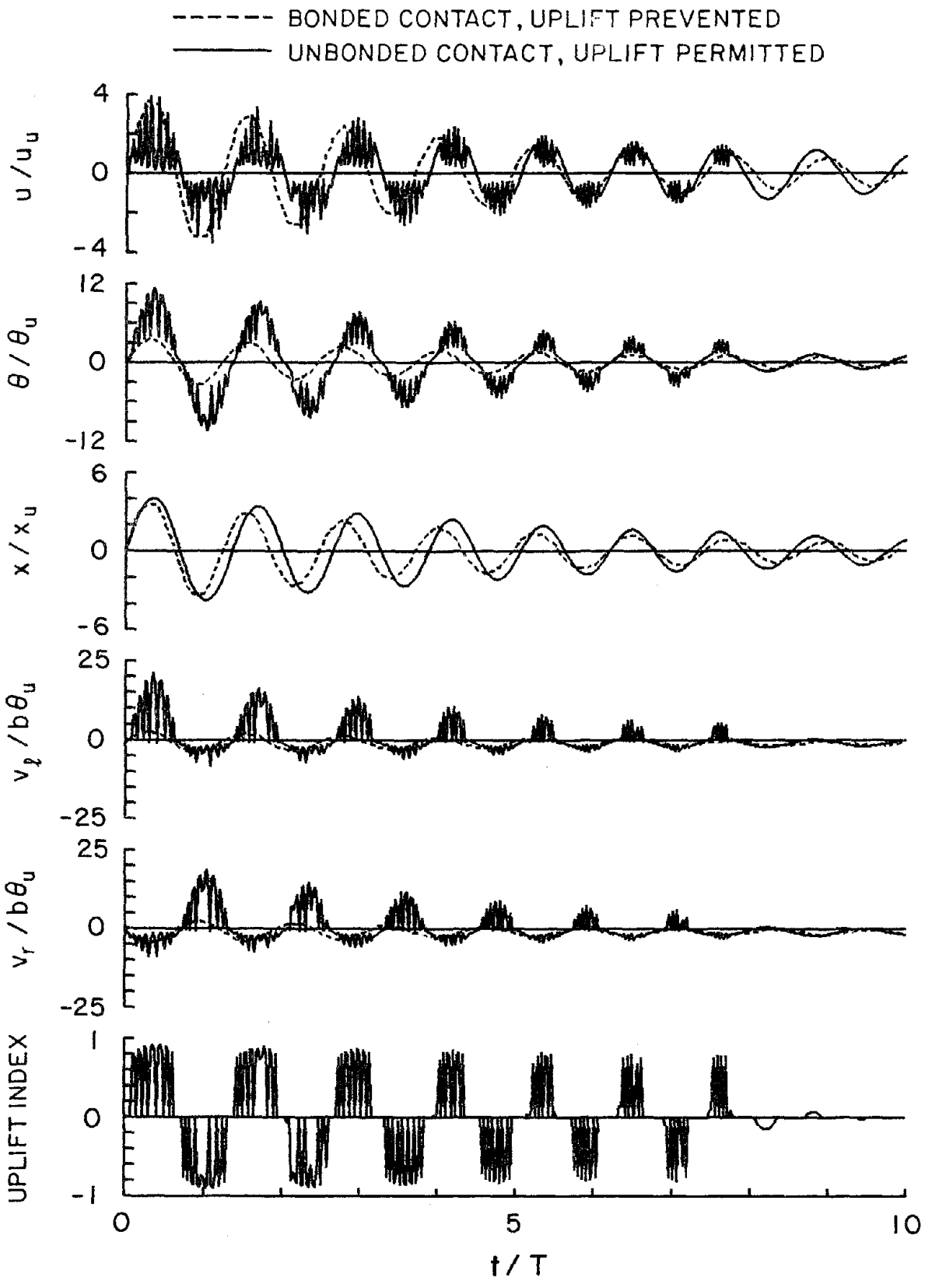

FIGURE 3.8 Response of a damped structure ($\xi = 0.05$, $\xi_v = 0.4$, $\alpha = 5$, $\beta = 12$, $\gamma = 0$) to initial velocity $\dot{\bar{x}}(0) = 4$, for two conditions of contact between the foundation mat and the supporting elements: (a) Bonded contact preventing uplift, and (b) Unbonded contact only through gravity with uplift permitted.

damping of the high frequency mode of the structure during large uplift. This response behavior also leads to the lack of damping effect in the first few vibration cycles, because while the first mode damping ratio is relatively larger than that of the first structure, it is small in absolute magnitude. This damping ratio and the large damping ratio of the second mode during full contact have significant influence only when the percentage of contact of the foundation mat with the supporting elements is relatively large. Thus when the average contact area over the cycle is small, as in the first few cycles, the damping effect based on full contact is also small. When the uplift duration is reduced, as in the later cycles, the average contact area over a cycle increases, and so does the damping effect.

3.6 Earthquake Responses

The response of a structural system to the north-south component of the El Centro, 1940 ground motion is presented in Figure 3.9. Responses are shown for two conditions of contact between the foundation mat and the supporting spring-damper elements: (a) bonded contact preventing uplift and (b) unbonded contact only through gravity with uplift permitted. In the first case, the structural response is entirely due to the first natural vibration mode of the system with the full width of the foundation mat in contact with the supporting elements (see Section 3.5). Thus the response behavior is similar to a SDOF system. When uplift of the foundation mat is permitted, the response behavior is much more complicated. During the initial phase of the ground shaking, the foundation mat remains in contact with the supporting elements over its entire width. As the ground motion intensity builds up, the two edges of the foundation mat alternately uplift in a vibration cycle, inducing partial separation of the mat from the supporting elements. In this example the foundation mat uplifts over a significant portion of its width in every vibration cycle during the strong phase of ground shaking, with the duration of uplift depending on the amplitudes of foundation-mat rotation. As the intensity of ground motion decays toward the later phase of the earthquake, the foundation-mat uplift becomes negligible and full contact is maintained for long durations.

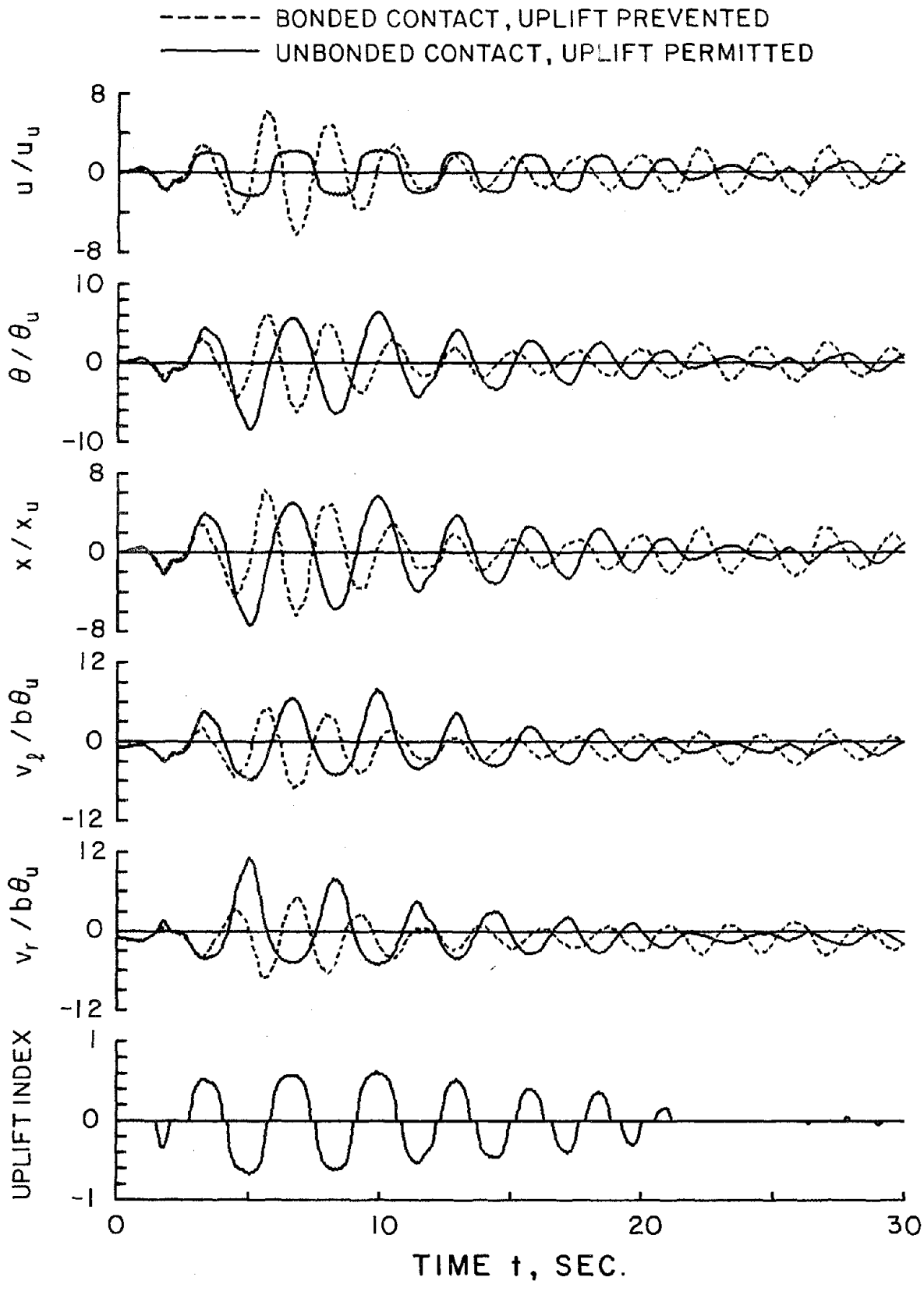

FIGURE 3.9 Response of a structure ($\alpha = 10$, $\beta = 8$, $\gamma = 0$, $T = 1$ sec., $\xi = 0.05$, $\xi_v = 0.4$) to El Centro ground motion for two conditions of contact between the foundation mat and the supporting elements: (a) Bonded contact preventing uplift, and (b) Unbonded contact only through gravity with uplift permitted.

The effects of foundation-mat uplift on the maximum response of the selected structure due to earthquake ground motion are similar to those observed in Section 3.5 during free vibration. When foundation-mat uplift is permitted, the maximum deformation of the structure is about twice the deformation u_{ii} at incipient-uplift of the foundation mat, which is a significant reduction compared to the response when foundation-mat uplift is prevented. Because of damping, the small-amplitude oscillations at a high frequency like those in Figure 3.4 damp out and are not present in the earthquake response results of Figure 3.9. The rotation of the foundation mat and vertical displacements of the two edges of the foundation mat are significantly increased due to the rigid body uplift motion of the system. This uplift motion provides the dominant contribution to these responses during uplift but does not affect the maximum response of the structural deformation.

The response of the relatively squatty system (smaller α) with higher stiffness in the vertical direction (larger β) to the El Centro ground motion is presented in Figure 3.10. While some features of the response are similar to those observed above from the previous case, important differences can be noted. In particular, foundation-mat uplift causes much larger rotation θ, and vertical edge displacements v_l and v_r of the foundation mat. As observed in the free vibration study (Section 3.5) the high frequency component in the deformation response is now much more pronounced, to the extent that foundation-mat uplift causes hardly any reduction in response and it leads to a slight increase in the maximum downward displacement of the foundation mat. Unlike in Figure 3.9, where the foundation-mat uplift was gradual, in this case the uplifted width of the foundation mat fluctuates very rapidly; once uplift is initiated, the uplifted width increases from zero to maximum value in almost no time; however, after a few cycles the tendency to uplift decreases. Thus, if uplift occurs in a cycle, the width is either very small or very near the maximum, but rarely an intermediate value.

In order to study the effects of foundation-mat uplift on the maximum response of structures, response spectra are presented. The base shear coefficient

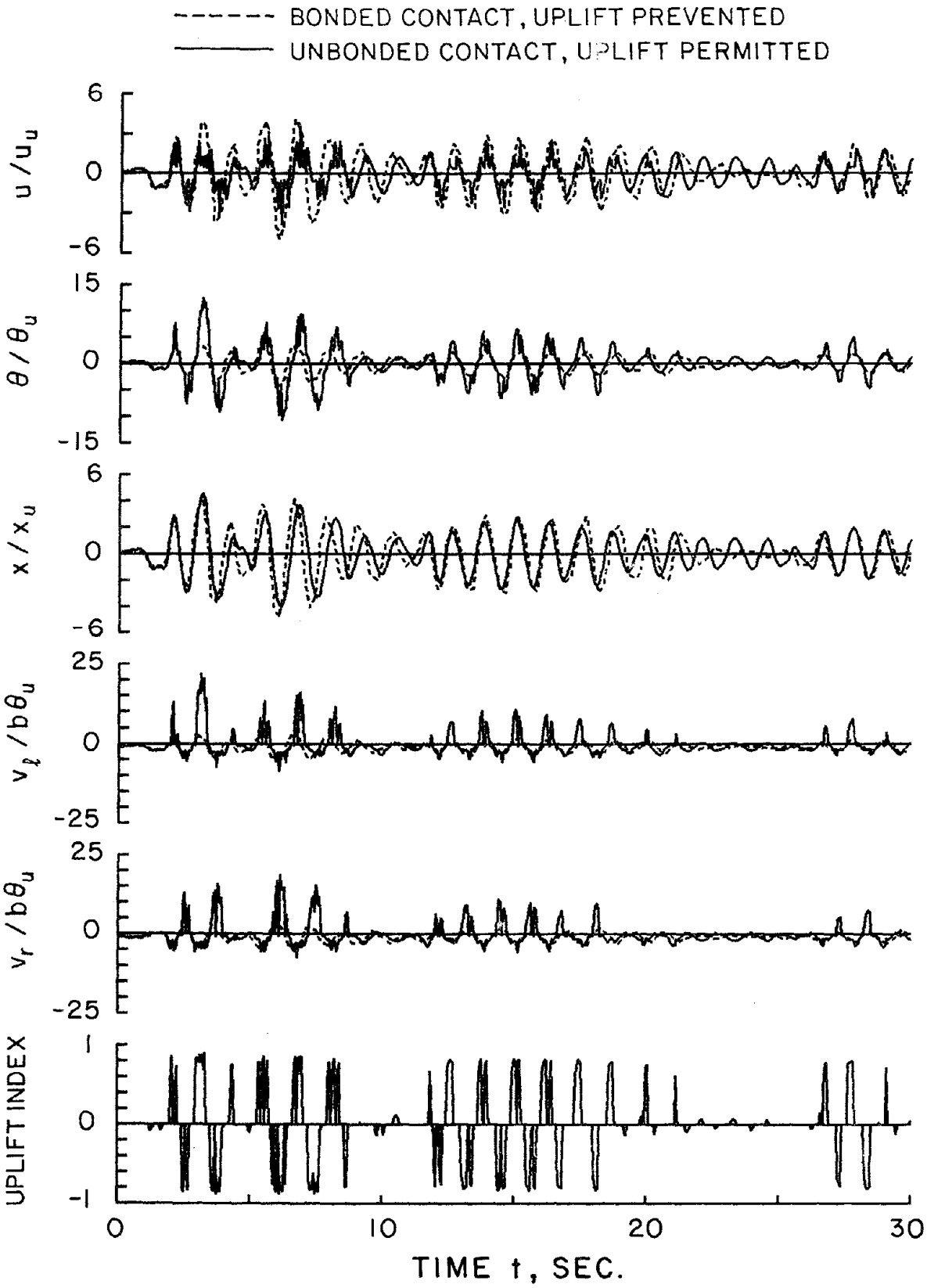

FIGURE 3.10 Response of a structure ($\alpha = 5$, $\beta = 12$, $\gamma = 0$, $T = 1$ sec., $\xi = 0.05$, $\xi_v = 0.4$) to El Centro ground motion for two conditions of contact between the foundation mat and the supporting elements: (a) Bonded contact preventing uplift, and (b) Unbonded contact only through gravity with uplift permitted.

$$V_{max} = \frac{\mathbf{V}_{max}}{w} = \frac{ku_{max}}{mg} = \left(\frac{2\pi}{T}\right)^2 \frac{u_{max}}{g} \tag{3.17}$$

where $\mathbf{V}_{max}$ is the maximum base shear, and w is the weight of the superstructure, is plotted as a function of the natural vibration period of the corresponding rigidly supported structure. For each set of system parameters α, β, γ, ξ and ξ_y, such a response spectrum plot is presented for two conditions of contact between the foundation mat and the supporting spring-damper elements: (a) bonded contact preventing uplift, and (b) unbonded contact with uplift permitted. Also presented are the results for the corresponding rigidly supported structure, which is simply the standard pseudo-acceleration response spectrum, normalized with respect to gravitational acceleration. Included in the response spectra plots is V_u, the base shear coefficient associated with the value of base shear, $\mathbf{V}_u$, at which uplift of an edge of the foundation mat is initiated (equation 3.1a):

$$V_u = \frac{\mathbf{V}_u}{w} = \frac{1+\gamma}{3\alpha} \tag{3.18}$$

Also included is V_c, the critical base shear coefficient associated with the static asymptotic base shear , $\mathbf{V}_c$, (see Section 3.1) which corresponds to the uplift of the foundation mat from its supporting springs over the entire width, i.e. the foundation mat is standing on its edge:

$$V_c = \frac{\mathbf{V}_c}{w} = \frac{1+\gamma}{\alpha} \tag{3.19}$$

These base shear coefficients depend on the mass ratio γ and slenderness-ratio parameter α, but are independent of the vibration period T.

The response spectra presented in Figure 3.11 are for systems with massless foundations ($\gamma = 0$) and a fixed set of system parameters α, β, ξ, and ξ_y subjected to El Centro ground motion. The differences between the response spectra for the two linear systems, the structure with foundation mat bonded to the supporting elements and the corresponding rigidly supported

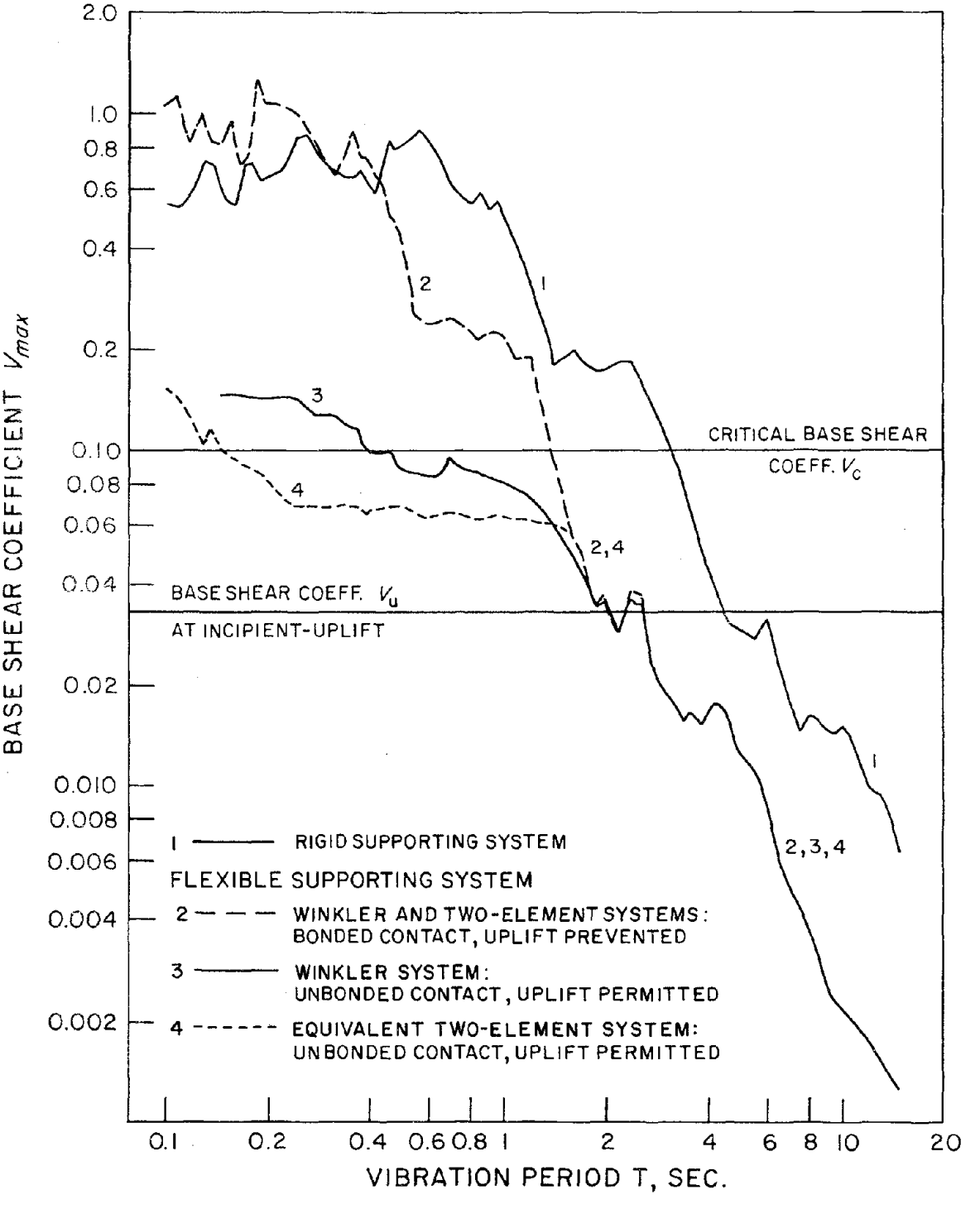

FIGURE 3.11 Response spectra for structures ($\alpha = 10$, $\beta = 8$, $\gamma = 0$, $\xi = 0.05$, $\xi_v = 0.4$) subjected to El Centro ground motion for four support conditions.

structure, are due to the change in period and damping resulting from support flexibility (equations 3.9 and 3.16). The base shear developed in structures with relatively long vibration periods is below the static value at incipient uplift and throughout the earthquake the foundation mat remains in contact over its entire width with the supporting elements. If foundation mat uplift is prevented, the maximum base shear at some vibration periods may exceed the incipient-uplift value. For the selected system parameters and ground motion, Figure 3.11 indicates that this occurs for all vibration periods shorter than the period where the linear spectrum first attains the incipient-uplift value. If the foundation mat of such a structure rests on the Winkler spring-damper elements only through gravity and is not bonded to these elements, partial separation occurs and this has the effect of reducing the base shear. However, the base shear exceeds the value at incipient-uplift because even under static forces the base moment, and hence base shear, continue to increase considerably beyond this value (Figure 3.2b). Furthermore the base shear is not reduced to as low as the critical value based on static consideration. Although this asymptotic value can never be exceeded under static forces, depending on the state -- displacement, velocity and acceleration -- of the system, the deformation and base shear may exceed the critical values during dynamic response as seen in Figure 3.11. Because the base shear developed in linear structures (foundation-mat uplift prevented) tends to exceed the incipient-uplift value by increasing margins as the vibration period decreases, the foundation mat of a shorter-period structure has a greater tendency to uplift over a greater portion of its width, which in turn results in the incipient-uplift base shear being exceed by a greater margin although it remains well below the linear response.

Also shown in Figure 3.11 is the response spectrum for the equivalent two-element system defined in Section 3.3. This response spectrum is identical to that for the Winkler system for the relatively long periods because the base shear developed is below the incipient-uplift value and the foundation mat does not uplift from its supporting elements and for this condition the two-element supporting system is exactly equivalent to the Winkler supporting system. Uplift occurs for any structure if the corresponding ordinate of the linear response spectrum

exceeds the static base shear coefficient at incipient uplift, which is $1/3\alpha$ for a Winkler system and $1/\sqrt{3}\alpha$ for the equivalent two-element system. Because the base shear developed in linear structures tends to increase as the vibration period decreases, uplift in a Winkler system is initiated at a longer period compared to the two-element system. However, because the uplift is limited in extent and duration in the range of periods bounded on the low side by the period at which uplift is initiated in a two-element system and on the high side by the period at which uplift is initiated in a Winkler system, the difference between the response spectra for the two systems is small in this period range. For shorter vibration periods outside this range the equivalent two-element system consistently underestimates the maximum response -- by a factor as large as two -- thus demonstrating that the equivalent two-element system does not adequately represent the moment-rotation relation for larger rotation angles (see Figure 3.3).

Presented in Figure 3.12 is the response spectrum for the downward displacement at either edge of the foundation mat for two conditions of contact between the foundation mat at its supporting spring-damper elements: (a) bonded contact preventing uplift and (b) unbonded contact with uplift permitted. The edge displacement is normalized with respect to the initial static displacement due to gravity. Just like the maximum deformation (Figure 3.11) the foundation mat edge displacement tends to be larger for shorter vibration period structures. Although this response quantity is affected by uplift of the foundation mat, these effects are not very significant, and over a wide range of periods a conservative estimate is provided by linear analyses preventing uplift.

The effects of ground motion intensity on the dynamic response of structures is displayed in Figure 3.13, wherein the response spectra for El Centro ground motion amplified by a factor of 2 are compared with the corresponding plots for the unscaled ground motion. If the foundation mat is bonded to the supporting elements and it can not uplift, the structural system is linear and the response spectrum is amplified by the same factor of 2. When uplift is permitted but the uplift is limited in extent, the response is only slightly reduced from the corresponding linear values with greater reduction for the more intense earthquake, the response spectrum is

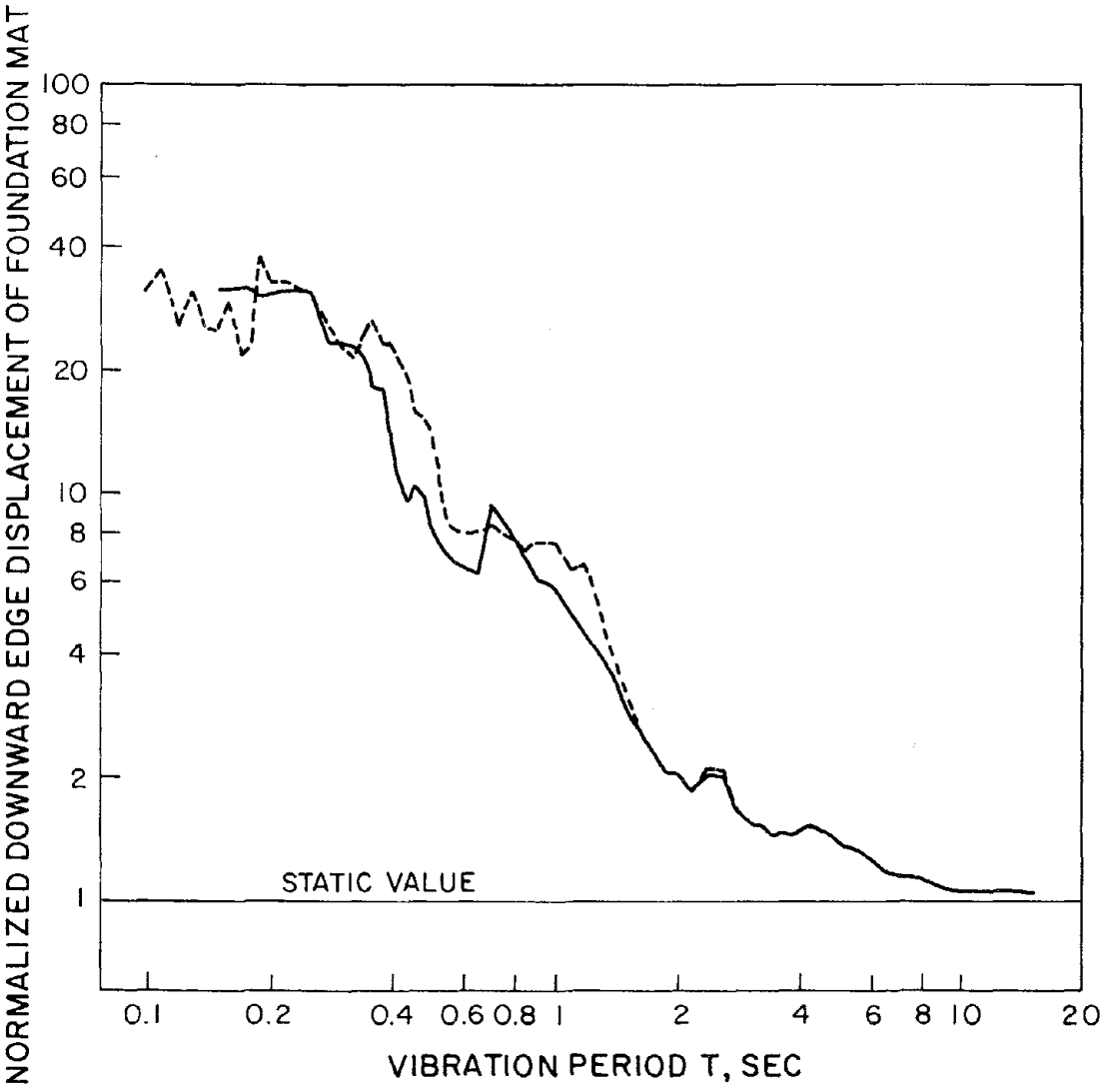

FIGURE 3.12 Response spectra for structures ($\alpha = 10$, $\beta = 8$, $\gamma = 0$, $\xi = 0.05$, $\xi_v = 0.4$) subjected to El Centro ground motion for two support conditions.

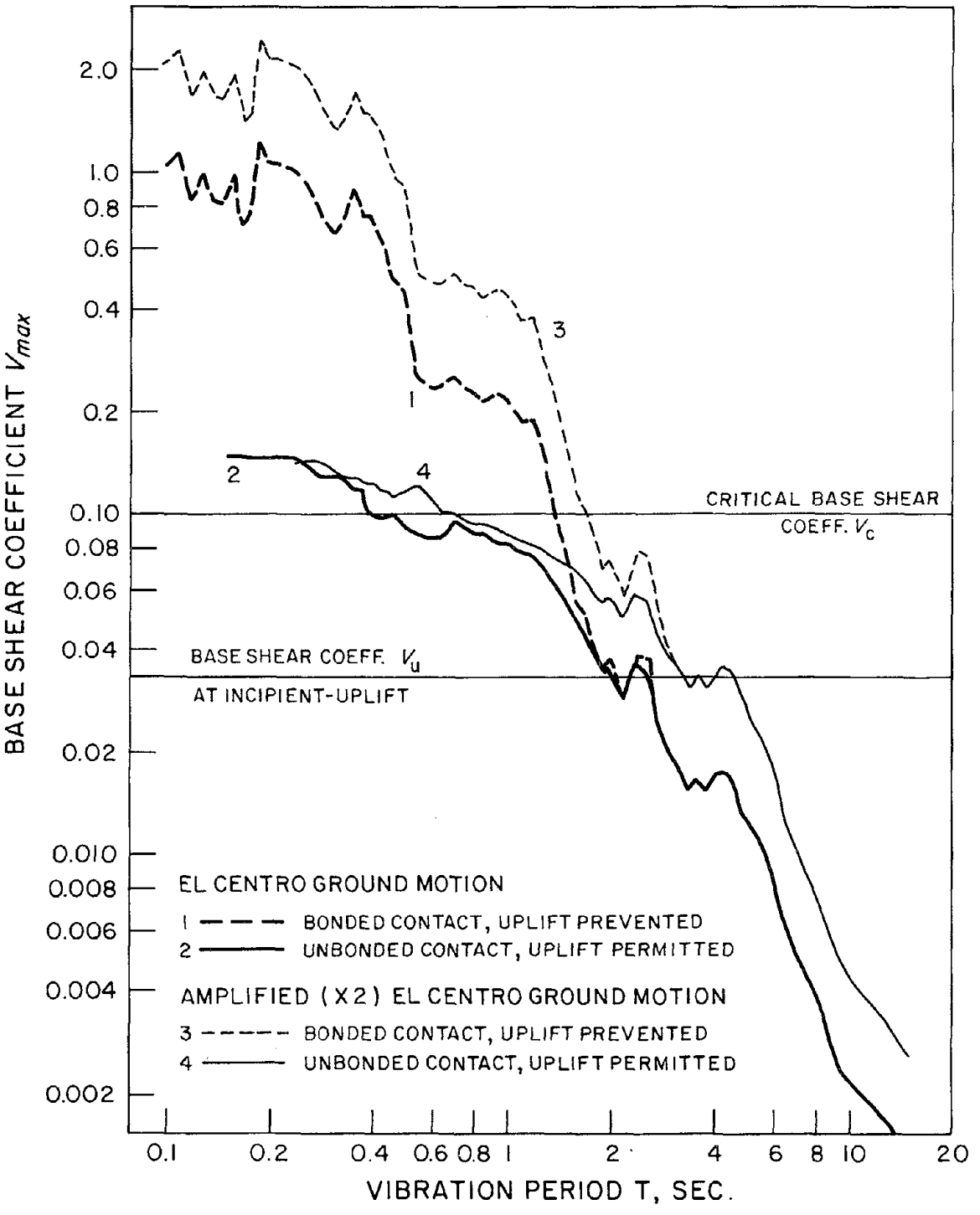

FIGURE 3.13 Effects of ground motion intensity on response spectra for structures ($\alpha = 10$, $\beta = 8$, $\gamma = 0$, $\xi = 0.05$, $\xi_v = 0.4$).

amplified by a factor somewhat less than 2. This behavior differs from the two-element system, where the foundation mat uplifts abruptly changing the state from full contact to no contact, and the response permitting foundation-mat uplift is essentially independent of the earthquake intensity. However, for structures with shorter periods the foundation mat uplifts over greater width and for more time and the base shear is controlled by the critical value V_c which is a property of the system, independent of ground motion. Thus like the two-element system, the base shear for short-period systems is increased only slightly although the earthquake intensity is doubled. Because the base shear attains its incipient-uplift value at a slightly longer period when earthquake intensity is increased, uplift of the foundation mat is initiated at a slightly longer period.

The response spectra presented in Figure 3.14 are for two values of the frequency ratio β with all other system parameters kept constant. As mentioned earlier, the differences in the response spectra for the two linear systems, the structure with foundation mat bonded to the supporting elements and the corresponding rigidly supported structure, are due to the change in period and damping resulting from support flexibility (equations 3.9 and 3.16). The period change appears as a shift in the response spectrum to the left, with larger shift for smaller values of β, i.e. for the more flexible supporting elements. The nonlinear response spectrum for the structure with foundation mat permitted to uplift shifts similarly to the left, with uplift initiated at longer periods as β increases. But for the period shift, the shapes of the linear as well as nonlinear response spectra are affected little by the frequency ratio β. These effects of varying β on the response of structures supported on Winkler foundation are similar to those observed in Section 2.6 for structures on two supporting elements.

As presented in equations 3.18 and 3.19, the incipient-uplift and critical base shear coefficients are inversely proportional to the slenderness-ratio parameter α. This would suggest that maximum base shear will be smaller for relatively slender structures, which is confirmed by response spectra presented in Figure 3.15. The foundation mat of a slender structure has a greater tendency to uplift resulting in greater reductions in the base shear. Uplift of the

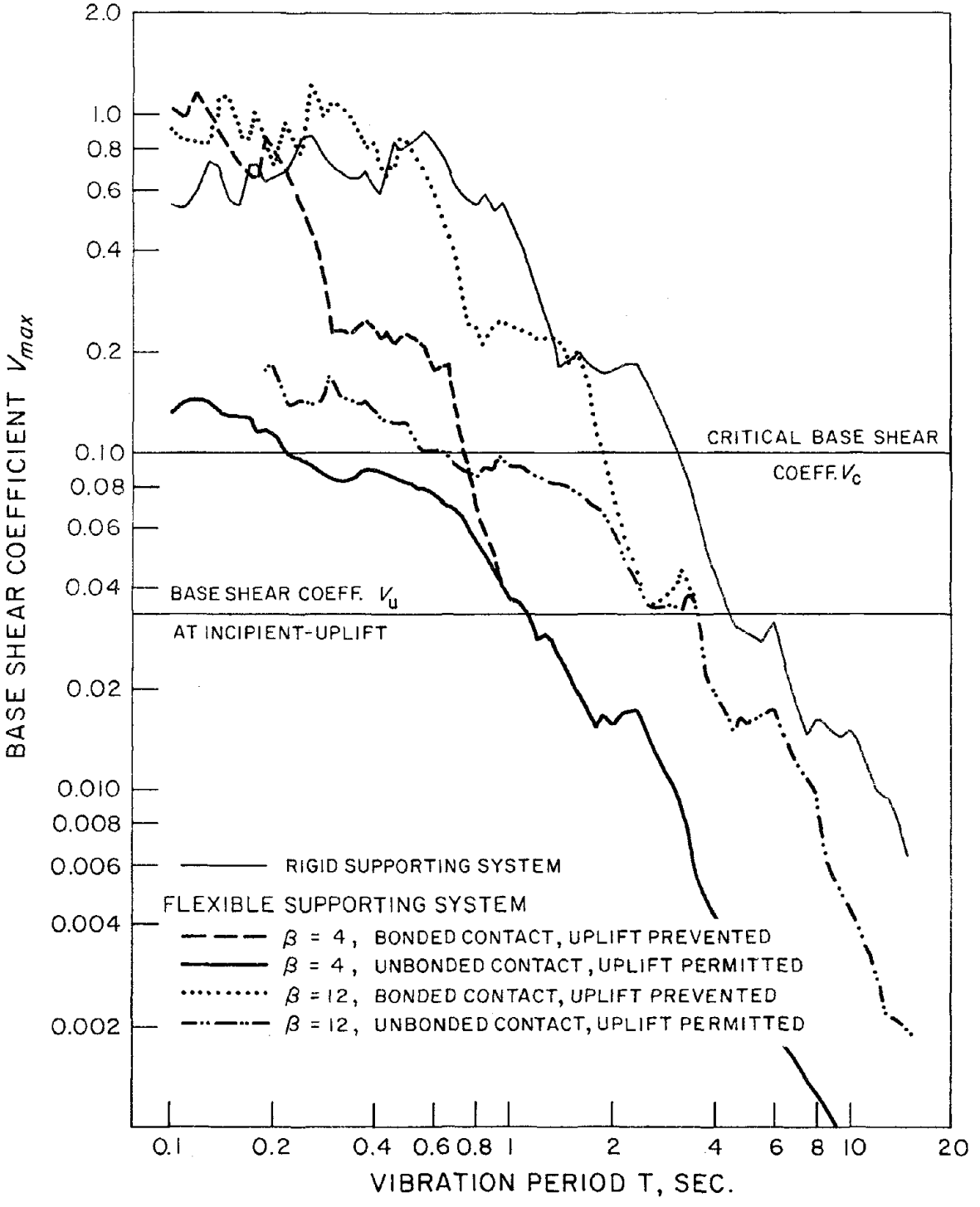

FIGURE 3.14 Response spectra for structures ($\alpha = 10$, $\gamma = 0$, $\xi = 0.05$, $\xi_v = 0.4$) subjected to El Centro ground motion for two values of frequency ratio $\beta = 4$ and 12.

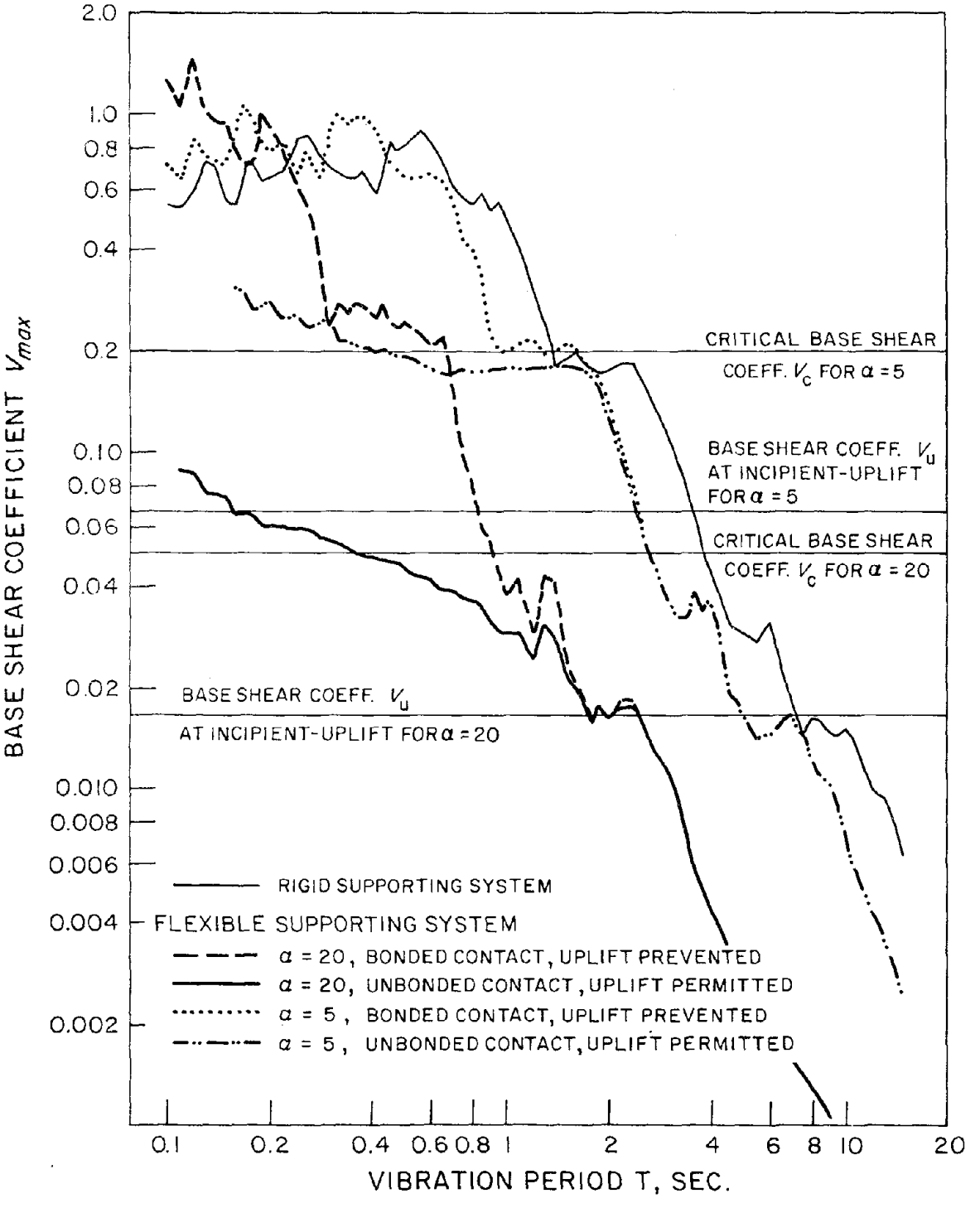

FIGURE 3.15 Response spectra for structures ($\beta = 8$, $\gamma = 0$, $\xi = 0.05$, $\xi_v = 0.4$) subjected to El Centro ground motion for two values of slenderness ratio parameter $\alpha = 5$ and 20.

foundation mat occurs at all vibration periods shorter than the period where the linear response spectrum attains the incipient-uplift value. This period, in general, depends on the slenderness ratio α in a complicated manner, because the incipient-uplift base shear coefficient as well as the period shift of the linear response spectrum (relative to the standard pseudo-acceleration spectrum) both depend on α; however, in this example, this period is essentially independent of α.

The incipient-uplift and critical base shear coefficients increase with mass ratio γ as indicated by equation 3.18 and 3.19; for systems with massless foundation mat ($\gamma = 0$) these coefficients are $1/3\alpha$ and $1/\alpha$ respectively, and they increase to $2/3\alpha$ and $2/\alpha$ for systems with equal foundation-mat and structural masses ($\gamma = 1$). The response spectra for these two mass ratios are presented in Figure 3.16 which indicate that the effects of foundation-mat mass are to reduce the short period range over which the foundation mat uplifts; to approximately double the maximum base shear over this period range; and to introduce a period shift in the linear response spectrum, with little influence on the shape of the spectrum.

These effects of varying parameters α, β and γ on the response of structures supported on Winkler foundation are similar to those identified in Section 2.6 from the response of structures with two supporting elements.

The effects of gravity and inertia forces in the vertical direction (the so-called $p-\delta$ effect) on the dynamic response of structures is displayed in Figure 3.17 wherein the response spectra are presented for two cases: (1) $p-\delta$ effect neglected and (2) $p-\delta$ effect included. Over a wide range of periods the response spectrum is essentially the same, with or without $p-\delta$ effects. For a fixed frequency ratio, the supporting system becomes increasingly flexible for structures with longer vibration periods, and the structure can overturn because of $p-\delta$ effects (Figure 3.17).

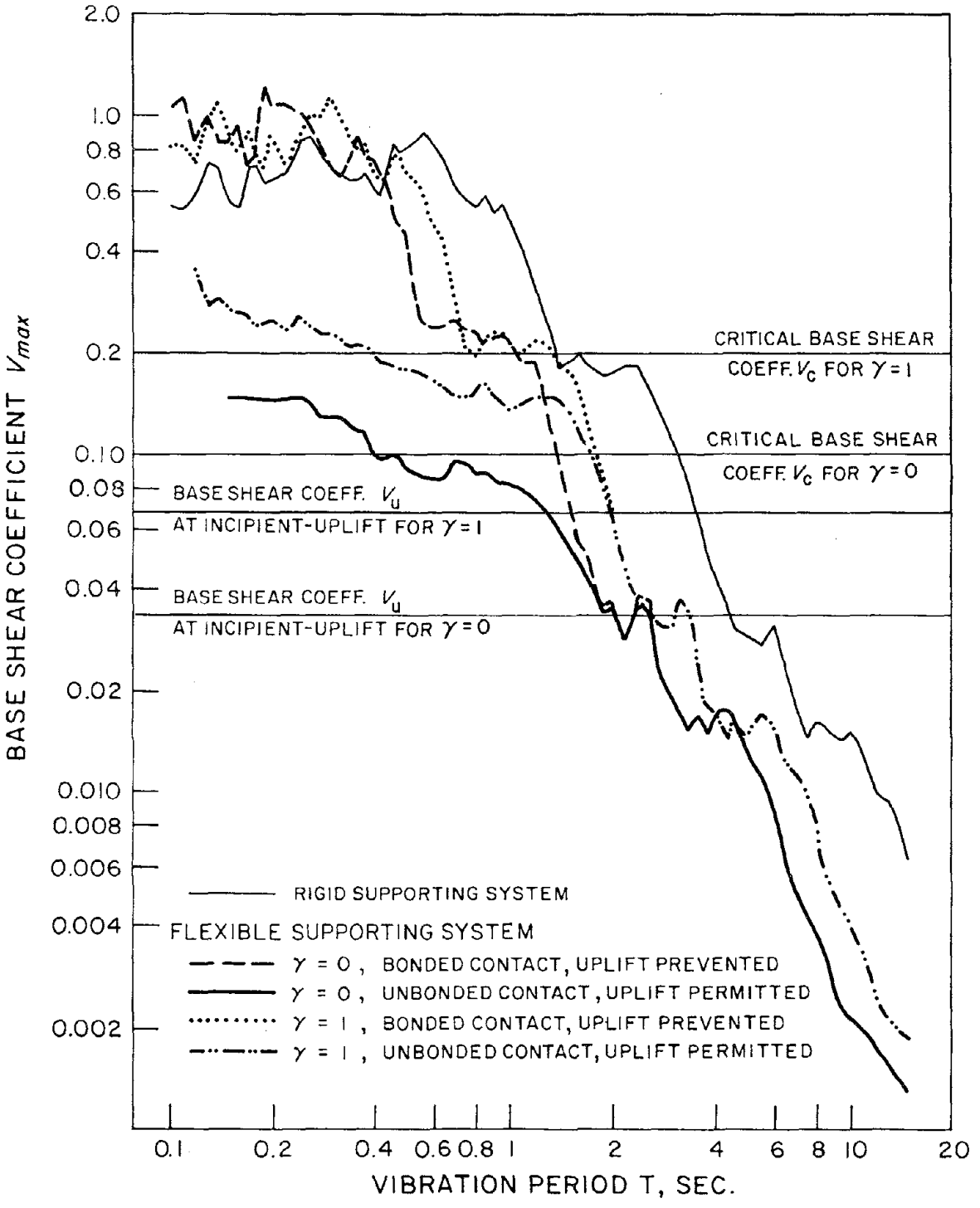

FIGURE 3.16 Response spectra for structures ($\alpha = 10$, $\beta = 8$, $\xi = 0.05$, $\xi_v = 0.4$) subjected to El Centro ground motion for two values of mass ratio $\gamma = 0$ and 1.

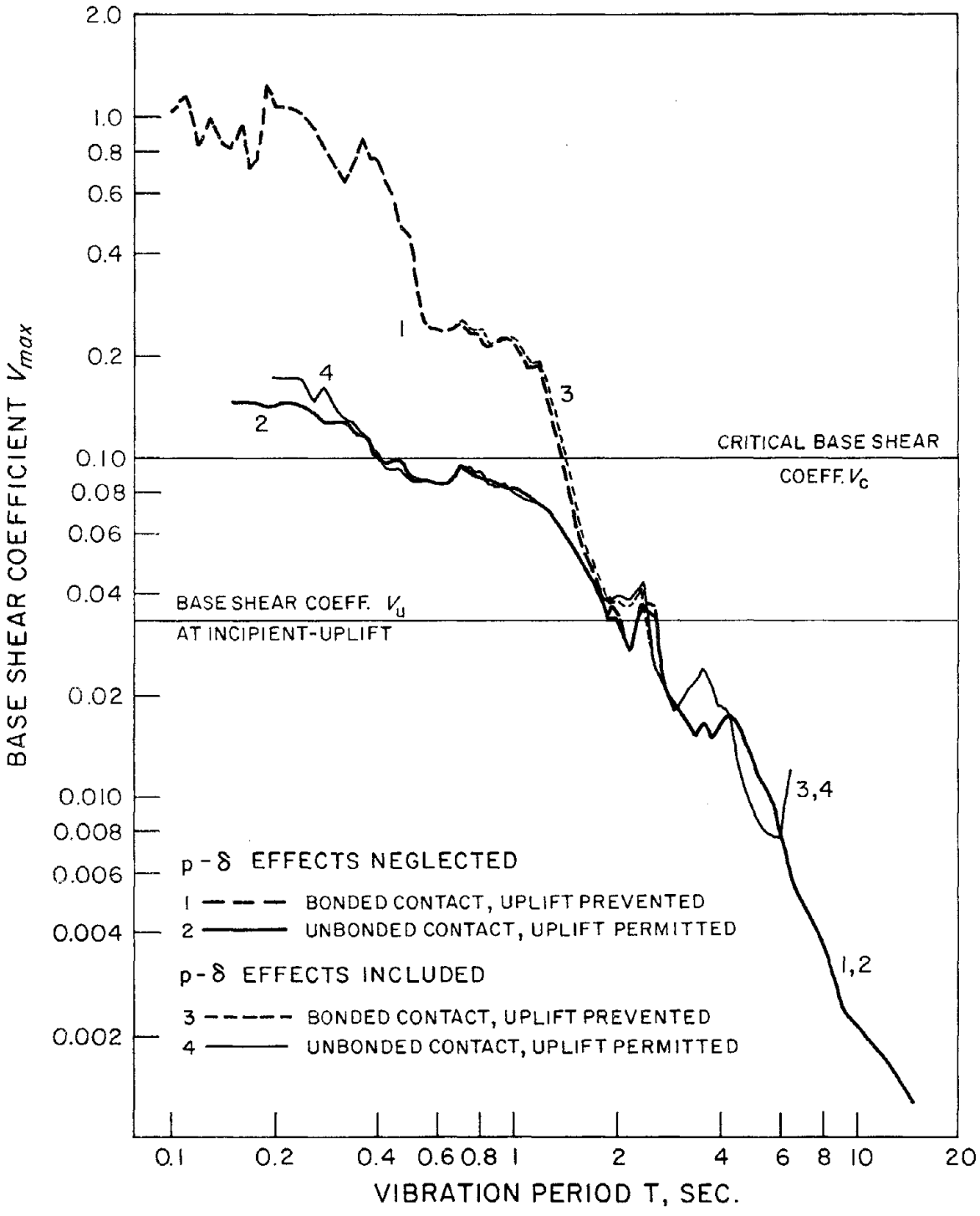

FIGURE 3.17 Response spectra for structures ($\alpha = 10$, $\beta = 8$, $\xi = 0.05$, $\xi_v = 0.4$) subjected to El Centro ground motion for two cases: (a) p–δ effects neglected, and (b) p–δ effects included.

4. CONCLUSION

The effects of transient foundation uplift on the earthquake response of buildings have been investigated. This study was based on structural idealizations that are relatively simple but realistic in the sense that they incorporate the most important features of foundation uplift. In its fixed base condition the structure itself was idealized as a single-degree-of-freedom system attached to a rigid foundation which is flexibly supported. The flexibility and damping of the supporting soil was represented by two alternative idealizations: (a) two spring-damper elements, one at each edge of the foundation mat, and (b) Winkler foundation with spring-damper elements distributed over the entire width of the foundation mat.

The critical base shear for a structure under the action of static lateral force, i.e. the maximum base shear that can be developed with its foundation mat supported only through gravity with uplift permitted, depends on the gravity force and slenderness-ratio parameter, and is the same for both idealizations of the supporting soil. The base shear in the structure at incipient uplift of the foundation mat depends on the model employed to represent the supporting soil. Uplift of the foundation mat supported on two-element foundation is not initiated until the base shear attains the critical value. In the case of Winkler foundation, uplift of the foundation mat is initiated when the base shear reaches one-third of the critical value; and as the base shear increases further the foundation mat separates over increasing width from its supporting elements.

The equations of motion for the structure with its foundation mat permitted to uplift are nonlinear with foundation stiffness and damping parameters dependent on whether the foundation mat is in contact with the supporting systems at one or both edges; and also on the extent of uplift in case of the Winkler foundation. However a linear system corresponding to any instantaneous contact condition of the foundation mat can be defined. This linear system has three degrees-of-freedom and the natural frequency of the third mode is at least an order of magnitude higher than the second mode frequency and it tends to infinity as the foundation-mat mass approaches zero. Because the contribution of this high frequency mode to the response is negligible, the Rayleigh-Ritz concept was employed to eliminate this mode from the

analysis. It was then possible to employ a much larger integration time-step than would otherwise be practical, resulting in considerable savings in computational effort.

Analytical examination of the governing equations and system properties and the numerical results obtained in this study indicate that the earthquake response of uplifting structures is controlled by the following system parameters, listed in more or less descending order of importance:

- natural vibration frequency ω of the rigidly supported structure
- slenderness-ratio parameter α
- ratio γ of foundation mass to superstructure mass
- $\beta = \omega_v / \omega$ where ω_v is the vertical vibration frequency of the system with its foundation mat bonded to supporting elements
- damping ratio ξ of the rigidly supported structure
- damping ratio ξ_v in vertical vibration of the system with its foundation mat bonded to the supporting elements.

If we had considered the large-amplitude motion of the structure including the possibility of its overturning the response of a structure would be influenced also by its size. Similarly the size influences even the small-amplitude response if p–δ effects are considered, but the results presented indicate that these effects are insignificant for most buildings.

In order to study the effects of foundation-mat uplift on the maximum response of buildings, response spectra were presented. For each set of system parameters the maximum base shear was plotted against the natural vibration period of the corresponding rigidly-supported structure for two conditions of contact between the foundation mat and the supporting spring-damper elements: (a) bonded contact preventing uplift and (b) unbonded contact with uplift permitted. A study of these response spectra plots led to the following conclusions:

1. The base shear developed in structures with relatively long vibration periods is below the static value at incipient uplift and the foundation mat does not uplift from its supporting elements.

2. For short period structures, the base shear exceeds the incipient-uplift value if foundation-mat uplift is prevented; for such structures, permitting uplift has the effect of reducing the base shear -- to values somewhat above the critical value.

3. Because the response of a structure with foundation mat permitted to uplift is controlled by the critical base shear, which is independent of the ground motion, the base shear is affected only slightly by earthquake intensity.

4. The foundation mat of a slender structure has a greater tendency to uplift resulting in greater reductions in base shear.

5. Because the critical base shear increases with mass ratio γ so does the maximum earthquake induced base shear.

6. The shape of the response spectrum is affected little by the frequency ratio β, but it does have the effect of shifting the response spectrum to the left with larger shift for smaller β, i.e. for the more flexible supporting elements.

The possibility of transient uplift of a portion of the foundation mat or of a few individual footings, as the case may be, should be considered in the analysis of response of structures subjected to intense earthquake ground motion. Because foundation uplift has the effect of reducing the structural deformations and forces, there is no need to prevent it but, on the contrary, it is desirable to permit it. The foundation, underlying soil and the structural columns should be properly designed to accommodate the transient uplift and the effects of subsequent impact on contact.

Note that the conclusions drawn in this study are based on the dynamic response of structures to horizontal ground excitations only, the vertical component of the ground excitation is assumed to be negligible for simplicity. However, this component of the ground motion may

have significant influence on the dynamic response of the flexible structure under some combinations of structure-foundation system parameters and ground excitations. This is especially true if the dominant frequency of the vertical excitation is close to the vertical free vibration frequency of the structure-foundation system, leading to large amplification in the vertical response and hence large influence on the uplift response.

Although the results of this work have provided an understanding of the basic effects of transient foundation uplift on the earthquake response of structures, there is an important limitation in the application of these results to actual buildings. In reality the foundation stiffness and damping parameters depend on the displacement amplitude and, excitation frequency, in contrast to the constant parameters employed in this work. In either case, the foundation parameters are very difficult to evaluate because they would depend on the details of the foundation design, including the degree of foundation embedment and the base deformability. Reliable methods to evaluate foundation parameters for actual buildings need to be developed, so that the beneficial effects of foundation uplift can be considered in the design of buildings.

REFERENCES

1. Psycharis, I.N., "Dynamic Behavior of Rocking Structures Allowed to Uplift," *Report No. EERL 81-02,* Earthquake Engineering Research Laboratory, California Institute of Technology, Pasadena, California, August, 1981.

2. Housner, G.W., "The Behavior of Inverted Pendulum Structures During Earthquakes," *Bulletin of the Seismological Society of America,* Vol. *53,* No. 2, Feb., 1963, pp. 403-417.

3. Beck, J.L. and Skinner, R.I., "The Seismic Response of a Reinforced Concrete Bridge Pier Designed to Step," *Earthquake Engineering and Structural Dynamics,* Vol. *2,* No. 4, April-June, 1974, pp. 343-358.

4. Muto, K., Umemura, H. and Sonobe, Y., "Study of the Overturning Vibrations of Slender Structures," *Proceedings of the Second World Conference on Earthquake Engineering,* Tokyo, 1960.

5. Meek, J.W., "Effects of Foundation Tipping on Dynamic Response," *Journal of the Structural Division,* American Society of Civil Engineers, Vol. *101,* No. ST7, July, 1975, pp. 1297-1311.

6. Meek, J.W., "Dynamic Response of Tipping Core Building," *Earthquake Engineering and Structural Dynamics,* Vol. *6,* No. 5, Sept.-Oct., 1978, pp. 437-454.

7. Clough, R.W., and Huckelbridge, A.A., "Earthquake Simulation Tests of a Three-Story Steel Frame with Columns Allowed to Uplift," *Report No. UCB/EERC 77-22,* Earthquake Engineering Research Center, University of California, Berkeley, California, August, 1977.

8. Huckelbridge, A.A., and Clough, R.W., "Seismic Response of Uplifting Building Frame," *Journal of the Structural Division,* American Society of Civil Engineers, Vol. *104,* No. ST8, August, 1978, pp. 1211-1229.

9. Wolf, J.P., "Soil-Structure Interaction with Separation of Base Mat from Soil (Lifting-off)," *Nuclear Engineering and Design,* Vol. *38,* No. 2, August, 1976, pp. 357-384.

10. Kennedy, R.P., Short, S.A., Wesley, D.A., and Lee, T.H., "Effect on Non-linear Soil-Stucture Interaction due to Base Slab Uplift on the Seismic Response of a High-Temperature Gas-Cooled Reactor (HTGR)," *Nuclear Engineering and Design,* Vol. *38,* No. 2, August, 1976, pp. 323-355.

11. Veletsos, A.S., and Verbic, B., "Vibration of Viscoelastic Foundations," *International Journal of Earthquake Engineering and Structural Dynamics,* Vol. *2,* No. 1, July-Sept., 1973, pp. 87-102.

12. Seed, H.Bolton, and Idriss, I.M., "Soil Moduli and Damping Factors for Dynamic Response Analyses," *Report No. UCB/EERC 70-10,* Earthquake Engineering Research Center, University of California, Berkeley, California, December, 1970.

APPENDIX A: NOTATION

b	half width of foundation mat
c	lateral damping coefficient of superstructure
c_f	damping coefficient of supporting element of two-element foundation
c_w	damping coefficient per unit width of Winkler foundation
f_s	lateral force applied to superstructure
f_{sc}	maximum static lateral force on structure at full uplift of foundation mat with contact reduced to one edge
f_{su}	static lateral force on structure at incipient uplift of foundation mat on Winkler foundation
g	acceleration of gravity
h	height of superstructure
I_o	moment of inertia of foundation mat
k	lateral stiffness of superstructure
k_f	stiffness of supporting element of two-element foundation
k_w	stiffness per unit width of Winkler foundation
m	mass of superstructure
m_o	mass of foundation mat
M	static base moment applied at c.g of foundation mat
M_c	maximum static base moment at full uplift of foundation mat with contact reduced to one edge
M_u	static base moment at incipient uplift of foundation mat supported on Winkler foundation

p	static vertical force on foundation mat
R_l	upward reaction of left supporting element of two-element foundation
R_r	upward reaction of right supporting element of two-element foundation
$\mathbf{r}$	displacement vector for structure-foundation system
$\bar{\mathbf{r}}$	reduced displacement vector of structure-foundation system
$t, t', \bar{t}$	time measured from a specified reference
T	natural vibration period of the rigidly supported structure
T_c	rocking vibration period of flexibly supported structure with uplift prevented
T_u	rocking vibration period of flexibly supported structure with uplift permitted
$\mathbf{T}$	displacement transformation matrix defined in equation 2.20a
u	structural deformation
u_c	maximum structural deformation under the action of static lateral force
$u_g(t)$	horizontal ground displacement
$\ddot{u}_g(t)$	horizontal ground acceleration
$u_{\max}$	maximum structural deformation during an earthquake
u_u	static structural deformation at incipient uplift of foundation mat on Winkler foundation
v	vertical displacement of c.g of foundation mat
v_l	vertical displacement of left edge of foundation mat
v_r	vertical displacement of right edge of foundation mat
v_s	vertical displacement of foundation mat under the action of gravity forces
$V_{\max}$	a base shear coefficient $= \mathbf{V}_{\max} / w$

V_c a base shear coefficient $= \mathbf{V}_c / w$

V_u a base shear coefficient $= \mathbf{V}_u / w$

$\mathbf{V_c}$ maximum base shear that can be deveolped under the action of static lateral force

$\mathbf{V_u}$ static base shear at incipient uplift of foundation mat on Winkler foundation

$\mathbf{V}_{max}$ maximum base shear

w weight of superstructure

x lateral displacement of structure relative to supporting foundation $= u + h\theta$

$\dot{x}(0)$ initial velocity of structure

$\dot{x}(0)_c$ minimum initial velocity of structure inducing foundation-mat uplift of structure supported on two-element foundation

$\dot{x}(0)_u$ minimum initial velocity of structure inducing foundation-mat uplift of structure supported on Winkler foundation

$\bar{\dot{x}}(0)$ normalized initial velocity of structure

$\mathbf{Z}$ vector of generalized coordinates Z_i

α slenderness ratio parameter

β $= \omega_v / \omega$

γ ratio of foundation mass to superstructure mass

Δt integration time-step

ϵ_i contact coefficients (defined in sections 2.2 and 3.2)

ζ_i damping ratio of the i^{th} vibration mode after uplift

θ rotation of foundation mat

θ_c static rotation of foundation mat at full uplift with contact reduced to one edge

θ_u static rotation of foundation mat on Winkler foundation at incipient uplift

λ_i undamped natural vibration frequency of the i^{th} mode after uplift

λ'_i damped natural vibration frequency of the i^{th} mode after uplift

ξ damping ratio of the rigidly supported structure

ξ_f damping ratio in vertical vibration of the system of Figure 2.1 with its foundation mat bonded to the two-element foundation

ξ_i damping ratio of the i^{th} vibration mode of system with both edges of foundation mat in contact with foundation

ξ_w damping ratio in vertical vibration of the system of Figure 3.1 with its foundation mat bonded to the Winkler foundation

ϕ_{ij} i^{th} element of the j^{th} free vibration mode $\boldsymbol{\phi}_j$

$\boldsymbol{\phi}_i$ i^{th} vibration mode of system with foundation mat in contact with both edges of foundation

ψ_{ij} i^{th} element of the j^{th} free vibration mode $\boldsymbol{\psi}_j$

$\boldsymbol{\psi}_i$ i^{th} vibration mode of system after uplift

$\boldsymbol{\Psi}$ displacement transformation matrix (see equation 3.7a)

ω natural vibration frequency of the rigidly supported structure

ω_i natural vibration frequency of the i^{th} mode of system with both edges of foundation mat in contact with supporting elements

ω_v vertical vibration frequency of the system with its foundation mat bonded to the supporting elements

ω'_i ω_i modified by damping

APPENDIX B: DERIVATION OF EQUATIONS OF MOTION

B.1 Equilibrium Equations

Free body diagrams of the top mass and the structure including foundation-mat mass and inertia are shown in Figures B.1a and b, respectively. Equations of motion for both systems with two-element as well as Winkler foundations can be derived by considering: (1) equilibrium of forces of the top mass in the horizontal direction, (2) equilibrium of moment of the entire structure about the center of the foundation mat and (3) equilibrium of forces of the entire structure in the vertical direction. The displacement of the top mass and the rotation of the foundation mat are assumed to be small enough that $\sin(\theta + \frac{u}{h})$ can be replaced by $(\theta + \frac{u}{h})$ and $\cos(\theta + \frac{u}{h})$ by unity. Except for the $p-\delta$ effects due to gravity acting on the top mass, all secondary nonlinear effects including the contribution of moment about the center of the foundation mat by the horizontal reaction forces of the supporting medium due to eccentricity are assumed to be negligible.

First, considering the top mass as a free body (Figure B.1a), equilibrium of forces in the horizontal direction ($\sum F_x = 0$) yields

$$m\ddot{u} + m(h\ddot{\theta}) + c\dot{u} + ku = -m\ddot{u}_g(t) - m\frac{(u + h\theta)}{h}(\ddot{v} + g) \tag{B.1}$$

and in the vertical direction ($\sum F_y = 0$) yields

$$p = m(\ddot{v} + g) \tag{B.2}$$

Then, considering the entire structure as a free body (Figure B.1b), equilibrium of moment of the structure about the center, o, of the foundation mat ($\sum M_o = 0$) yields

$$I_o\ddot{\theta} + mh(\ddot{u} + h\ddot{\theta}) + M_f = -mh\ddot{u}_g(t) + m(u + h\theta)(\ddot{v} + g) \tag{B.3}$$

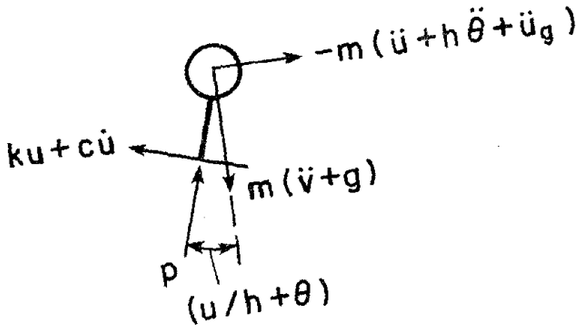

(a) Top mass

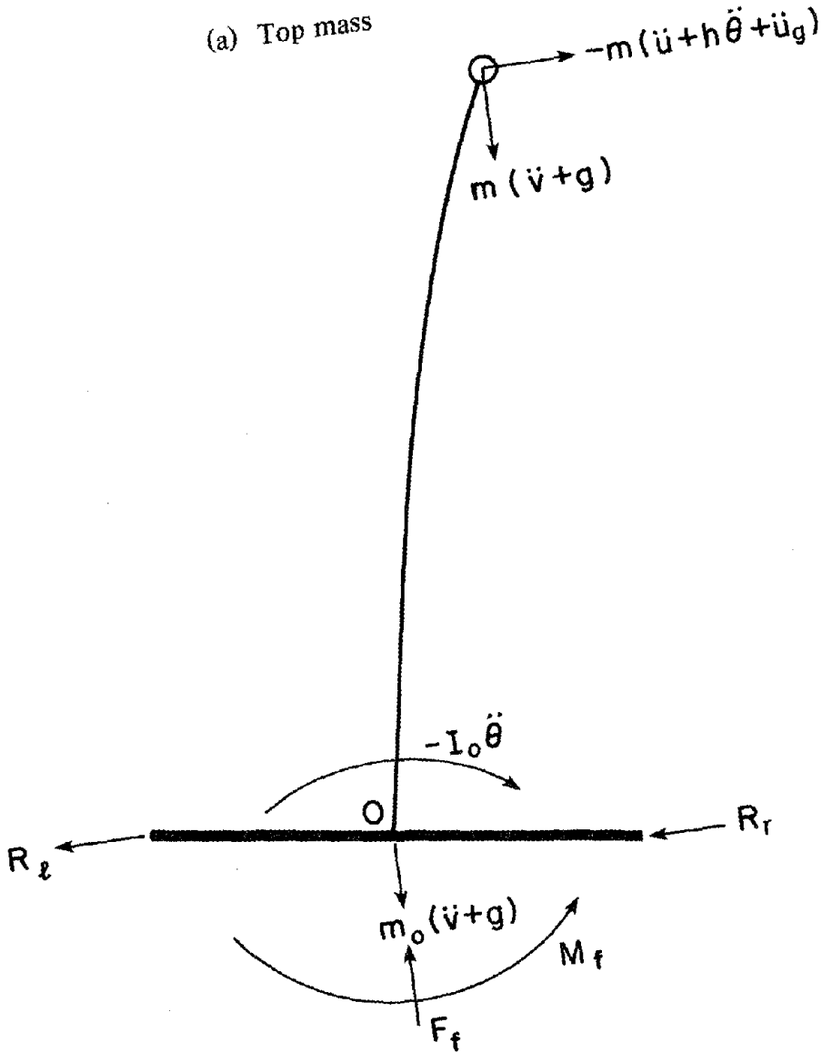

(b) Structure

FIGURE B.1 Free-body diagrams for top mass and structure.

and equilibrium of forces of the structure in the vertical direction ($\sum F_y = 0$) yields

$$(m + m_o)\ddot{v} - F_f = -(m + m_o)g \tag{B.4}$$

The thickness of the rigid foundation mat is assumed to be small compare to the width $2b$ so that $I_o = m_o b^2/3$. Equations B.1, B.2 and B.4 form a set of general equations governing the motion of the structural system for both types of foundation support. While equation B.1 is already in explicit form equations B.3 and B.4 need further specialization for each system.

B.2 Structure on Two-Element Foundation

For the system with two-element foundation, the upward reaction force, F_f, and restoring moment, M_f, about the c.g of the foundation mat, are the sum and the moment of the reaction forces of the two elements, F_l and F_r, acting at the left and right edges of the foundation mat respectively (Figure B.2a) :

$$F_f = F_l + F_r \tag{B.5a}$$

and

$$M_f = b(F_r - F_l) \tag{B.5b}$$

where

$$F_l = \begin{cases} -k_f(v + b\theta) - c_f(\dot{v} + b\dot{\theta}) & \textit{left edge in contact} \\ 0 & \textit{left edge uplifted} \end{cases} \tag{B.6a}$$

and

$$F_r = \begin{cases} -k_f(v - b\theta) - c_f(\dot{v} - b\dot{\theta}) & \textit{right edge in contact} \\ 0 & \textit{right edge uplifted} \end{cases} \tag{B.6b}$$

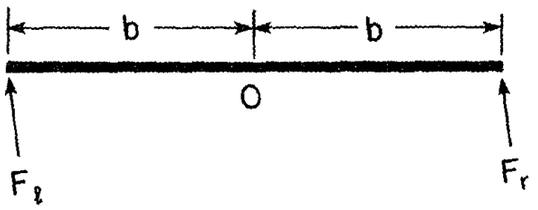

(a) Two spring-damper element foundation

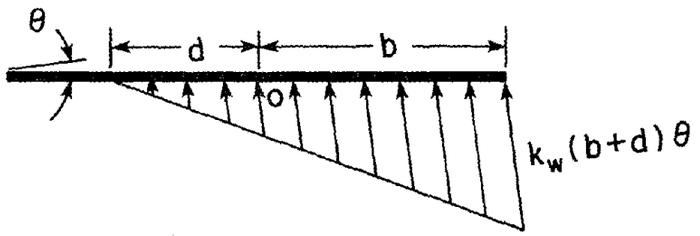

(b) Winkler foundation

FIGURE B.2 Foundation reaction forces.

Substituting equations B.5 and B.6 into equations B.3 and B.4 and simplifying using equation B.1, the equations for equilibrium of moment about the c.g of the foundation mat and equilibrium of forces in the vertical direction become

$$\frac{m_o b^2}{3h^2}(h\ddot{\theta}) - c\dot{u} + \epsilon_1 c_f \frac{b^2}{h^2}(h\dot{\theta}) + \epsilon_2 c_f \frac{b}{h}\dot{v}$$

$$- ku + \epsilon_1 k_f \frac{b^2}{h^2}(h\theta) + \epsilon_2 k_f \frac{b}{h} v = 0 \tag{B.7a}$$

and

$$(m + m_o)\ddot{v} + \epsilon_1 c_f \dot{v} + \epsilon_2 c_f \frac{b}{h}(h\dot{\theta}) + \epsilon_1 k_f v + \epsilon_2 k_f \frac{b}{h}(h\theta) = -(m + m_o) g \tag{B.7b}$$

respectively, where ϵ_1 and ϵ_2 depend on the contact conditions:

$$\epsilon_1 = \begin{cases} 2 & \textit{contact at both edges} \\ 1 & \textit{left or right edge uplifted} \end{cases} \tag{B.8a}$$

and

$$\epsilon_2 = \begin{cases} -1 & \textit{left edge uplifted} \\ 0 & \textit{contact at both edges} \\ 1 & \textit{right edge uplifted} \end{cases} \tag{B.8b}$$

Equations B.7a and b together with equation B.1 constitute the equations of motion 2.2 presented in Chapter 2.

B.3 Structure on Winkler Foundation

For the system with Winkler foundation, evaluation of the reaction force, F_f, and restoring moment about the c.g of the foundation mat, M_f, are more complicated with partial uplift than with full contact, and the two cases are discussed separately.

B.3.1 Full Contact

During full contact, the force-displacement and moment-rotation relations at the c.g of the foundation mat are linear and uncoupled. The upward reaction force, F_f, is dependent only on vertical displacement, v, and velocity $\dot{v}$, alone but is independent of base rotation θ and angular velocity $\dot{\theta}$; whereas the restoring moment, M_f, is a function of base rotation θ and angular rotation $\dot{\theta}$ alone but is independent of vertical displacement, v, and vertical velocity, $\dot{v}$. These relations may be expressed as follow:

$$F_f = -2k_w bv - 2c_w b\dot{v} \tag{B.9a}$$

and

$$M_f = \frac{2}{3} k_w b^3\theta + \frac{2}{3} c_w b^3\dot{\theta} \tag{B.9b}$$

B.3.2 Partial Uplift

For the case with partial uplift, the upward reaction force, F_f, and the restoring moment, M_f, about the c.g of the foundation mat can be obtained by integrating the distributed force and moment about center o, due to elastic spring reaction and damping, over the region of contact (Figure B.2b).

$$F_f = \int_0^{b+d} k_w |\theta| x\, dx - \int_{-d}^{b} c_w (\dot{v} + \epsilon_2 \dot{\theta} x)\, dx$$

$$= k_w \frac{(b+d)^2}{2} |\theta| - c_w \left\{ (b+d)\dot{v} + \epsilon_2 \frac{(b^2 - d^2)}{2} \dot{\theta} \right\} \tag{B.10a}$$

and

$$M_f = \int_0^{b+d} k_w \theta (x - d) x \, dx + \epsilon_2 \int_{-d}^{b} c_w (\dot{v} + \epsilon_2 \dot{\theta} x) x \, dx$$

$$= k_w \frac{(2b - d)(b + d)^2}{6} \theta + c_w \left\{ \frac{\epsilon_2 (b^2 - d^2)}{2} \dot{v} + \epsilon_2 \frac{(b^3 + d^3)}{3} \dot{\theta} \right\} \qquad \text{(B.10b)}$$

where

$$\epsilon_2 = \begin{cases} -1 & \textit{left edge uplifted} \\ 0 & \textit{contact at both edges} \\ 1 & \textit{right edge uplifted} \end{cases} \qquad \text{(B.11a)}$$

The distance, d, from the point where partial uplift begins to the c.g of the foundation mat, o, is a function of the vertical displacement, v, and rotation of the c.g of the mat:

$$d = \begin{cases} -\dfrac{v}{b} / |\theta| & \theta \neq 0 \quad \textit{partially uplifted} \\ & \textit{contact at both edges} \end{cases}$$

and

$$|d| \leqslant b$$

Note that when the system is at incipient uplift or during full contact, the distance between the point of separation and c.g is equal to b, i.e. $d = b$ and equations B.9 and B.10 are identical. Thus equation B.9 can be considered as a special case of equation B.10. Defining ϵ_1 as the quotient of d and half-base-width b, i.e.

$$\epsilon_1 = \frac{d}{b} \qquad \text{(B.11b)}$$

and substituting equations B.11a and b into equations B.3 and B.4 and simplifying the resulting expressions using equation B.1 yield:

$$\frac{m_o b^2}{3h^2}(h\ddot{\theta}) - c\dot{u} + (1+\epsilon_1^3)\, c_w \frac{b^3}{3h^2}(h\theta) + (1-\epsilon_1^2)\,\epsilon_2 c_w \frac{b^2}{2h}\, \dot{v}$$

$$- ku + (1+\epsilon_1^3)\, k_w \frac{b^3}{3h^2}(h\theta) + (1-\epsilon_1^2)\,\epsilon_2 k_w \frac{b^2}{2h}\, v = 0 \qquad \text{(B.12)}$$

$$(m+m_o)\,\ddot{v} + (1+\epsilon_1)\, c_w b\dot{v} + (1-\epsilon_1^2)\,\epsilon_2 c_w \frac{b^2}{2h}(h\dot{\theta})$$

$$+ (1+\epsilon_1)\, k_w bv + (1-\epsilon_1^2)\,\epsilon_2 k_w \frac{b^2}{2h}(h\theta) = -(m+m_o)\, g \qquad \text{(B.13)}$$

Equations B.12 and B.13 together with equation B.1 constitute the equations of motion for the system with Winkler foundation (equation 3.2) presented in Chapter 3.

APPENDIX C: MODAL RESPONSE CONTRIBUTIONS

C.1 Frequencies and Mode Shapes

The frequencies and mode shapes of the systems with two-element as well as Winkler foundations can be obtained by solving the well known eigenvalue problem

$$\left[\mathbf{k} - \omega_i^2 \mathbf{m}\right] \boldsymbol{\phi}_i = 0 \tag{C.1}$$

where $\mathbf{m}$ and $\mathbf{k}$ are the mass and stiffness matrices respectively, and $\boldsymbol{\phi}_i$, $i = 1,..., n$, are the mode shapes corresponding to the n frequencies ω_i's of the n-DOF system considered. The mass and stiffness matrices for the two-element and Winkler systems can be derived from equation 2.2 in Chapter 2 and equation 3.2 in Chapter 3 respectively. These matrices are put into symmetric form by adding the first row of each matrix to their corresponding second row before solving the eigenvalue problem for each system.

C.1.1 Structure on Two-Element Foundation

As discussed in section 2.3, the linear systems representing the system with two-element foundation during full contact and after uplift have different vibration properties. These linear systems are studied separately in the following subsections.

Full Contact

During full contact, the symmetric mass matrix, $\mathbf{m}$, and stiffness matrix, $\mathbf{k}$, can be obtained from equation 2.2 by using the appropriate values for the contact coefficients ($\epsilon_1 = 2$ and $\epsilon_2 = 0$):

$$\mathbf{m} = \begin{bmatrix} m & m & 0 \\ m & m+\dfrac{m_o b^2}{3h^2} & 0 \\ 0 & 0 & m+m_o \end{bmatrix} \tag{C.2a}$$

and

$$\mathbf{k} = \begin{bmatrix} k & 0 & 0 \\ 0 & 2k_f \dfrac{b^2}{h^2} & 0 \\ 0 & 0 & 2k_f \end{bmatrix} \tag{C.2b}$$

The resulting frequencies obtained by solving equation C.1 are:

$$\begin{aligned} \omega_1 &= \omega\bar{\omega}_1 \\ \omega_2 &= \omega\beta \\ \omega_3 &= \omega\bar{\omega}_3 \end{aligned} \tag{C.3a}$$

with corresponding mode shapes

$$\begin{aligned} \boldsymbol{\phi}_1^T &= \left\{ \begin{array}{ccc} \bar{\omega}_1^2 & (1-\bar{\omega}_1^2) & 0 \end{array} \right\} \\ \boldsymbol{\phi}_2^T &= \left\{ \begin{array}{ccc} 0 & 0 & 1 \end{array} \right\} \\ \boldsymbol{\phi}_3^T &= \left\{ \begin{array}{ccc} \bar{\omega}_3^2 & (1-\bar{\omega}_3^2) & 0 \end{array} \right\} \end{aligned} \tag{C.3b}$$

where

$$\bar{\omega}_{1,3} = \left\{ \frac{\tau_1 \mp \left[\tau_1^2 - \frac{4\gamma}{3}(1+\gamma)\beta^2 \right]^{1/2}}{\frac{2}{3}\gamma} \right\}^{1/2} \tag{C.3c}$$

and

$$\tau_1 = (1+\gamma)\beta^2 + \alpha^2 + \frac{\gamma}{3}$$

and $\bar{\omega}_1$ and $\bar{\omega}_3$ corresponding to the upper and lower signs respectively.

After Uplift

When one of the edges is uplifted from its supporting element, the mass matrix, **m**, remains unchanged. However, the stiffness matrix, **k**, derived from equation 2.2 with appropriate contact coefficients ($\epsilon_1 = 1$ and $\epsilon_2 = \mp 1$) becomes

$$\mathbf{k} = \begin{bmatrix} k & 0 & 0 \\ 0 & k_f \frac{b^2}{h^2} & \mp k_f \frac{b}{h} \\ o & \mp k_f \frac{b}{h} & k_f \end{bmatrix} \tag{C.4}$$

The resulting frequencies obtained by solving equation C.1 are:

$$\lambda_1 = 0$$

$$\lambda_2 = \omega\bar{\lambda}_2 \tag{C.5a}$$

$$\lambda_3 = \omega\bar{\lambda}_3$$

with corresponding mode shapes

$$\psi_1^T = \left\{ \begin{array}{ccc} 0 & 1 & \pm 1/\alpha \end{array} \right\}$$

$$\psi_2^T = \left\{ \begin{array}{ccc} \bar{\lambda}_2^2 & \pm(1-\bar{\lambda}_2^2) & \dfrac{(1-\bar{\lambda}_2^2)}{\alpha\left\{1-2\dfrac{\bar{\lambda}_2^2}{\beta^2}\right\}} \end{array} \right\} \tag{C.5b}$$

$$\psi_3^T = \left\{ \begin{array}{ccc} \bar{\lambda}_3^2 & \pm(1-\bar{\lambda}_3^2) & \dfrac{(1-\bar{\lambda}_3^2)}{\alpha\left\{1-2\dfrac{\bar{\lambda}_3^2}{\beta^2}\right\}} \end{array} \right\}$$

where

$$\bar{\lambda}_{2,3} = \left\{ \frac{\tau_2 \mp \left[\tau_2^2 - \dfrac{2\gamma\beta^2}{9}(4\gamma + 3\alpha^2 + 3)\right]^{1/2}}{\dfrac{2}{3}\gamma} \right\}^{1/2} \tag{C.5c}$$

and

$$\tau_2 = \frac{2}{3}\beta^2\gamma + \frac{\beta^2}{2} + \frac{\gamma}{3}$$

with $\bar{\lambda}_2$ and $\bar{\lambda}_3$ corresponding to the upper and lower signs respectively. Note that ψ_1, corresponding to a zero frequency, is a rigid body mode; and the upper and lower signs in ψ_2 and ψ_3 correspond to left and right edge uplifted, respectively.

C.1.2 Structure on Winkler Foundation

Because the system with Winkler foundation during partial separation of the foundation mat from the supporting elements is continuous and nonlinear, no conventional discrete frequencies and mode shapes exist. Thus only the case with full contact is considered here. Modal analysis of the system with partial uplift using the notion of instantaneous frequencies and modes is discussed in section 3.4.

Full Contact

For the system during full contact, the symmetric mass matrix, **m**, and stiffness matrix, **k**, derived from equation 3.2 with contact coefficients $\epsilon_1 = 1$ and $\epsilon_2 = 0$ are:

$$\mathbf{m} = \begin{bmatrix} m & m & 0 \\ m & m + \dfrac{m_o b^2}{3h^2} & 0 \\ 0 & 0 & m + m_o \end{bmatrix} \tag{C.6a}$$

and

$$\mathbf{k} = \begin{bmatrix} k & 0 & 0 \\ 0 & \dfrac{2}{3} k_w \dfrac{b^3}{h^3} & 0 \\ 0 & 0 & 2k_w \end{bmatrix} \tag{C.6b}$$

respectively.

The associated frequencies are:

$$\begin{aligned} \omega_1 &= \omega\bar{\omega}_1 \\ \omega_2 &= \omega\beta \\ \omega_3 &= \omega\bar{\omega}_3 \end{aligned} \tag{C.7a}$$

with corresponding mode shapes

$$\boldsymbol{\phi}_1^T = \left\{ \begin{array}{ccc} \bar{\omega}_1^2 & (1-\bar{\omega}_1^2) & 0 \end{array} \right\}$$

$$\boldsymbol{\phi}_2^T = \left\{ \begin{array}{ccc} 0 & 0 & 1 \end{array} \right\} \qquad \text{(C.7b)}$$

$$\boldsymbol{\phi}_3^T = \left\{ \begin{array}{ccc} \bar{\omega}_3^2 & (1-\bar{\omega}_3^2) & 0 \end{array} \right\}$$

where

$$\bar{\omega}_{1,3} = \left\{ \frac{\tau \mp \left[\tau^2 - \frac{4}{9}\gamma(1+\gamma)\beta^2\right]^{1/2}}{\frac{2}{3}\gamma} \right\}^{1/2} \qquad \text{(C.7c)}$$

with

$$\tau = \frac{(1+\gamma)\beta^2}{2} + \alpha + \frac{\gamma}{3}$$

and $\bar{\omega}_1$ and $\bar{\omega}_3$ correspond to the upper and lower signs respectively. Because there is an equivalent relation between the systems with two-element and Winkler foundation during full contact (see section 3.3) only the two-element system need to be considered in the subsequent linear analysis in this appendix.

C.2 Limiting Values of High Frequencies

In general, the range of the numerical values of the base mass varies from as low as negligible ($\gamma = 0$) to about the same as the top mass ($\gamma = 1$). While the frequency coefficients $\bar{\omega}_2$ ($= \beta$) during full contact and $\bar{\lambda}_1$ ($= 0$) After uplift are independent of γ, $\bar{\omega}_1$ and $\bar{\lambda}_2$ do not vary significantly for most combinations of aspect ratio parameter α and frequency ratio β.

On the contrary the two coefficients for the high frequency modes, $\bar{\omega}_3$ during full contact and $\bar{\lambda}_3$ after uplift are very sensitive to the variations in the mass ratio γ in this range and approach infinity as γ approaches zero. This observation can be demonstrated mathematically by first rewriting the expressions for $\bar{\omega}_3$ and $\bar{\lambda}_3$ as follows:

$$\bar{\omega}_3 = \left\{ \frac{\tau_1}{\frac{2\gamma}{3}} \left\{ 1 + \left[1 - \frac{4\gamma}{3} \frac{(1+\gamma)\beta^2}{\tau_1^2} \right]^{1/2} \right\} \right\}^{1/2} \tag{C.8a}$$

$$\bar{\lambda}_3 = \left\{ \frac{\tau_2}{\frac{2\gamma}{3}} \left\{ 1 + \left[1 - \frac{2\gamma\beta^2}{9} \frac{(4\gamma + 3\alpha^2 + 3)}{\tau_2^2} \right]^{1/2} \right\} \right\}^{1/2} \tag{C.8b}$$

Taking the limit as $\gamma \to 0$:

$$\tau_1 \to \beta^2 + \alpha^2$$

$$\tau_2 \to \frac{\beta^2 + 2\alpha^2}{2}$$

and the second term inside the large square brackets in both equations C.8a and b approach zero, thus

$$\lim_{\gamma \to 0} \approx \left\{ \frac{\beta^2 + \alpha^2}{2\gamma/3} \cdot 2 \right\}^{1/2} = \left[\frac{3(\beta^2 + \alpha^2)}{\gamma} \right]^{1/2} \to \infty$$

$$\lim_{\gamma \to 0} \approx \left\{ \frac{(\beta^2 + 2\alpha^2)/2}{2\gamma/3} \cdot 2 \right\}^{1/2} = \left[\frac{3(\beta^2 + 2\alpha^2)}{2\gamma} \right]^{1/2} \to \infty$$

Hence, for a given fixed-base frequency, ω, the frequency of the third mode during full contact ($\omega_3 = \omega\bar{\omega}_3$) and after uplift ($\lambda_3 = \omega\bar{\lambda}_3$) approach infinity as the mass ratio γ approaches zero.

C.3 Relative Contribution to Deformation Response

It is well known that for linear systems, the contribution of high frequency modes to the dynamic response of the system subject to earthquake type ground excitations are usually negligible. In this section the significance of the contribution of the high frequency modes to the deformation response, u, during full contact and after uplift, for the system with two-element foundation are examined.

C.3.1 Equations of Motion in Modal Coordinates

Denoting the matrix formed by the mode shapes during full contact, $\boldsymbol{\phi}$, and after uplift, $\boldsymbol{\psi}$, the displacement response in geometric coordinates, $\mathbf{v}$, of the two-element system may be expressed in terms of modal coordinates, $\mathbf{Z}$, during full contact as

$$\mathbf{v} = \boldsymbol{\Phi}\mathbf{Z} \tag{C.9a}$$

and after uplift as

$$\mathbf{v} = \boldsymbol{\Psi}\mathbf{Z} \tag{C.9b}$$

where

$$\boldsymbol{\Phi} = \begin{bmatrix} \boldsymbol{\phi}_1 & \boldsymbol{\phi}_2 & \boldsymbol{\phi}_3 \end{bmatrix} \tag{C.10a}$$

$$\boldsymbol{\Psi} = \begin{bmatrix} \boldsymbol{\psi}_1 & \boldsymbol{\psi}_2 & \boldsymbol{\psi}_3 \end{bmatrix} \tag{C.10b}$$

and

$$\mathbf{Z}^T = \begin{Bmatrix} Z_1 & Z_2 & Z_3 \end{Bmatrix} \tag{C.10c}$$

The equations of motion in modal coordinates can be obtained by substituting equation C.9 into the original equations of motion (2.2) and premultiplying the resulting matrix equation with the transpose of equation C.10.

$$\mathbf{M}\ddot{\mathbf{Z}} + \mathbf{C}\dot{\mathbf{z}} + \mathbf{K}\mathbf{z} = \mathbf{P}(t) \tag{C.11}$$

where

$$\mathbf{M} = \Phi^T \mathbf{m} \Phi \tag{C.12a}$$

$$\mathbf{C} = \Phi^T \mathbf{c} \Phi \tag{C.12b}$$

$$\mathbf{K} = \Phi^T \mathbf{k} \Phi \tag{C.12c}$$

$$\mathbf{P} = \Phi^T \mathbf{p} \tag{C.12d}$$

during full contact, and

$$\mathbf{M} = \Psi^T \mathbf{m} \Psi \tag{C.13a}$$

$$\mathbf{C} = \Psi^T \mathbf{c} \Psi \tag{C.13b}$$

$$\mathbf{K} = \Psi^T \mathbf{k} \Psi \tag{C.13c}$$

$$\mathbf{P} = \Psi^T \mathbf{p} \tag{C.13d}$$

after uplift.

C.3.2 Modal Contributions to Deformation Response

During full contact, the vertical vibration mode, $\boldsymbol{\phi}_2$, which does not contain structural deformation, u, is uncoupled with the rocking modes, $\boldsymbol{\phi}_1$ and $\boldsymbol{\phi}_3$, and will not be excited by horizontal ground motion. Thus the deformation response, u, is equal to the sum of the deformation responses of the first and third mode, i.e.,

$$u = \phi_{11} Z_1 + \phi_{13} Z_3 = \bar{\omega}_1^2 Z_1 + \bar{\omega}_3^2 Z_3 \tag{C.14}$$

After uplift, the rigid-body mode, $\boldsymbol{\phi}_1$, does not contain structural deformation, and the deformation response, u, is equal to the sum of the deformation responses of second and third mode.

$$u = \psi_{12} Z_2 + \psi_{13} Z_3 = \bar{\lambda}_2^2 Z_2 + \bar{\lambda}_3^2 Z_3 \tag{C.15}$$

The relative contributions of the high frequency modes to deformation, u, may be determined by examining their complex frequency response functions.

C.3.3 Complex Frequency Responses

Neglecting the static response due to gravity (i.e. the constant terms in the load vector $\mathbf{p}$) and assuming the horizontal ground motion to be a complex excitation of the form

$$\ddot{u}_g(t) = a\ e^{i\bar{\omega}t} \tag{C.16}$$

where a is a real constant representing the magnitude of the ground acceleration. Then, the steady state response in modal coordinates are also of the form

$$\mathbf{Z} = \bar{\mathbf{Z}}\ e^{i\bar{\omega}t} \tag{C.17}$$

where $\bar{\mathbf{Z}}$ is a function of the ratio of the excitation frequency, $\bar{\omega}$, to the fixed-base frequency, ω, of the structure alone. Successive differentiation of equation C.17 with respect to time, t,

yields the velocity and acceleration vectors

$$\dot{\mathbf{Z}} = i\bar{\omega}\bar{\mathbf{Z}}\, e^{i\bar{\omega}t} \tag{C.18a}$$

and

$$\ddot{\mathbf{Z}} = -\bar{\omega}^2\bar{\mathbf{Z}}\, e^{i\bar{\omega}t} \tag{C.18b}$$

Substituting equations C.16-18 into equation C.11 and cancelling the time dependent exponential term, $e^{i\bar{\omega}t}$, from both sides, a complex matrix equation as a function of the ratio of excitation frequency, $\bar{\omega}$, to the fixed-base frequency, ω, alone is obtained:

$$\left[\mathbf{K} - \bar{\omega}^2\mathbf{M} + i\bar{\omega}\mathbf{C}\right]\bar{\mathbf{Z}} = \bar{\mathbf{P}} \tag{C.19}$$

It can be shown that $\bar{\mathbf{P}}$ is real and constant during full contact as well as after uplift. However, the generalized coordinates vector $\bar{\mathbf{Z}}$, which is obtained by formally inverting the complex matrix equation C.19, is in general complex. Once the complex frequency response in modal coordinates of the system is known, the relative contribution of the high frequency modes during full contact and after uplift can be determined by examining the relative magnitudes of the pseudo acceleration responses normalized with respect to maximum ground acceleration a, including the high frequency modes contributions

$$|\omega^2 u|/a = \begin{cases} \omega^2|\bar{\omega}_1^2 z_1 + \bar{\omega}_3^2 z_3|/a & \textit{full contact} \\ \omega^2|\bar{\lambda}_2^2 z_2 + \bar{\omega}_3^2 z_3|/a & \textit{after uplift} \end{cases} \tag{C.20a}$$

and neglecting the high frequency mode contributions

$$|\omega^2 u'|/a = \begin{cases} \omega^2|\overline{\omega_1}^2 z_1|/a & \textit{full contact} \\ \omega^2|\overline{\lambda_2}^2 z_2|/a & \textit{after uplift} \end{cases} \tag{C.20b}$$

respectively.

The normalized pseudo acceleration responses as functions of the frequency ratio $\bar{\omega}/\omega$ for a series of typical two-element systems with mass ratio $\gamma = 0$, varying slenderness ratio parameter α and frequency ratio β for both full contact and after uplift are obtained by solving equation C.19 numerically. Small structural and foundation damping ratios ($\xi = 0.05$ and $\xi_v = 0.15$) are used to emphasize the responses. It was observed that for the case with full contact, the pseudo acceleration responses including and neglecting the high frequency mode are practically identical; whereas the agreement between the two responses for the case after uplift is also very good with maximum difference of less than 5 percent in relative magnitude. Further more, varying mass ratio γ, aspect ratio parameter α, and frequency ratio β does not seem to affect the quality of the agreement between the two responses.

Thus the contributions of the high frequency modes to the deformation response during full contact and after uplift are negligible and can be analytically eliminated in the numerical study of the behavior of the structural foundation system.

APPENDIX D: NUMERICAL PROCEDURES

The reduced systems of equations of motion of a structure on two-element foundation described in Section 2.5 and a structure on Winkler foundation described in Section 3.4 are integrated directly using the Newmark method assuming linear variation of acceleration. For systems with constant mass, stiffness and damping matrices, this implicit method, which satisfies dynamic equilibrium at the end of each time-step, is unconditionally stable. The details are well documented and will not be repeated here.* At each time-step, the displacement $\mathbf{v}_{t+\Delta t}$ is obtained by solving the following matrix equation:

$$\mathbf{K}_e \mathbf{v}_{t+\Delta t} = \mathbf{R}_{t+\Delta t} \tag{D.1}$$

where $\mathbf{K}_e$ and $\mathbf{R}_{t+\Delta t}$ are the effective stiffness matrix and effective load respectively. For the structural systems considered here, the effective stiffness matrices are two-by-two and equation D.1 can be solved efficiently using Cramer's rule. Because the transformation matrices used in reducing the original equations of motion -- $\mathbf{T}$ (equation 2.20) -- for the system with two-element foundation and -- $\mathbf{\Psi}$ (equation 3.7) -- for the system with Winkler foundation as well as the stiffness and damping matrices for both systems depend on the contact condition through the contact coefficients ϵ_1 and ϵ_2 (equations 2.2 and 3.2), the effective stiffness matrix for both systems also depend on the contact condition. Satisfying equilibrium at the end of the time-step requires that the effective stiffness matrix $\mathbf{K}_e$ used in obtaining the displacement $\mathbf{v}_{t+\Delta t}$ be constant over the entire time interval Δt and correspond to the contact condition at time $t+\Delta t$ governed by the yet unknown displacement $\mathbf{v}_{t+\Delta t}$. To ensure this correspondence, special procedures are incorporated into the original integration scheme.

* Bathe, K.-J., and Wilson, E.L., *Numerical Methods in Finite Element Analysis,* Prentice-Hall, 1976.

D.1 Structure on Two-Element Foundation

As discussed in Section 2.2, there are three contact conditions for a structure on two-element foundation: (1) contact at both edges, (2) left edge uplifted, and (3) right edge uplifted. Under each contact condition, the mass, stiffness, damping as well as the transformation matrices are constant. Based on numerical results observed, the effective stiffness matrix corresponding to each contact condition differ significantly from the others. Constancy of the effective stiffness matrix over the entire interval of integration implies that the contact condition corresponding to the displacement at the end of the time-step must be the same as the one at the beginning of the time-step. Otherwise, the interval of integration has to be divided into two subintervals with the first ending at incipient uplift or recontact so that within each subinterval constant effective stiffness matrix corresponding to the same contact condition may apply. Fortunately, due to the nature of the system and the excitations, the displacement response varies smoothly with time. The system stays under each particular contact condition for relatively long periods of time and only a few transitions from one contact condition to another occur over the entire duration of the response.

To avoid recomputation of the effective at each time-step, the effective stiffness matrices $\mathbf{K}_{e,j}$, $j = 1,2,3$, for the three contact condition are stored. At each time-step, the effective stiffness corresponding to the contact condition at the beginning of the time-step is used in equation D.1 to obtain the displacement $\mathbf{v}_{t+\Delta t}$. Then the contact condition at the end of the time-step corresponding to $\mathbf{v}_{t+\Delta t}$ is evaluated. If the resulting contact condition is equal to the one at the beginning of the time-step, the integration for the time-step is completed and no iteration is necessary.

However, in the few occasions when the contact condition corresponding to the displacement at the end of the time-step is not equal to the assumed one, i.e. a transition occurs, iteration is required to ensure that the edge involved is at incipient uplift or recontact, i.e. $v_i = 0$, $i = l$ *or* r, at the instant effective stiffness matrix is changed in the integration procedure. The

time-step is divided into two subintervals: $\eta\Delta t$ and $(1-\eta)\Delta t$, with $t+\eta\Delta t$ being the time at which one edge of the foundation mat is at incipient uplift or recontact. The ratio η is obtained iteratively base on the ratio of the magnitude of the edge displacement from $v_{i,t}$ at time t to $v_{i,t+\eta\Delta t}=0$ at time $t+\eta\Delta t$ to the magnitude of displacement from $v_{i,t+\Delta t}$ at time t to $v_{i,t+\Delta t}$ at time $t+\Delta t$ assuming no transition has occurred. This linear interpolation is repeated until the magnitude of the edge displacement obtained at time $t+\eta\Delta t$ is less than a predetermined tolerance limit. The displacement, velocity, and acceleration at corresponding to this transition time $t+\eta\Delta t$ is determined. Then the integration is carried out for the remaining part of the time-step with step size equal to $(1-\eta)\Delta t$ using the new contact condition and the displacement, velocity, and acceleration at the transition as initial values. The typical step size used in this procedure is $\Delta t = 0.01$, which is significantly larger than that required to accurately integrate the original three degrees-of-freedom system as discussed in Section 2.5.

D.2 Structure on Winkler Foundation

The reduced system of equations is integrated numerically using the same implicit Newmark method assuming linear variation of acceleration as mentioned above. At each time-step the displacements in modal coordinates $\mathbf{Z}_{t+\Delta t}$ is obtained by solving iteratively the nonlinear matrix equation

$$\mathbf{K}_e(\epsilon_1)\,\mathbf{Z}_{t+\Delta t} = \mathbf{R}_{t+\Delta t} \tag{D.2}$$

where the effective stiffness matrix $\mathbf{K}_e(\epsilon_1)$ and the effective load $\mathbf{R}_{t+\Delta t}$ depend continuously on contact coefficient ϵ_1. Unlike the system of a structure on two-element foundation, the system of a structure on Winkler foundation has, theoretically, infinitely many contact conditions due to the continuous nature of supporting spring-damper elements. Fortunately, like the system supported on a two-element foundation, the displacement response of the system supported on a Winkler foundation is also smooth. Under this assumption, the changes in the coefficients of the stiffness, damping, transformation, as well as effective stiffness matrix over

the time interval Δt are small for sufficient small Δt's, and the requirement for matching contact conditions at the beginning and ending of the time-step may be relaxed.

To avoid costly computation of the effective stiffness matrix $\mathbf{K}_e(\epsilon_1)$ at each iteration corresponding to the new set of foundation-mat rotation and vertical displacement, only a finite (yet sufficiently large) number (say n) of effective stiffness matrices $\{ \mathbf{K}_{e,1}, ..., \mathbf{K}_{e,n} \}$ corresponding to a set of discrete values of contact coefficient $\{ \epsilon_{1_1}, ..., \epsilon_{1_n} \}$ are determined and stored. At each time step, dynamic equilibrium is satisfied at the end of the time step with the effective stiffness matrix $\mathbf{K}_{e,j} = \mathbf{K}_e(\epsilon_{1_j})$ chosen from the ones stored corresponding to the contact coefficient ϵ_{1_j} closest to the one given by equation 3.3a using the foundation-mat rotation and vertical displacement obtained from the previous iteration. Convergence is achieved at the i^{th} cycles when the effective stiffness matrix $\mathbf{K}_{e,j(i)}$ used for the particular iteration is identical to the effective matrix $\mathbf{K}_{e,j(i+1)}$ corresponding to contact coefficient $\epsilon_{1_{j(i+1)}}$ given by the resulting displacement $\{ h\theta_{t+\Delta t}^{(i+1)}, v_{t+\Delta t}^{(i+1)} \}$ which are in turn derived from the generalized displacement vector $\mathbf{Z}_{t+\Delta t}^{(i+1)}$ through the transformation equation 3.7; or equivalently convergence is achieved when $\epsilon_{1_{j(i+1)}} = \epsilon_{1_{j(i)}}$.

This procedure to eliminate the contribution of the high frequency component is similar to the Ritz method used in the two-element system analysis. If the foundation mat is massless, this procedure is equivalent to the static condensation approach outlined in section 3.2. The typical step size used in this procedure is 0.001 second. Such small step size is needed to obtain stable and accurate solutions and ensure convergence of the solutions of equation D.2 within a few cycles at each time-step.

The numerical procedure may be summarized as follows:

1. For $i = 0$, using the known generalized displacement $\mathbf{Z}_t$, velocity $\dot{\mathbf{Z}}_t$ and acceleration $\ddot{\mathbf{Z}}_t$ at time step t as initial estimate of generalized displacement, velocity and acceleration of the system $\mathbf{Z}_{t+\Delta t}^{(0)}$, $\dot{\mathbf{Z}}_{t+\Delta t}^{(0)}$ and $\ddot{\mathbf{Z}}_{t+\Delta t}^{(0)}$

respectively, determine contact coefficient $\epsilon_{l_{j(i)}}$, effective stiffness matrix $\mathbf{K}_{e,j(i)}$, and effective load $\mathbf{R}^{(i)}_{t+\Delta t}$ based on $\{ h\theta^{(i)}_{t+\Delta t}, \nu^{(i)}_{t+\Delta t} \}$ derived from $\mathbf{Z}^{(i)}_{t+\Delta t}$.

2. Solve equation D.2 to obtain the new values of generalized displacement, velocity and acceleration:

$$\mathbf{Z}^{(i+1)}_{t+\Delta t},\ \dot{\mathbf{Z}}^{(i+1)}_{t+\Delta t},\ \ddot{\mathbf{Z}}^{(i+1)}_{t+\Delta t}.$$

3. Evaluate new coefficient of contact $\epsilon_{l_{j(i+1)}}$ base on $\{ h\theta^{(i+1)}_{t+\Delta t}, \nu^{(i+1)}_{t+\Delta t} \}$ derived from $\mathbf{Z}^{(i+1)}_{t+\Delta t}$.

4. Check convergence:

$$\epsilon_{l_{j(i+1)}} = \epsilon_{l_{j(i)}} \quad ?$$

If yes, iteration for this time step has completed.

5. Otherwise, using the new $\epsilon_{l_{j(i+1)}}$, determine new effective stiffness matrix $\mathbf{K}_{e,j(i+1)}$ and evaluate new effective load $\mathbf{R}^{(i+1)}_{t+\Delta t}$.

6. Advance counter: $i = i + 1$ and repeat procedure starting at step 2.

EARTHQUAKE ENGINEERING RESEARCH CENTER REPORTS

NOTE: Numbers in parentheses are Accession Numbers assigned by the National Technical Information Service; these are followed by a price code. Copies of the reports may be ordered from the National Technical Information Service, 5285 Port Royal Road, Springfield, Virginia, 22161. Accession Numbers should be quoted on orders for reports (PB --- ---) and remittance must accompany each order. Reports without this information were not available at time of printing. The complete list of EERC reports (from EERC 67-1) is available upon request from the Earthquake Engineering Research Center, University of California, Berkeley, 47th Street and Hoffman Boulevard, Richmond, California 94804.

UCB/EERC-77/01 "PLUSH - A Computer Program for Probabilistic Finite Element Analysis of Seismic Soil-Structure Interaction," by M.P. Romo Organista, J. Lysmer and H.B. Seed - 1977 (PB81 177 651)A05

UCB/EERC-77/02 "Soil-Structure Interaction Effects at the Humboldt Bay Power Plant in the Ferndale Earthquake of June 7, 1975," by J.E. Valera, H.B. Seed, C.F. Tsai and J. Lysmer - 1977 (PB 265 795)A04

UCB/EERC-77/03 "Influence of Sample Disturbance on Sand Response to Cyclic Loading," by K. Mori, H.B. Seed and C.K. Chan - 1977 (PB 267 352)A04

UCB/EERC-77/04 "Seismological Studies of Strong Motion Records," by J. Shoja-Taheri - 1977 (PB 269 655)A10

UCB/EERC-77/05 Unassigned

UCB/EERC-77/06 "Developing Methodologies for Evaluating the Earthquake Safety of Existing Buildings," by No. 1 - B. Bresler; No. 2 - B. Bresler, T. Okada and D. Zisling; No. 3 - T. Okada and B. Bresler; No. 4 - V.V. Bertero and B. Bresler - 1977 (PB 267 354)A08

UCB/EERC-77/07 "A Literature Survey - Transverse Strength of Masonry Walls," by Y. Omote, R.L. Mayes, S.W. Chen and R.W. Clough - 1977 (PB 277 933)A07

UCB/EERC-77/08 "DRAIN-TABS: A Computer Program for Inelastic Earthquake Response of Three Dimensional Buildings," by R. Guendelman-Israel and G.H. Powell - 1977 (PB 270 693)A07

UCB/EERC-77/09 "SUBWALL: A Special Purpose Finite Element Computer Program for Practical Elastic Analysis and Design of Structural Walls with Substructure Option," by D.Q. Le, H. Peterson and E.P. Popov - 1977 (PB 270 567)A05

UCB/EERC-77/10 "Experimental Evaluation of Seismic Design Methods for Broad Cylindrical Tanks," by D.P. Clough (PB 272 280)A13

UCB/EERC-77/11 "Earthquake Engineering Research at Berkeley - 1976," - 1977 (PB 273 507)A09

UCB/EERC-77/12 "Automated Design of Earthquake Resistant Multistory Steel Building Frames," by N.D. Walker, Jr. - 1977 (PB 276 526)A09

UCB/EERC-77/13 "Concrete Confined by Rectangular Hoops Subjected to Axial Loads," by J. Vallenas, V.V. Bertero and E.P. Popov - 1977 (PB 275 165)A06

UCB/EERC-77/14 "Seismic Strain Induced in the Ground During Earthquakes," by Y. Sugimura - 1977 (PB 284 201)A04

UCB/EERC-77/15 Unassigned

UCB/EERC-77/16 "Computer Aided Optimum Design of Ductile Reinforced Concrete Moment Resisting Frames," by S.W. Zagajeski and V.V. Bertero - 1977 (PB 280 137)A07

UCB/EERC-77/17 "Earthquake Simulation Testing of a Stepping Frame with Energy-Absorbing Devices," by J.M. Kelly and D.F. Tsztoo - 1977 (PB 273 506)A04

UCB/EERC-77/18 "Inelastic Behavior of Eccentrically Braced Steel Frames under Cyclic Loadings," by C.W. Roeder and E.P. Popov - 1977 (PB 275 526)A15

UCB/EERC-77/19 "A Simplified Procedure for Estimating Earthquake-Induced Deformations in Dams and Embankments," by F.I. Makdisi and H.B. Seed - 1977 (PB 276 820)A04

UCB/EERC-77/20 "The Performance of Earth Dams during Earthquakes," by H.B. Seed, F.I. Makdisi and P. de Alba - 1977 (PB 276 821)A04

UCB/EERC-77/21 "Dynamic Plastic Analysis Using Stress Resultant Finite Element Formulation," by P. Lukkunapvasit and J.M. Kelly - 1977 (PB 275 453)A04

UCB/EERC-77/22 "Preliminary Experimental Study of Seismic Uplift of a Steel Frame," by R.W. Clough and A.A. Huckelbridge 1977 (PB 278 769)A08

UCB/EERC-77/23 "Earthquake Simulator Tests of a Nine-Story Steel Frame with Columns Allowed to Uplift," by A.A. Huckelbridge - 1977 (PB 277 944)A09

UCB/EERC-77/24 "Nonlinear Soil-Structure Interaction of Skew Highway Bridges," by M.-C. Chen and J. Penzien - 1977 (PB 276 176)A07

UCB/EERC-77/25 "Seismic Analysis of an Offshore Structure Supported on Pile Foundations," by D.D.-N. Liou and J. Penzien 1977 (PB 283 180)A06

UCB/EERC-77/26 "Dynamic Stiffness Matrices for Homogeneous Viscoelastic Half-Planes," by G. Dasgupta and A.K. Chopra - 1977 (PB 279 654)A06

UCB/EERC-77/27 "A Practical Soft Story Earthquake Isolation System," by J.M. Kelly, J.M. Eidinger and C.J. Derham - 1977 (PB 276 814)A07

UCB/EERC-77/28 "Seismic Safety of Existing Buildings and Incentives for Hazard Mitigation in San Francisco: An Exploratory Study," by A.J. Meltsner - 1977 (PB 281 970)A05

UCB/EERC-77/29 "Dynamic Analysis of Electrohydraulic Shaking Tables," by D. Rea, S. Abedi-Hayati and Y. Takahashi 1977 (PB 282 569)A04

UCB/EERC-77/30 "An Approach for Improving Seismic - Resistant Behavior of Reinforced Concrete Interior Joints," by B. Galunic, V.V. Bertero and E.P. Popov - 1977 (PB 290 870)A06

UCB/EERC-78/01 "The Development of Energy-Absorbing Devices for Aseismic Base Isolation Systems," by J.M. Kelly and D.F. Tsztoo - 1978 (PB 284 978)A04

UCB/EERC-78/02 "Effect of Tensile Prestrain on the Cyclic Response of Structural Steel Connections, by J.G. Bouwkamp and A. Mukhopadhyay - 1978

UCB/EERC-78/03 "Experimental Results of an Earthquake Isolation System using Natural Rubber Bearings," by J.M. Eidinger and J.M. Kelly - 1978 (PB 281 686)A04

UCB/EERC-78/04 "Seismic Behavior of Tall Liquid Storage Tanks," by A. Niwa - 1978 (PB 284 017)A14

UCB/EERC-78/05 "Hysteretic Behavior of Reinforced Concrete Columns Subjected to High Axial and Cyclic Shear Forces," by S.W. Zagajeski, V.V. Bertero and J.G. Bouwkamp - 1978 (PB 283 858)A13

UCB/EERC-78/06 "Three Dimensional Inelastic Frame Elements for the ANSR-I Program," by A. Riahi, D.G. Row and G.H. Powell - 1978 (PB 295 755)A04

UCB/EERC-78/07 "Studies of Structural Response to Earthquake Ground Motion," by O.A. Lopez and A.K. Chopra - 1978 (PB 282 790)A05

UCB/EERC-78/08 "A Laboratory Study of the Fluid-Structure Interaction of Submerged Tanks and Caissons in Earthquakes," by R.C. Byrd - 1978 (PB 284 957)A08

UCB/EERC-78/09 Unassigned

UCB/EERC-78/10 "Seismic Performance of Nonstructural and Secondary Structural Elements," by I. Sakamoto - 1978 (PB81 154 593)A05

UCB/EERC-78/11 "Mathematical Modelling of Hysteresis Loops for Reinforced Concrete Columns," by S. Nakata, T. Sproul and J. Penzien - 1978 (PB 298 274)A05

UCB/EERC-78/12 "Damageability in Existing Buildings," by T. Blejwas and B. Bresler - 1978 (PB 80 166 978)A05

UCB/EERC-78/13 "Dynamic Behavior of a Pedestal Base Multistory Building," by R.M. Stephen, E.L. Wilson, J.G. Bouwkamp and M. Button - 1978 (PB 286 650)A08

UCB/EERC-78/14 "Seismic Response of Bridges - Case Studies," by R.A. Imbsen, V. Nutt and J. Penzien - 1978 (PB 286 503)A10

UCB/EERC-78/15 "A Substructure Technique for Nonlinear Static and Dynamic Analysis," by D.G. Row and G.H. Powell - 1978 (PB 288 077)A10

UCB/EERC-78/16 "Seismic Risk Studies for San Francisco and for the Greater San Francisco Bay Area," by C.S. Oliveira - 1978 (PB 81 120 115)A07

UCB/EERC-78/17 "Strength of Timber Roof Connections Subjected to Cyclic Loads," by P. Gülkan, R.L. Mayes and R.W. Clough - 1978 (HUD-000 1491)A07

UCB/EERC-78/18 "Response of K-Braced Steel Frame Models to Lateral Loads," by J.G. Bouwkamp, R.M. Stephen and E.P. Popov - 1978

UCB/EERC-78/19 "Rational Design Methods for Light Equipment in Structures Subjected to Ground Motion," by J.L. Sackman and J.M. Kelly - 1978 (PB 292 357)A04

UCB/EERC-78/20 "Testing of a Wind Restraint for Aseismic Base Isolation," by J.M. Kelly and D.E. Chitty - 1978 (PB 292 833)A03

UCB/EERC-78/21 "APOLLO - A Computer Program for the Analysis of Pore Pressure Generation and Dissipation in Horizontal Sand Layers During Cyclic or Earthquake Loading," by P.P. Martin and H.B. Seed - 1978 (PB 292 835)A04

UCB/EERC-78/22 "Optimal Design of an Earthquake Isolation System," by M.A. Bhatti, K.S. Pister and E. Polak - 1978 (PB 294 735)A06

UCB/EERC-78/23 "MASH - A Computer Program for the Non-Linear Analysis of Vertically Propagating Shear Waves in Horizontally Layered Deposits," by P.P. Martin and H.B. Seed - 1978 (PB 293 101)A05

UCB/EERC-78/24 "Investigation of the Elastic Characteristics of a Three Story Steel Frame Using System Identification," by I. Kaya and H.D. McNiven - 1978 (PB 296 225)A06

UCB/EERC-78/25 "Investigation of the Nonlinear Characteristics of a Three-Story Steel Frame Using System Identification," by I. Kaya and H.D. McNiven - 1978 (PB 301 363)A05

UCB/EERC-78/26 "Studies of Strong Ground Motion in Taiwan," by Y.M. Hsiung, B.A. Bolt and J. Penzien - 1978 (PB 298 436)A06

UCB/EERC-78/27 "Cyclic Loading Tests of Masonry Single Piers: Volume 1 - Height to Width Ratio of 2," by P.A. Hidalgo, R.L. Mayes, H.D. McNiven and R.W. Clough - 1978 (PB 296 211)A07

UCB/EERC-78/28 "Cyclic Loading Tests of Masonry Single Piers: Volume 2 - Height to Width Ratio of 1," by S.-W.J. Chen, P.A. Hidalgo, R.L. Mayes, R.W. Clough and H.D. McNiven - 1978 (PB 296 212)A09

UCB/EERC-78/29 "Analytical Procedures in Soil Dynamics," by J. Lysmer - 1978 (PB 298 445)A06

UCB/EERC-79/01 "Hysteretic Behavior of Lightweight Reinforced Concrete Beam-Column Subassemblages," by B. Forzani, E.P. Popov and V.V. Bertero - April 1979(PB 298 267)A06

UCB/EERC-79/02 "The Development of a Mathematical Model to Predict the Flexural Response of Reinforced Concrete Beams to Cyclic Loads, Using System Identification," by J. Stanton & H. McNiven - Jan. 1979(PB 295 875)A10

UCB/EERC-79/03 "Linear and Nonlinear Earthquake Response of Simple Torsionally Coupled Systems," by C.L. Kan and A.K. Chopra - Feb. 1979(PB 298 262)A06

UCB/EERC-79/04 "A Mathematical Model of Masonry for Predicting its Linear Seismic Response Characteristics," by Y. Mengi and H.D. McNiven - Feb. 1979(PB 298 266)A06

UCB/EERC-79/05 "Mechanical Behavior of Lightweight Concrete Confined by Different Types of Lateral Reinforcement," by M.A. Manrique, V.V. Bertero and E.P. Popov - May 1979(PB 301 114)A06

UCB/EERC-79/06 "Static Tilt Tests of a Tall Cylindrical Liquid Storage Tank," by R.W. Clough and A. Niwa - Feb. 1979 (PB 301 167)A06

UCB/EERC-79/07 "The Design of Steel Energy Absorbing Restrainers and Their Incorporation into Nuclear Power Plants for Enhanced Safety: Volume 1 - Summary Report," by P.N. Spencer, V.F. Zackay, and E.R. Parker - Feb. 1979(UCB/EERC-79/07)A09

UCB/EERC-79/08 "The Design of Steel Energy Absorbing Restrainers and Their Incorporation into Nuclear Power Plants for Enhanced Safety: Volume 2 - The Development of Analyses for Reactor System Piping,""Simple Systems" by M.C. Lee, J. Penzien, A.K. Chopra and K, Suzuki "Complex Systems" by G.H. Powell, E.L. Wilson, R.W. Clough and D.G. Row - Feb. 1979(UCB/EERC-79/08)A10

UCB/EERC-79/09 "The Design of Steel Energy Absorbing Restrainers and Their Incorporation into Nuclear Power Plants for Enhanced Safety: Volume 3 - Evaluation of Commercial Steels," by W.S. Owen, R.M.N. Pelloux, R.O. Ritchie, M. Faral, T. Ohhashi, J. Toplosky, S.J. Hartman, V.F. Zackay and E.R. Parker - Feb. 1979(UCB/EERC-79/09)A04

UCB/EERC-79/10 "The Design of Steel Energy Absorbing Restrainers and Their Incorporation into Nuclear Power Plants for Enhanced Safety: Volume 4 - A Review of Energy-Absorbing Devices," by J.M. Kelly and M.S. Skinner - Feb. 1979(UCB/EERC-79/10)A04

UCB/EERC-79/11 "Conservatism In Summation Rules for Closely Spaced Modes," by J.M. Kelly and J.L. Sackman - May 1979(PB 301 328)A03

UCB/EERC-79/12 "Cyclic Loading Tests of Masonry Single Piers; Volume 3 - Height to Width Ratio of 0.5," by P.A. Hidalgo, R.L. Mayes, H.D. McNiven and R.W. Clough - May 1979(PB 301 321)A08

UCB/EERC-79/13 "Cyclic Behavior of Dense Course-Grained Materials in Relation to the Seismic Stability of Dams," by N.G. Banerjee, H.B. Seed and C.K. Chan - June 1979(PB 301 373)A13

UCB/EERC-79/14 "Seismic Behavior of Reinforced Concrete Interior Beam-Column Subassemblages," by S. Viwathanatepa, E.P. Popov and V.V. Bertero - June 1979(PB 301 326)A10

UCB/EERC-79/15 "Optimal Design of Localized Nonlinear Systems with Dual Performance Criteria Under Earthquake Excitations," by M.A. Bhatti - July 1979(PB 80 167 109)A06

UCB/EERC-79/16 "OPTDYN - A General Purpose Optimization Program for Problems with or without Dynamic Constraints," by M.A. Bhatti, E. Polak and K.S. Pister - July 1979(PB 80 167 091)A05

UCB/EERC-79/17 "ANSR-II, Analysis of Nonlinear Structural Response, Users Manual," by D.P. Mondkar and G.H. Powell July 1979(PB 80 113 301)A05

UCB/EERC-79/18 "Soil Structure Interaction in Different Seismic Environments," A. Gomez-Masso, J. Lysmer, J.-C. Chen and H.B. Seed - August 1979(PB 80 101 520)A04

UCB/EERC-79/19 "ARMA Models for Earthquake Ground Motions," by M.K. Chang, J.W. Kwiatkowski, R.F. Nau, R.M. Oliver and K.S. Pister - July 1979(PB 301 166)A05

UCB/EERC-79/20 "Hysteretic Behavior of Reinforced Concrete Structural Walls," by J.M. Vallenas, V.V. Bertero and E.P. Popov - August 1979(PB 80 165 905)A12

UCB/EERC-79/21 "Studies on High-Frequency Vibrations of Buildings - 1: The Column Effect," by J. Lubliner - August 1979 (PB 80 158 553)A03

UCB/EERC-79/22 "Effects of Generalized Loadings on Bond Reinforcing Bars Embedded in Confined Concrete Blocks," by S. Viwathanatepa, E.P. Popov and V.V. Bertero - August 1979(PB 81 124 018)A14

UCB/EERC-79/23 "Shaking Table Study of Single-Story Masonry Houses, Volume 1: Test Structures 1 and 2," by P. Gülkan, R.L. Mayes and R.W. Clough - Sept. 1979 (HUD-000 1763)A12

UCB/EERC-79/24 "Shaking Table Study of Single-Story Masonry Houses, Volume 2: Test Structures 3 and 4," by P. Gülkan, R.L. Mayes and R.W. Clough - Sept. 1979 (HUD-000 1836)A12

UCB/EERC-79/25 "Shaking Table Study of Single-Story Masonry Houses, Volume 3: Summary, Conclusions and Recommendations," by R.W. Clough, R.L. Mayes and P. Gülkan - Sept. 1979 (HUD-000 1837)A06

UCB/EERC-79/26 "Recommendations for a U.S.-Japan Cooperative Research Program Utilizing Large-Scale Testing Facilities," by U.S.-Japan Planning Group - Sept. 1979(PB 301 407)A06

UCB/EERC-79/27 "Earthquake-Induced Liquefaction Near Lake Amatitlan, Guatemala," by H.B. Seed, I. Arango, C.K. Chan, A. Gomez-Masso and R. Grant de Ascoli - Sept. 1979(NUREG-CR1341)A03

UCB/EERC-79/28 "Infill Panels: Their Influence on Seismic Response of Buildings," by J.W. Axley and V.V. Bertero Sept. 1979(PB 80 163 371)A10

UCB/EERC-79/29 "3D Truss Bar Element (Type 1) for the ANSR-II Program," by D.P. Mondkar and G.H. Powell - Nov. 1979 (PB 80 169 709)A02

UCB/EERC-79/30 "2D Beam-Column Element (Type 5 - Parallel Element Theory) for the ANSR-II Program," by D.G. Row, G.H. Powell and D.P. Mondkar - Dec. 1979(PB 80 167 224)A03

UCB/EERC-79/31 "3D Beam-Column Element (Type 2 - Parallel Element Theory) for the ANSR-II Program," by A. Riahi, G.H. Powell and D.P. Mondkar - Dec. 1979(PB 80 167 216)A03

UCB/EERC-79/32 "On Response of Structures to Stationary Excitation," by A. Der Kiureghian - Dec. 1979(PB 80166 929)A03

UCB/EERC-79/33 "Undisturbed Sampling and Cyclic Load Testing of Sands," by S. Singh, H.B. Seed and C.K. Chan Dec. 1979(ADA 087 298)A07

UCB/EERC-79/34 "Interaction Effects of Simultaneous Torsional and Compressional Cyclic Loading of Sand," by P.M. Griffin and W.N. Houston - Dec. 1979(ADA 092 352)A15

UCB/EERC-80/01 "Earthquake Response of Concrete Gravity Dams Including Hydrodynamic and Foundation Interaction Effects," by A.K. Chopra, P. Chakrabarti and S. Gupta - Jan. 1980(AD-A087297)A10

UCB/EERC-80/02 "Rocking Response of Rigid Blocks to Earthquakes," by C.S. Yim, A.K. Chopra and J. Penzien - Jan. 1980 (PB80 166 002)A04

UCB/EERC-80/03 "Optimum Inelastic Design of Seismic-Resistant Reinforced Concrete Frame Structures," by S.W. Zagajeski and V.V. Bertero - Jan. 1980(PB80 164 635)A06

UCB/EERC-80/04 "Effects of Amount and Arrangement of Wall-Panel Reinforcement on Hysteretic Behavior of Reinforced Concrete Walls," by R. Iliya and V.V. Bertero - Feb. 1980(PB81 122 525)A09

UCB/EERC-80/05 "Shaking Table Research on Concrete Dam Models," by A. Niwa and R.W. Clough - Sept. 1980(PB81 122 368)A06

UCB/EERC-80/06 "The Design of Steel Energy-Absorbing Restrainers and their Incorporation into Nuclear Power Plants for Enhanced Safety (Vol 1A): Piping with Energy Absorbing Restrainers: Parameter Study on Small Systems," by G.H. Powell, C. Oughourlian and J. Simons - June 1980

UCB/EERC-80/07 "Inelastic Torsional Response of Structures Subjected to Earthquake Ground Motions," by Y. Yamazaki April 1980(PB81 122 327)A08

UCB/EERC-80/08 "Study of X-Braced Steel Frame Structures Under Earthquake Simulation," by Y. Ghanaat - April 1980 (PB81 122 335)A11

UCB/EERC-80/09 "Hybrid Modelling of Soil-Structure Interaction," by S. Gupta, T.W. Lin, J. Penzien and C.S. Yeh May 1980(PB81 122 319)A07

UCB/EERC-80/10 "General Applicability of a Nonlinear Model of a One Story Steel Frame," by B.I. Sveinsson and H.D. McNiven - May 1980(PB81 124 877)A06

UCB/EERC-80/11 "A Green-Function Method for Wave Interaction with a Submerged Body," by W. Kioka - April 1980 (PB81 122 269)A07

UCB/EERC-80/12 "Hydrodynamic Pressure and Added Mass for Axisymmetric Bodies," by F. Nilrat - May 1980(PB81 122 343)A08

UCB/EERC-80/13 "Treatment of Non-Linear Drag Forces Acting on Offshore Platforms," by B.V. Dao and J. Penzien May 1980(PB81 153 413)A07

UCB/EERC-80/14 "2D Plane/Axisymmetric Solid Element (Type 3 - Elastic or Elastic-Perfectly Plastic) for the ANSR-II Program," by D.P. Mondkar and G.H. Powell - July 1980(PB81 122 350)A03

UCB/EERC-80/15 "A Response Spectrum Method for Random Vibrations," by A. Der Kiureghian - June 1980(PB81 122 301)A03

UCB/EERC-80/16 "Cyclic Inelastic Buckling of Tubular Steel Braces," by V.A. Zayas, E.P. Popov and S.A. Mahin June 1980(PB81 124 885)A10

UCB/EERC-80/17 "Dynamic Response of Simple Arch Dams Including Hydrodynamic Interaction," by C.S. Porter and A.K. Chopra - July 1980(PB81 124 000)A13

UCB/EERC-80/18 "Experimental Testing of a Friction Damped Aseismic Base Isolation System with Fail-Safe Characteristics," by J.M. Kelly, K.E. Beucke and M.S. Skinner - July 1980(PB81 148 595)A04

UCB/EERC-80/19 "The Design of Steel Energy-Absorbing Restrainers and their Incorporation into Nuclear Power Plants for Enhanced Safety (Vol 1B): Stochastic Seismic Analyses of Nuclear Power Plant Structures and Piping Systems Subjected to Multiple Support Excitations," by M.C. Lee and J. Penzien - June 1980

UCB/EERC-80/20 "The Design of Steel Energy-Absorbing Restrainers and their Incorporation into Nuclear Power Plants for Enhanced Safety (Vol 1C): Numerical Method for Dynamic Substructure Analysis," by J.M. Dickens and E.L. Wilson - June 1980

UCB/EERC-80/21 "The Design of Steel Energy-Absorbing Restrainers and their Incorporation into Nuclear Power Plants for Enhanced Safety (Vol 2): Development and Testing of Restraints for Nuclear Piping Systems," by J.M. Kelly and M.E. Skinner - June 1980

UCB/EERC-80/22 "3D Solid Element (Type 4-Elastic or Elastic-Perfectly-Plastic) for the ANSR-II Program," by D.P. Mondkar and G.H. Powell - July 1980(PB81 123 242)A03

UCB/EERC-80/23 "Gap-Friction Element (Type 5) for the ANSR-II Program," by D.P. Mondkar and G.H. Powell - July 1980 (PB81 122 285)A03

UCB/EERC-80/24 "U-Bar Restraint Element (Type 11) for the ANSR-II Program," by C. Oughourlian and G.H. Powell July 1980(PB81 122 293)A03

UCB/EERC-80/25 "Testing of a Natural Rubber Base Isolation System by an Explosively Simulated Earthquake," by J.M. Kelly - August 1980(PB81 201 360)A04

UCB/EERC-80/26 "Input Identification from Structural Vibrational Response," by Y. Hu - August 1980(PB81 152 308)A05

UCB/EERC-80/27 "Cyclic Inelastic Behavior of Steel Offshore Structures," by V.A. Zayas, S.A. Mahin and E.P. Popov August 1980(PB81 196 180)A15

UCB/EERC-80/28 "Shaking Table Testing of a Reinforced Concrete Frame with Biaxial Response," by M.G. Oliva October 1980(PB81 154 304)A10

UCB/EERC-80/29 "Dynamic Properties of a Twelve-Story Prefabricated Panel Building," by J.G. Bouwkamp, J.P. Kollegger and R.M. Stephen - October 1980(PB82 117 128)A06

UCB/EERC-80/30 "Dynamic Properties of an Eight-Story Prefabricated Panel Building," by J.G. Bouwkamp, J.P. Kollegger and R.M. Stephen - October 1980(PB81 200 313)A05

UCB/EERC-80/31 "Predictive Dynamic Response of Panel Type Structures Under Earthquakes," by J.P. Kollegger and J.G. Bouwkamp - October 1980(PB81 152 316)A04

UCB/EERC-80/32 "The Design of Steel Energy-Absorbing Restrainers and their Incorporation into Nuclear Power Plants for Enhanced Safety (Vol 3): Testing of Commercial Steels in Low-Cycle Torsional Fatigue," by P. Spencer, E.R. Parker, E. Jongewaard and M. Drory

UCB/EERC-80/33 "The Design of Steel Energy-Absorbing Restrainers and their Incorporation into Nuclear Power Plants for Enhanced Safety (Vol 4): Shaking Table Tests of Piping Systems with Energy-Absorbing Restrainers," by S.F. Stiemer and W.G. Godden - Sept. 1980

UCB/EERC-80/34 "The Design of Steel Energy-Absorbing Restrainers and their Incorporation into Nuclear Power Plants for Enhanced Safety (Vol 5): Summary Report," by P. Spencer

UCB/EERC-80/35 "Experimental Testing of an Energy-Absorbing Base Isolation System," by J.M. Kelly, M.S. Skinner and K.E. Beucke - October 1980(PB81 154 072)A04

UCB/EERC-80/36 "Simulating and Analyzing Artificial Non-Stationary Earthquake Ground Motions," by R.F. Nau, R.M. Oliver and K.S. Pister - October 1980(PB81 153 397)A04

UCB/EERC-80/37 "Earthquake Engineering at Berkeley - 1980," - Sept. 1980(PB81 205 374)A09

UCB/EERC-80/38 "Inelastic Seismic Analysis of Large Panel Buildings," by V. Schricker and G.H. Powell - Sept. 1980 (PB81 154 338)A13

UCB/EERC-80/39 "Dynamic Response of Embankment, Concrete-Gravity and Arch Dams Including Hydrodynamic Interaction," by J.F. Hall and A.K. Chopra - October 1980(PB81 152 324)A11

UCB/EERC-80/40 "Inelastic Buckling of Steel Struts Under Cyclic Load Reversal," by R.G. Black, W.A. Wenger and E.P. Popov - October 1980(PB81 154 312)A08

UCB/EERC-80/41 "Influence of Site Characteristics on Building Damage During the October 3, 1974 Lima Earthquake," by P. Repetto, I. Arango and H.B. Seed - Sept. 1980(PB81 161 739)A05

UCB/EERC-80/42 "Evaluation of a Shaking Table Test Program on Response Behavior of a Two Story Reinforced Concrete Frame," by J.M. Blondet, R.W. Clough and S.A. Mahin

UCB/EERC-80/43 "Modelling of Soil-Structure Interaction by Finite and Infinite Elements," by F. Medina - December 1980(PB81 229 270)A04

UCB/EERC-81/01 "Control of Seismic Response of Piping Systems and Other Structures by Base Isolation," edited by J.M. Kelly - January 1981 (PB81 200 735)A05

UCB/EERC-81/02 "OPTNSR - An Interactive Software System for Optimal Design of Statically and Dynamically Loaded Structures with Nonlinear Response," by M.A. Bhatti, V. Ciampi and K.S. Pister - January 1961 (PB81 218 851)A09

UCB/EERC-81/03 "Analysis of Local Variations in Free Field Seismic Ground Motions," by J.-C. Chen, J. Lysmer and H.B. Seed - January 1981 (AD-A099508)A13

UCB/EERC-81/04 "Inelastic Structural Modeling of Braced Offshore Platforms for Seismic Loading," by V.A. Zayas, P.-S.B. Shing, S.A. Mahin and E.P. Popov - January 1981(PB82 138 777)A07

UCB/EERC-81/05 "Dynamic Response of Light Equipment in Structures," by A. Der Kiureghian, J.L. Sackman and B. Nour-Omid - April 1981 (PB81 218 497)A04

UCB/EERC-81/06 "Preliminary Experimental Investigation of a Broad Base Liquid Storage Tank," by J.G. Bouwkamp, J.P. Kollegger and R.M. Stephen - May 1981(PB82 140 385)A03

UCB/EERC-81/07 "The Seismic Resistant Design of Reinforced Concrete Coupled Structural Walls," by A.E. Aktan and V.V. Bertero - June 1981(PB82 113 358)A11

UCB/EERC-81/08 "The Undrained Shearing Resistance of Cohesive Soils at Large Deformations," by M.R. Pyles and H.B. Seed - August 1981

UCB/EERC-81/09 "Experimental Behavior of a Spatial Piping System with Steel Energy Absorbers Subjected to a Simulated Differential Seismic Input," by S.F. Stiemer, W.G. Godden and J.M. Kelly - July 1981

UCB/EERC-81/10 "Evaluation of Seismic Design Provisions for Masonry in the United States," by B.I. Sveinsson, R.L. Mayes and H.D. McNiven - August 1981 (PB82 166 075)A08

UCB/EERC-81/11 "Two-Dimensional Hybrid Modelling of Soil-Structure Interaction," by T.-J. Tzong, S. Gupta and J. Penzien - August 1981(PB82 142 118)A04

UCB/EERC-81/12 "Studies on Effects of Infills in Seismic Resistant R/C Construction," by S. Brokken and V.V. Bertero - September 1981 (PB82 166 190)A09

UCB/EERC-81/13 "Linear Models to Predict the Nonlinear Seismic Behavior of a One-Story Steel Frame," by H. Valdimarsson, A.H. Shah and H.D. McNiven - September 1981(PB82 138 793)A07

UCB/EERC-81/14 "TLUSH: A Computer Program for the Three-Dimensional Dynamic Analysis of Earth Dams," by T. Kagawa, L.H. Mejia, H.B. Seed and J. Lysmer - September 1981(PB82 139 940)A06

UCB/EERC-81/15 "Three Dimensional Dynamic Response Analysis of Earth Dams," by L.H. Mejia and H.B. Seed - September 1981 (PB82 137 274)A12

UCB/EERC-81/16 "Experimental Study of Lead and Elastomeric Dampers for Base Isolation Systems," by J.M. Kelly and S.B. Hodder - October 1981 (PB82 166 182)A05

UCB/EERC-81/17 "The Influence of Base Isolation on the Seismic Response of Light Secondary Equipment," by J.M. Kelly - April 1981 (PB82 255 266)A04

UCB/EERC-81/18 "Studies on Evaluation of Shaking Table Response Analysis Procedures," by J. Marcial Blondet - November 1981 (PB82 197 278)A10

UCB/EERC-81/19 "DELIGHT.STRUCT: A Computer-Aided Design Environment for Structural Engineering," by R.J. Balling, K.S. Pister and E. Polak - December 1981 (PB82 218 496)A07

UCB/EERC-81/20 "Optimal Design of Seismic-Resistant Planar Steel Frames," by R.J. Balling, V. Ciampi, K.S. Pister and E. Polak - December 1981 (PB82 220 179)A07

UCB/EERC-82/01 "Dynamic Behavior of Ground for Seismic Analysis of Lifeline Systems," by T. Sato and A. Der Kiureghian - January 1982 (PB82 218 926)A05

UCB/EERC-82/02 "Shaking Table Tests of a Tubular Steel Frame Model," by Y. Ghanaat and R. W. Clough - January 1982 (PB82 220 161)A07

UCB/EERC-82/03 "Behavior of a Piping System under Seismic Excitation: Experimental Investigations of a Spatial Piping System supported by Mechanical Shock Arrestors and Steel Energy Absorbing Devices under Seismic Excitation," by S. Schneider, H.-M. Lee and W. G. Godden - May 1982 (PB83 172 544)A09

UCB/EERC-82/04 "New Approaches for the Dynamic Analysis of Large Structural Systems," by E. L. Wilson - June 1982 (PB83 148 080)A05

UCB/EERC-82/05 "Model Study of Effects of Damage on the Vibration Properties of Steel Offshore Platforms," by F. Shahrivar and J. G. Bouwkamp - June 1982 (PB83 148 742)A10

UCB/EERC-82/06 "States of the Art and Practice in the Optimum Seismic Design and Analytical Response Prediction of R/C Frame-Wall Structures," by A. E. Aktan and V. V. Bertero - July 1982 (PB83 147 736)A05

UCB/EERC-82/07 "Further Study of the Earthquake Response of a Broad Cylindrical Liquid-Storage Tank Model," by G. C. Manos and R. W. Clough - July 1982 (PB83 147 744)A11

UCB/EERC-82/08 "An Evaluation of the Design and Analytical Seismic Response of a Seven Story Reinforced Concrete Frame - Wall Structure," by F. A. Charney and V. V. Bertero - July 1982(PB83 157 628)A09

UCB/EERC-82/09 "Fluid-Structure Interactions: Added Mass Computations for Incompressible Fluid," by J. S.-H. Kuo - August 1982 (PB83 156 281)A07

UCB/EERC-82/10 "Joint-Opening Nonlinear Mechanism: Interface Smeared Crack Model," by J. S.-H. Kuo - August 1982 (PB83 149 195)A05

UCB/EERC-82/11 "Dynamic Response Analysis of Techi Dam," by R. W. Clough, R. M. Stephen and J. S.-H. Kuo - August 1982 (PB83 147 496)A06

UCB/EERC-82/12 "Prediction of the Seismic Responses of R/C Frame-Coupled Wall Structures," by A. E. Aktan, V. V. Bertero and M. Piazza - August 1982 (PB83 149 203)A09

UCB/EERC-82/13 "Preliminary Report on the SMART 1 Strong Motion Array in Taiwan," by B. A. Bolt, C. H. Loh, J. Penzien, Y. B. Tsai and Y. T. Yeh - August 1982 (PB83 159 400)A10

UCB/EERC-82/14 "Shaking-Table Studies of an Eccentrically X-Braced Steel Structure," by M. S. Yang - September 1982

UCB/EERC-82/15 "The Performance of Stairways in Earthquakes," by C. Roha, J. W. Axley and V. V. Bertero - September 1982 (PB83 157 693)A07

UCB/EERC-82/16 "The Behavior of Submerged Multiple Bodies in Earthquakes," by W.-G. Liao - Sept. 1982 (PB83 158 709)A07

UCB/EERC-82/17 "Effects of Concrete Types and Loading Conditions on Local Bond-Slip Relationships," by A. D. Cowell, E. P. Popov and V. V. Bertero - September 1982 (PB83 153 577)A04

UCB/EERC-82/18 "Mechanical Behavior of Shear Wall Vertical Boundary Members: An Experimental Investigation," by M. T. Wagner and V. V. Bertero - October 1982 (PB83 159 764)A05

UCB/EERC-82/19 "Experimental Studies of Multi-support Seismic Loading on Piping Systems," by J. M. Kelly and A. D. Cowell - November 1982

UCB/EERC-82/20 "Generalized Plastic Hinge Concepts for 3D Beam-Column Elements," by P. F.-S. Chen and G. H. Powell - November 1982

UCB/EERC-82/21 "ANSR-III: General Purpose Computer Program for Nonlinear Structural Analysis," by C. V. Oughourlian and G. H. Powell - November 1982

UCB/EERC-82/22 "Solution Strategies for Statically Loaded Nonlinear Structures," by J. W. Simons and G. H. Powell - November 1982

UCB/EERC-82/23 "Analytical Model of Deformed Bar Anchorages under Generalized Excitations," by V. Ciampi, R. Eligehausen, V. V. Bertero and E. P. Popov - November 1982 (PB83 169 532)A06

UCB/EERC-82/24 "A Mathematical Model for the Response of Masonry Walls to Dynamic Excitations," by H. Sucuoğlu, Y. Mengi and H. D. McNiven - November 1982 (PB83 169 011)A07

UCB/EERC-82/25 "Earthquake Response Considerations of Broad Liquid Storage Tanks," by F. J. Cambra - November 1982

UCB/EERC-82/26 "Computational Models for Cyclic Plasticity, Rate Dependence and Creep," by B. Mosaddad and G. H. Powell - November 1982

UCB/EERC-82/27 "Inelastic Analysis of Piping and Tubular Structures," by M. Mahasuverachai and G. H. Powell - November 1982

UCB/EERC-83/01 "The Economic Feasibility of Seismic Rehabilitation of Buildings by Base Isolation," by J. M. Kelly - January 1983

UCB/EERC-83/02 "Seismic Moment Connections for Moment-Resisting Steel Frames," by E. P. Popov - January 1983

UCB/EERC-83/03 "Design of Links and Beam-to-Column Connections for Eccentrically Braced Steel Frames," by E. P. Popov and J. O. Malley - January 1983

UCB/EERC-83/04 "Numerical Techniques for the Evaluation of Soil-Structure Interaction Effects in the Time Domain," by E. Bayo and E. L. Wilson - February 1983

UCB/EERC-83/05 "A Transducer for Measuring the Internal Forces in the Columns of a Frame-Wall Reinforced Concrete Structure," by R. Sause and V. V. Bertero - May 1983

UCB/EERC-83/06 "Dynamic Interactions between Floating Ice and Offshore Structures," by P. Croteau - May 1983

UCB/EERC-83/07 "Dynamic Analysis of Multiply Tunnelled and Arbitrarily Supported Secondary Systems," by T. Igusa and A. Der Kiureghian - June 1983

UCB/EERC-83/08 "A Laboratory Study of Submerged Multi-body Systems in Earthquakes," by G. R. Ansari - June 1983

UCB/EERC-83/09 "Effects of Transient Foundation Uplift on Earthquake Response of Structures," by C.-S. Yim and A. K. Chopra - June 1983